Room Fires and Combustible Linings

Karlsson, Björn

1989

LUND UNIVERSITY

PO Box 117
221 00 Lund
+46 46-222 00 00

LUND UNIVERSITY · SWEDEN
INSTITUTE OF SCIENCE AND TECHNOLOGY
DEPARTMENT OF FIRE SAFETY ENGINEERING
CODEN: SE - LUTVDG/TVBB - 3050
ISSN 0284 - 933X

BJÖRN KARLSSON

ROOM FIRES AND COMBUSTIBLE LININGS

LUND 1989

Research project financed by the Swedish Fire Research Board (BRANDFORSK)

Acknowledgments

This report was prepared at the Department of Fire Safety Engineering, Lund Institute of Technology as a part of the requirements for a licentiate degree.

I would like to express my sincere gratitude to my supervisor, Professor Sven Erik Magnusson, for instigating this work and for supporting me with his broad experience. This work builds, to a large extent, on his preceeding work in the field.

It is a pleasure to acknowledge the work of Berit Andersson who collected and compared different bench-scale data referred to in this report.

Lund, October 1989

Björn Karlsson

Abstract

An extensive research program on combustible wall lining materials has been carried out in Sweden.

Several lining materials were tested in full scale room tests and 1/3 scale model room tests for two different scenarios, A and B. Scenario A refers to the case where walls and ceiling are covered by the lining material, scenario B where lining materials are mounted on walls only.

A model is presented using material properties derived from standardized bench-scale tests as input data. The model predicts the fire growth in the full or 1/3 scale tests, which includes predicting the rate of heat release, gastemperatures, radiation to walls, wall surface temperatures and downward flame spread on the wall lining material.

List of symbols

A_p	=	Pyrolysis area
A_o	=	Area of opening
A_w	=	Wall surface area
C	=	Flame spread constant in eqn. (5)
C	=	Constant in eqn. (14)
c_p	=	Heat capacity (of air unless otherwise stated)
F	=	Configuration factor
g	=	Gravitational acceleration
h	=	Convective and radiative heat transfer coefficient
h_k	=	Convective heat transfer coefficient
H_o	=	Height of opening
k	=	Constant in eqn. (12)
$k\rho c$	=	Thermal inertia
q''	=	Radiative heat transfer per area
$q''_{0,ig}$	=	Minimum radiant heat flux per area for sustained piloted ignition
q''_e	=	External radiant heat flux per area
Q''	=	Energy release rate per fuel area
Q''_{av}	=	Average heat release rate per fuel area in bench-scale test
Q_{cf}	=	Non-combustible part of wall-corne flame reaching the ceiling
Q_{gb}	=	Heat release from gas burner
Q''_{max}	=	Maximum energy release rate per fuel area in bench-scale test
Q_{start}	=	Total heat release from gas burner and lining material behind burner
t_h	=	Time for pyrolysis front to move horizontally along wall-ceiling intersection to opposite corner
t_{ign}	=	Time to ignition in bench-scale test
t_p	=	Time to reach pyrolises temperature
t_{start}	=	Time to reach Q_{start}
T	=	Temperature
$T_{fl.f}$	=	Material surface temperature just ahead of the flame front
T_{ig}	=	Ignition temperature
T_i	=	Initial temperature
T_s	=	Surface temperature
V_f	=	Flame spread velocity
V_p	=	Velocity of pyrolysis front
x_f	=	Position of the flame front in eqn. (4)
x_f	=	Flame height
x_p	=	Position of the pyrolysis front
α	=	Entrainment coefficient in eqn. (17)
α	=	Correlation coefficient

β	=	Correlation coefficient
λ	=	Decay coefficient
ρ_0	=	Density of ambient air
σ	=	Stefan-Boltzmann constant
ϕ	=	Flame spread parameter
ε	=	Emissivity

Table of contents

1 Introduction

This report presents experimental and theoretical results from a study within the project "Fire Hazard - Fire Growth in Compartments in the Early Stage of Development (Preflashover)". The project is carried out jointly by the department of Fire Safety Engineering at Lund University and the Division of Fire Technology at the Swedish National Testing Institute. An outline of the research program is given by Pettersson [1].

Room fire growth on combustible linings has been a problem of concern to the legislators and authorities since the advent of building fire safety regulations. Work in this area has included development of bench-scale tests to derive basic flammability characteristics which could rationally be used as classification criteria. Also, full-scale standard tests have been developed to evaluate the fire performance of materials of products under actual in-use situations. The contribution of a specimen to the fire growth within a previously calibrated compartment can then be used to rate materials and to evaluate the validity of existing bench-scale test methods.

The purpose of the work presented here is to use results from bench-scale flammability tests as input to a mathematical model which could rationally predict full scale fire growth on combustible linings. Only two scenarios are considered here; scenario A, where the lining materials are mounted on compartment walls and ceiling; and, scenario B where the material is mounted on walls only.

Two room sizes were considered; the full scale test room with a single door opening in accordance with methods proposed by ASTM, ISO and NORDTEST; and, a 1/3 scale model of the full scale compartment.

The study reported here is of pilot character and should be seen as a first, preliminary attempt to arrive at a rational engineering solution of a recognized and important fire safety problem.

2 Bench-scale tests

2.1 Surface spread of flame test

The 13 materials listed in Table I were tested in the IMO and ISO surface spread of flame tests. The velocity of the flame front, V_f, and the corresponding external heat flux, q''_e, were measured at several positions along the sample. The sample surface temperature was also measured at some of these positions during the test. A detailed description of the test apparatus, procedure and results is given in [2].

2.1.1 Determination of the minimum radiant heat flux to sustain piloted ignition.

Harkleroad, Quintiere and Walton [3] determined $q''_{0,ig}$ from the surface spread of flame test. The method of plotting $1/\sqrt{V_f}$ versus q''_e F(t) was introduced, where the intercept on the latter axes gave $q''_{0,ig}$. An expression for the minimum radiant heat flux to sustained piloted ignition was given as

$$q''_{0,ig} = h\ (T_{ig} - T_i) \qquad (1)$$

The values of $q''_{0,ig}$ used in this work were reported in Ref. 2. Andersson [4] used data from Ref. 2 and the method of plotting $1/\sqrt{V_f}$ versus q''_e F(t) to obtain the flame spread parameter C. Figure 1 shows, as an example, the plot for material no.3 from in Table I. The slope of the line resulting from the plot of $1/\sqrt{V_f}$ versus q''_e F(t) gives this parameter. The values of C reported in Ref. 4 and the values obtained in Ref. 3 were compared and there seemed to be no large differences in the data except for material no. 12, wood panel, spruce. Data are reproduced in Appendix A.

2.1.2 Determination of ignition temperature

The ignition temperature, T_{ig}, is an important material parameter when studying opposed flow flame spread over a solid. This temperature can be calculated from equation (1) but to do this the parameters $q''_{0,ig}$, h and T_i need to be determined.

The values of $q''_{0,ig}$ used here were those derived by Sundström [2]. Ref. 3 gives an expression for the heat transfer coefficient, h:

$$h = 0.01\ (1 + 0.0085\ (T_s - T_i)) \qquad (2)$$

The initial temperature, T_i, was fixed at 20° C for all materials. By assuming a value for T_{ig} and substituting it for T_s when calculating h, T_{ig} could be calculated by an iterative process. The values of T_{ig} obtained in Ref. 3 were compared with similar materials from Ref. 4, the agreement was relatively good. Data are reproduced in Appendix A.

2.1.3 Determination of the flame spread parameter, ϕ

The following well known expression has been given ([5], [6], etc) for the velocity of the flame front for a slab initially at the temperature $T = T_s$

$$V_f = \phi/(T_{ig} - T_s)^2 \qquad (3)$$

where ϕ depends on the thermal properties of the solid, the ambient oxygen concentration, flow speed and the heat flux ahead of the advancing flame. V_f is determined from the surface spread of flame test as

$$V_f = dx_f/dt \qquad (4)$$

The flame spread parameter ϕ can be determined from the experimentally-determined parameter C

$$\phi = V_f/(T_{ig} - T_s)^2 = 1/(Ch)^2 \qquad (5)$$

The heat transfer coefficient, h, and the flame spread constant, C, were determined as discussed above. Andersson [4] compared the resulting values of the flame spread parameter, ϕ, to those reported in Ref. 3 and found the agreement satisfactory. Data are reproduced in Appendix A. The values of ϕ used in this work are listed in Table I.

2.2 Ignitability test

The test - ISO TC92 TR5657, Fire Tests, Reaction to Fire, Ignitability of Building Products - is described in [28]. The main quantitative information from the test is a set of values of t_{ig} for a set of exposure radiation levels q''_e. Data can also be extrapolated to give the minimum level of impressed flux to cause ignition, $q''_{0,ig}$.

The time to ignition is closely related to the thermal inertia, $k\rho c$, of the tested material. With additional thermocouples attached to both sides of the sample the test can be used to derive parameters such as thermal conductivity, k, and thermal capacity, ρc, of the tested specimen. The values of thermal inertia used in this study were derived in this way and are listed in Table I. A full description of the method used to derive these parameters is given in Ref. 11.

2.3 Rate of Heat Release measurements

The 13 materials were tested in three different RHR apparatuses: the Ohio State University apparatus [7], an open configuration [8] based on a design originally developed by the National Institute of Standards and Technology (formerly National

Bureau of Standards)[9], and the cone calorimeter [10]. The measurements referred to here were reported in Ref. 8.

The equipment consists of a vertical sampleholder and an electrical radiation panel placed under an open hood. The samples were tested at 5, 3 and 2 W/cm^2 and some easily ignitable materials also at 1 W/cm^2. An example of the test output is given in Fig. 2 for material 3.

An attempt to calculate the mass loss and RHR analytically was not successful, as described in [11]. Therefore it was decided to describe and make use of the RHR characteristics of the involved material directly, using a mathematical approximation of the curves shown in Fig. 2, primarily the curves valid for external flux equal to 3 W/cm^2. In the full scale experiments, heat fluxes to the lining material will vary considerably with time and location. A study of available literature indicated that an average value of 3 W/cm^2 might be more representative than 5 W/cm^2, but this has not been substantiated.

The experimental curves were idealized as seen in Fig. 3, resulting in the expression

$$Q''(t) = Q''_{max}\, e^{-\lambda(t - t_p)} \qquad (6)$$

Equation (6) assumes semi - infinite sample (no returning heatwave) and may have to be changed. The Q_{max} values were taken directly from measurements and are given together with the corresponding regression values of λ in Table I. Equation (6) seemed phenomenologically correct except for materials 9 and 10. Full results are given in Ref. 11.

3 Corner test experiments carried out in Sweden

3.1 Full scale tests carried out at the Swedish National Testing Institute, Borås, Sweden

The full scale tests, scenario A, were carried out according to the standard test method NT FIRE 025 [12]. The fire test room is 3.6 m long, 2.4 m wide and 2.4 m high with a doorway measuring 0.8 m wide and 2.0 m high. The walls are of lightweight concrete, 150 mm thick. The ignition source was a propane gas burner situated on the floor, in a corner of the room, with an effect of 100 kw. If this effect did not cause flashover in 10 minutes the effect was raised to 300 kw for another 10 minutes. The 13 different lining materials tested are listed in Table I. All tests were terminated after flashover, defined as flames emerging out of the doorway.

A detailed description of this test series is given by Sundström [13].

For scenario B, the same room, ignition source and procedure were used as described above for scenario A, except that no lining material was mounted on the ceiling. Only 3 materials were tested, namely materials no. 2, 3 and 8 in Table I.

Ondrus [14] described the test series summarily.

3.2 1/3 scale experiments carried out at the Department of Fire Safety Engineering, Lund University

The experiments were carried out in a room with a length of 1.2 m, width of 0.8m and height of 0.8 m. A description of the test procedure and results is given by Andersson [15]. The room is a 1/3 scale model of the full scale compartment at the National Testing Institute in Borås. Scaling criteria was to achieve the same upper layer gas temperature in full- and 1/3 scale. The ignition source was a gas burner with an effect of 11 kw for 10 minutes and, if no flashover occurred, 33 kw for another 10 minutes.

For scenario A, where lining material was mounted on both ceiling and walls, the doorway measured 0.56 m wide and 0.67 m high.

In scenario B, where the lining material was mounted on walls only, the door opening measured 0.46 m wide and 0.67 m high.

3.3 Results from 1/3 scale and full scale tests

The four experimental series discussed above were carried out over the period of four years and therefore not very coherent. In some series heat flux was measured at floor level only, in others at different heights at the lining material surface as well as at the floor level. Similarly, gastemperatures and surface temperatures were measured at different heights resulting in difficulties when comparing results between series.

4 Calculation of RHR in room fire experiments

4.1 RHR in scenario A

Magnusson [11] developed a model allowing the RHR in scenario A to be calculated. The method presented in this chapter is based on that work. Scenario A, as mentioned above, refers to the case where lining materials are on three walls and ceiling. Soon after the gas burner is started in the corner test, the wall material behind it ignites. The time for this to happen must be evaluated as well as the RHR from the burning wall and ceiling lining material.

4.1.1 Time to ignition

A quantity Q_{start} is defined as the sum of the heat release from the ignition source and the vertical wall area behind the burner, assuming complete combustion. The corresponding time t_{start} denotes the time necessary for the whole of the the lining material behind the burner to be pyrolysing. t_{start} is taken directly from the experimental time - RHR curves and thus includes time delay components such as transportation time in the measurement system.

Comparison of t_{start} values with results from the ISO ignitability test can be done in various ways. It was found that the simple procedure of correlating ignition time at the 30 kw/m^2 impressed radiation level with t_{start} seemed to work best. For the full scale series

$$t_{start} = t_{ign} + 5$$

and for the 1/3 scale series

$$t_{start} = t_{ign} *1.85$$

gives a reasonable approximation of t_{start}. The different dependencies of t_{start} on t_{ign} reflects the difference in thermal load from the 100 kw and 11 kw gas burner flame respectively. Observe that the strength of the ignition source means that the total height of the corner is covered by flame from the start of the experiment.

4.1.2 Calculation of RHR

The model is based on the concepts presented in [16], [17] and [18] from which A_p may be considered as a driving force in a process where the rate of increase of A_p is proportional to the quantity A_p itself; i.e. A_p is exponentially increasing with time. In the regression model of ceiling flame spread and combustion presented in [11], which includes the horizontal wall flame propagation along the intersection ceiling - wall, pyrolysis area A_p was written as

$$A_p(t) = \alpha(e^{at} - 1)^\beta \tag{7}$$

where $a = h^2/k\rho c$ and α and β were coefficients to be determined statistically. The rate of heat release could then be expressed as

$$Q(t) = A_p(t) * Q''_{av} \tag{8}$$

where Q''_{av} denotes a suitable time and space averaged measure of material rate of heat release per unit area. It was shown in chapter 2.4 that $Q''(t)$ for a certain constant impressed heat flux could be written as

$$Q''(t) = Q''_{max}\, e^{-\lambda(t - t_p)} \tag{9}$$

Combining equations 7 to 9 and describing the interaction of flame spread and rate of heat release by a superposition, Duhamel-type integral [19], a final, non-dimensional form of the regression equation was given in Ref. 11 as

$$\frac{\dot{Q}_{rt} - \dot{Q}_{start}}{\dot{Q}_{cf}} = \alpha\left(e^{at} - e^{-\lambda t}\right)^\beta \dot{Q}''_{max}\left(\frac{a}{a + \lambda}\right) \tag{10}$$

where Q_{start} is as defined earlier, Q_{rt} denoting measured RHR (rt meaning room test) and Q_{cf} the non-combusted part of wall corner flame reaching the ceiling (= Q_{start} minus combustion in the vertical part of the corner flame). The time t is measured from t = t_{start}. For the relatively short, initial period $0 < t < t_{start}$ the rate of heat release is assumed to grow linearly up to Q_{start}.

The overall average values and coefficients of variations for the parameters in model eqn (10) were given as:

$\alpha'_{aver} = -4.58$ (=ln α) $\qquad \sigma_\alpha/\alpha'_{aver} = 0.13$

$\beta_{aver} = 1.15 \qquad \sigma_\beta/\beta_{aver} = 0.276$

It remains to be studied how well time-RHR curves from the experiments can be recalculated using average values of α and β. Fig. 4 a) shows the results of using the regression equation on material 3 in Table I for the full scale test. Fig. 4 b) shows the same for the 1/3 scale test. The regression equation has been used for 6 materials in both full scale and 1/3 scale tests, showing similar results. The complete set of curves are shown in Appendicies B and C (B1-B3 and C1-C3 respectively). Observe that the downward flamespread is not included in equation (10). Further comments on this point are found in Chapter 8.

4.2 RHR in scenario B

The procedure for calculating rate of heat release in scenario B builds on the same principles as the one described above. In this scenario there is, however, no material on the ceiling.

The total rate of heat release in the room is assumed to come from five sources; the gas burner, the vertical wall area behind the burner, a horizontal strip of material corresponding to the vertical height og the ceiling jet at the ceiling-wall intersection, the wall material in the upper layer and, when downward flame spread has started, from the wall linings below the hot gas layer.

The scenario we are considering is the following one: The walls of the test room are lined with the material. The ignition source in the corner ignites the wall corner material and spreads upward on an area, A_w, approximately equal to the width of the burner times the distance from the burner to the ceiling. In this initial period, $0 < t < t_{start}$, the rate of heat release is calculated in the same way as above, i.e. assumed to grow linearly up to Q_{start} at time t_{start}.

The resulting ceiling jet, or flame, spreads along the intersections between the walls and the ceiling in the mode of concurrent flame propagation. After a time t_h the pyrolysing area has propagated to the nearest corner in the room and a strip of material at the top of the walls is pyroysing. In the experiments discussed here this strip has a height of around 5% of the room height. We assume we can calculate how long it will take for the pyrolysing area to reach the nearest corner. In the period $t_{start} < t < t_h$ there are thus three sources that contribute to the total heat release; the gas burner, the diminishing effect of the pyrolysing area behind the gas burner and the increasing pyrolysis area of the horizontal strip at the wall-ceiling intersection.

It remains to give expressions for t_h, the time at which the horizontal pyrolysing area reaches the an opposite corner. Saito, Quintiere and Williams [20] have given the upward spread velocity of the pyrolysis front as

$$V_p = 4\,(q''_0)^2\,(x_f - x_p)/[\pi k \rho c (T_p - T_a)^2] \qquad (11)$$

which has been employed in some recent studies by several workers ([21], [22] and others). The flame height x_f has been shown to only depend on the energy release rate per unit wall width ([21], [22], [23] and [24]) and several expressions for x_f have been given.

Efforts are being made to apply the above method to the horizontal concurrent flame spread. Some problems have been encountered in estimating the horizontal flame length x_f since earlier reported flame height correlations may not be valid in the horizontal ceiling-wall intersection configuration. Results from this part of the study will be reported later.

The problem of estimating t_h, the flame spread along intersection wall - ceiling and the resulting rate of heat release was therefore solved rather crudely as a first effort and is considered to be a temporary solution. Magnusson [25] suggested a simple expression for the calculation of A_{ph}, the horizontal pyrolysing area, assumed to increase linearly with time

$$A_{ph}(t) = k * t * (Q_{start} - Q_{gb})/k\rho c \qquad (12)$$

The factor k was derived from experiments to be ≈ 0.004 w/(m K)^2. For each Δt the pyrolysis area increases by ΔA_{ph}. As mentioned above, equation (12) will eventually be changed, using for example the methodology described in [24] instead.

Following a similar procedure as for scenario A, the expression for the rate of heat release for the time period $t_{start} < t < t_h$ is then written at time step j (counted from t_{start}) as

$$Q(t) = Q_{gb} + A_w * Q''_{max} * e^{(-\lambda*\Delta t*j)} + \Sigma[\Delta A_{ph} * Q''_{max} * e^{(-\lambda*\Delta t*i)}] \qquad (13)$$

where Q_{gb} stand for the effect from the gas burner, Q''_{max} is the maximum energy release rate per fuel area from the bench-scale test and A_w is the area of wall material behind the burner.

The first term is the effect from the gas burner, the second the contribution from the wall behind the burner and the third from the part of the horizontal strip which is pyrolysing.

For the period $t > t_h$ the downward flame spread contributes to the increasing rate of heat release. To equation (13) is then added the contribution of the downward flame spread in the upper layer and, once the flames reach the intersection of the hot gas layer and the lower ambient layer, the downward flame spread below the hot layer.

Fig. 4 c) shows the results of using this procedure on material 3 in Table I for the full scale test. Fig. 4 d) shows the same for the 1/3 scale test. Appendix E shows results for other materials in the 1/3 scale test series, scenario B.

The following sections describe how the gastemperatures, surface temperatures in the hot layer and below the hot layer and the downward flame spread are calculated, thus adding to the rate of heat release.

5 Calculation of gastemperatures

The basic principle used to calculate the temperature in a compartment fire is the conservation of mass and energy. Since the energy release rate and the compartment temperature change with time, the application of the conservation laws will lead to a series of differential equations.

By making certain assumptions on the energy and mass transfer in and out of the compartment boundaries, the laws of mass and energy conservation can result in a relatively complete set of equations. Due to the complexity and the large number of equations involved, a complete solution of the set of equations would usually only be obtained from computer programs.

However, now there exist regression formulae which, with a number of limiting assumptions, allow the gastemperature in a naturally or mechanically ventilated compartment to be calculated by hand.

McCaffrey, Quintiere and Harkleroad [26] used a simple conservation of energy expression and a correlation of a relatively wide range of data to develop a hand-calculation formula for the hot layer temperature in a naturally ventilated compartment.

The upper layer temperature was written as a function of two dimensionless groups

$$\frac{\Delta T}{T_0} = C \cdot X_1^N \cdot X_2^M \qquad (14)$$

The constants C, N and M were determined from a wide range experimental data, the final form of the regression equation in [26] was given as

$$\frac{\Delta T}{T_0} = 1.63 \left(\frac{\dot{Q}}{\sqrt{g}\, c_p\, \rho_o\, T_o\, A_o \sqrt{H_o}} \right)^{2/3} \left(\frac{h_k\, A_w}{\sqrt{g}\, c_p\, \rho_o\, A_o \sqrt{H_o}} \right)^{-1/3} \qquad (15)$$

The heat transfer coefficient, h_k, depends on the duration of the fire and the thermal characteristics of the compartment boundaries. The thickness of the lining materials treated here and the short duration of the corner test is such that the outer boundaries of the test compartment do not have an effect on the heat transfer coefficient. It can therefore be written as:

$$h_k = \sqrt{k\rho c/t} \qquad (16)$$

5.1 Calculation of gastemperatures in the current paper

The energy released within the compartment in flame and upper layer combustion is restricted by the availability of oxygen. The heat release measured in the experiments includes the energy released in the flames coming out through the opening. This part of the heat release does not influence the gastemperature within the compartment. The availability of oxygen in the upper layer can be approximated by using a simple flame formula [27], calculating the entrainment of air into the corner flame

$$m'_{air} = 2/3\ \alpha\ \rho_a \sqrt{2g\ (1 - T_a/T_{fl})}\ X_f^{3/2} \qquad (17)$$

where X_f is the effective entrainment flame height, α is the entrainment coefficient and T_{fl} is the flame temperature. Thus, the maximum rate of heat release inside the compartment was found to be approximately 600 kw for the full scale room and 40 kw for the 1/3 scale room.

The method developed in [26] was followed to calculate the upper layer gastemperatures in the corner test experiments. An attempt was made to determine the constants C, N and M by regression analysis but results were not satisfactory. The two constants, N and M, as they appear in equation {4} did however seem to describe the slope and shape of the experimental curves well. The constant C was then determined for each of the experimental series with the following results:

Full scale, scenario A	C_{aver} = 2.048
1/3 scale, scenario A	C_{aver} = 2.237
Full scale, scenario B	C_{aver} = 2.700
1/3 scale, scenario B	C_{aver} = 2.240

The experimental gastemperature was measured by thermocouples 5 cm from the ceiling in both 1/3 scale tests series and 30 cm from the ceiling in full scale test, scenario A. But in the full scale B test series the gastemperature was measured only 10 cm from the ceiling, resulting in relatively much higher gastemperature values than in the other test series. This accounts for the much higher C_{aver} in the last mentioned test series.

The procedure of limiting the RHR by the air entrainment into the corner flame and finding a pre-exponential factor for each test series proved to be very robust and showed good agreement with experimental results. Fig. 5 a), b), c) and d) show results of using the above procedure on material 3 in Table I for both scenarios and both compartment sizes. This has also been done for most of the materials in Table I, showing similar results. The results are partly shown in Appendicies B, C, D and E.

6. Heat transfer to walls

When the fire in the corner starts and the lining material in the corner ignites, combustion products and plume entrained air are transferred to the ceiling. The hot gas layer forms, descends and increases in temperature with time. Relatively early in the test the layer reaches the top of the opening, stabilizes and hot gases start flowing out through the opening.

Classical heat transfer provides expressions for quantities such as view factors, radiation and temperature fields in semi-infinite bodies. The lining materials studied here were treated as semi-infinite bodies since the test duration is relatively short.

One long side of the compartment wall was split into a large number of thin, horizontal strips and the instantaneous heat flux from the gas layer to the center of each strip calculated using the expression

$$q'' = \varepsilon F \sigma (T_g^4 - T_0^4) \qquad (18)$$

The emission coefficient was taken to be a constant value close to unity. The configuration factor, F, was calculated in a conventional way, treating the center of each strip as a point. Once the downward flame spread started the radiation from the wall flames and the pyrolysing lining material behind the flames was added to the smoke layer radiation. The instantaneous heat flux to the walls was then calculated from the expression

$$q'' = \varepsilon_g F_g \sigma (T_g^4 - T_0^4) + \varepsilon_f F_f \sigma (T_f^4 - T_0^4) + \varepsilon_p F_p \sigma (T_p^4 - T_0^4) \qquad (19)$$

where the subscript g refers to the gaslayer, f to the flame and p to the pyrolysing wall material. The view factors from the flame and the pyrolysing wall material were assumed to be identical and equal to the total burning area of lining material. The flame temperature was taken to be ≈ 1100° K and the pyrolysing material surface temperature was assumed to be ≈ 750° K. Further, the flame emission coefficient was taken to be = 0.5 as was the surface of the pyrolysing material. A sensitivity analysis is necessary.

7 Wall surface temperatures

As explained above, one long side of the compartment wall was split into a large number of thin strips and the heat flux to the center of each strip calculated. Solving the general one-dimensional heat conduction equation by means of Laplace transformations the wall surface temperature at time t can be calculated from

$$T_s - T_0 = (q''/h) * (1 - e^{h^2 t/k\rho c} * \mathrm{erfc}(\sqrt{h^2 t/k\rho c})) \qquad (20)$$

This assumes a semi-infinite wall and a constant heat flux q".

Knowing the heat flux as a function of time, the wall surface temperature at timestep n can be calculated using the superposition principle. Equation (20) then becomes

$$T_s(n) - T_0 = \sum_{i=1}^{n} \frac{\dot{q}''(i) - \dot{q}''(i-1)}{h} \exp\left(h^2 (n-i)dt \Big/ k\rho c\right) \mathrm{erfc}\left(h \sqrt{(n-i)dt \Big/ k\rho c}\right) \qquad (21)$$

where dt is the size of the timestep.

The surface temperature can thus be calculated as a function of time and height from the floor. Here, the Newtonian cooling coefficient, h, was assumed to be a constant value equal to 30 w/m^2, throughout the test. An explicit form of the superposition integrals can be found in [29].

Similarly, the surface temperature of the wall material emerged in the hot layer can be calculated from the expression

$$T_s(n) - T_0 = \sum_{i=1}^{n} T_g(i) - T_g(i-1) \exp\left(h^2 (n-i)dt \Big/ k\rho c\right) \mathrm{erfc}\left(h \sqrt{(n-i)dt \Big/ k\rho c}\right) \qquad (22)$$

using the superposition principle and assuming a constant heat transfer coefficient. Putting the Newtonian cooling coefficient in (21) and the heat transfer coefficient in (22) equal to a constant value is of course an oversimplification and is seen only as a temporary measure.

No wall surface temperatures were measured in the full scale test series, scenario A and in the 1/3 scale test series, scenario B. Fig. 6 a) shows the experimental and calculated wall surface temperatures, at a height of 0.45 m from the floor, for material 3, 1/3 scale test, scenario A. Fig. 6 b) shows the same, but at a height of 1.2 m from the floor, for the full scale test, scenario B. Appendicies C and D show surface temperatures for other materials and at different heights from the floor.

8 Downward flame spread

The RHR in scenario A is calculated from a regression equation (10) where the only dependent variable is time. Calculation according to equation (10) stops before downward flamespread has become significant or dominant.

In scenario B, however, both the horizontal concurrent flame spread and the downward flame spread, in and below the hot gas layer, are directly linked to the rate of heat release.

8.1 Downward flame spread for scenario A

Relatively early in the test the hot gas layer reaches the top of the opening, stabilizes and hot gases flow out through the opening. We have assumed that at the beginning of the test the hot layer is already stabilized at the height of the opening, this has a relatively small influence on the radiation from the hot layer to the walls since the the layer is relatively cold to begin with.

No attempt is made to predict what happens within the hot smoke layer for scenario A. The smoke is quite thick in this scenario and it is difficult to visually see what happens there. When the smoke layer has been heating the wall surfaces for some time, occasional flames start appearing at the interface of the smoke layer and the walls. Shortly after, a thin, horizontal line of flames has been established on the lining material at this interface. The downward flame spread is quite slow to begin with but accelerates with time and can be calculated from a similar expression to equation (3)

$$V_f = \phi/(T_{ig} - T_{fl.f})^2 \qquad (23)$$

where T_{ig} and ϕ are obtained from the bench-scale tests discussed in Chapter 2 of the current paper. $T_{fl.f}$ is the material surface temperature just ahead of the flame front. If the position of the flame front is known, this surface temperature at a certain wall height and certain time, can be extrapolated from the surface temperatures calculated at the center of each wall strip at each time step. The downward flame spread can thus be calculated.

Since what happens in the gaslayer is not treated in scenario A, the wall flames are assumed to start at the intersection of the walls and the hot layer, i.e. 40 cm from the ceiling in the full scale tests and 13 cm from the ceiling in the 1/3 scale tests.

In the full scale test series, scenario A, the test was terminated at flashover so no data is available for the downward flame spread in this series. Fig. 6 c) shows the experimental and calculated downward flame spread for material 3, 1/3 scale test, scenario A. Appendix C shows results for other materials (C11 - C13).

8.2 Downward flame spread for scenario B

Once the horizontal, concurrent flame spread along the wall ceiling intersection has reached an opposite corner in the compartment the downward flame spread in the upper layer starts. In reality, this could possibly start happening during the concurrent flame spread time interval. In the current version of the model, no account is taken of the relatively low oxygen concentration in the upper layer. The flame spread is quite slow at first since the wall material has a relatively low surface temperature. It then accelerates until it reaches the interface of the smoke layer and walls.

At this point the flame spread slows down since the walls beneath the smoke layer have a lower surface temperature than the walls immersed in the hot layer. The downward spread then accelerates again. The flame spread is calculated from equation (23) as above.

Fig 6 d) shows the experimental and calculated downward flame spread for material 3, full scale test, scenario B.

No results of the downward flamespread in the 1/3 scale test, scenario B are shown, due to lack of accurate experimental data. Some indicational data was available from slides taken during the experiments. Comparing this with the calculated downward flamespread it can be stated that the methodology outlined above seems to work. However, it is clear that the various sub-processes in the methodology and the parameters included in these, such as A_{ph}, will have to be investigated in greater detail.

It should be noted that the calculated rate of heat release for this test series (see Appendix E) shows a good agreement with the experimental results for all four lining materials presented. This is taken as an indirect confirmation of the validity of the model for downward flamespread.

9 Remarks on the results

No sensitivity testing has so far been carried out with respect to the different assumptions and procedures just enumerated. Changes will certainly be introduced, especially regarding the horizontal concurrent flame spread which will follow the methods outlined in [21], [22] and [24]. The Newtonian cooling coefficient and the heat transfer coefficient in equations (21) and (22) will be calculated as functions of surface temperatures. Certain other areas in the procedure need to be looked at more closely, a sensitivity analyses with regards to emission coefficients and heat transfer coefficients, as well as other input parameters, will need to be carried out.

The ISO surface spread of flame test seems to correlate well with room test behavior when directly comparing times to ignition and rates of opposed flow flame spread. For the RHR-test the correlation is more implicit. A simple model incorporating data from this test and the ignitability test is capable of predicting the first phases of room fire growth in scenario A. The basic structure of the model for predicting fire growth in scenario B seems acceptable although it needs improving. This is valid for both full scale and the 1/3 scale test room.

References

[1] Pettersson, O., "Fire Hazards and the Compartment Fire Growth Process - Outline of a Swedish Joint Research Program", FoU-brand No 1, 1980.

[2] Sundström, B. "Results and Analysis of Building Materials Tested According to ISO and IMO Spread of Flame Tests", SP-RAPP 1984:36, Swedish National Testing Institute, Borås, 1984.

[3] Harkelroad, M., Quintiere, J., Walton, W., "Radiative Ignition and Opposed Flow Flame Spread Measurements on Materials", Report No. DOT/FAA-CT-83/28, FAA Technical Center, Atlantic City Airport, N.J., 1983

[4] Andersson, B., Internal Memorandum, Department of Fire Safety Engineering, Lund University, Lund 1988.

[5] DeRis, J.N., "Spread of Laminar Diffusion Flame", 12th Symposium (International) on Combustion, the Combustion Institute, Pittsburgh, PA, 1969.

[6] Quintiere, J. G., "An Approach to Modeling Wall Fire Spread in a Room", Fire Safety Journal Vol 3, 1981.

[7] Blomqvist, J., "RHR of Building Materials - Experiments with an OSU Apparatus Using Oxygen Consumption", Report LUTVDG/(TVBB-3017), Division of Building Fire Safety and Technology, Lund University, Lund, Sweden, 1983.

[8] Svensson, G., Östman, B., "Rate of Heat Release By Oxygen Consumption Testing of Building Materials", Meddelande Serie A Nr 812, Swedish Institute for Wood Research, Stockholm, 1983.

[9] Sensenig, D. L., "An Oxygen Consumption Method for Determining the Contribution of Interior Wall Finishes to Room Fires" NBS Technical Note 1128, National Bureau of Standards, Washington DC, 1980.

[10] Babrauskas, V., "Development of the Cone Calorimeter - A Bench-Scale Heat Release Apparatus Based on Oxygen Consumption" NBSIR 82-2611, National Bureau of Standards, Washington DC, 1982.

[11] Magnusson, S.E., Sundström, B., "Combustable Linings and Room Fire Growth - A First Analysis", Report LUTVDG/(TVBB 3030), Department of Fire Safety Engineering, Lund University, Lund 1985. Appears also in ASTM STP 882, Ed Harmathy

[12] "Room Fire Test in Full Scale for Surface Products", NORDTEST Fire Test Method. NT FIRE 025.

[13] Sundström, B., "Full Scale Fire Testing of Surface Materials", Technical Report SP-RAPP 1986:45, Swedish National Testing Institute, Borås 1986.

[14] Ondrus, J., Internal Memorandum, Department of Fire Safety Engineering, Lund University, Lund 1988.

[15] Andersson, B., "Model Scale Compartment Fire Tests With Wall Lining Materials", Report LUTVDG/(TVBB-3041), Department of Fire Safety Engineering, Lund University, Lund 1988.

[16] Orloff, L., DeRis, J., Markstein, G. M.,Upward Turbulent Fire Spread and Burning of Fuel Surfaces", 15th Symposium (International) of Combustion, 1975.

[17] Fernadez-Pello, A. C., Mao, C. P., Comb. Sci. Tech., Vol. 26, Gordon and Breach Science Publishers, London, England, 1981, pp 147 - 155.

[18] Parker, W. J., "An Assessment of Correlations Between Laboratory and Full-Scale Experiments for the FAA Aircraft Fire Safety Program, Part 3: ASTM E 84", NBSIR 82-2564, Center for Fire Research, Washington DC, August 1982.

[19] Wickström, U., Internal Working Memorandum, Swedish National Testing Institute, Borås, Sweden, 1983.

[20] Saito, K., Quintiere, J.G., Williams, F.A., "Upward Turbulent Flame Spread", Int. Assoc. for Fire Safety Science. Fire Safety Science Proceedings. 1st Int. Symposium. October 7-11 1985. Grant, C. E., and Pagni, P. J., Editors, Gaithersburg, MD, Hemisphere Publishing Corp., New York, 1985.

[21] Quintiere, J. G., Harkleroad, M., Hasemi, Y., Comb. Sci. Tech., 48, p. 191, 1986.

[22] Hasemi, Y., "Thermal Modeling of Upward Wall Flamespread", Int. Assoc. for Fire Safety Science. Fire Safety Science Proceedings. 1st Int. Symposium. October 7-11 1985. Grant, C. E., and Pagni, P. J., Editors, Gaithersburg, MD, Hemisphere Publishing Corp., New York, 1985.

[23] Delichatsios, M. A., "Flame Heights in Turbulent Wall Fires with Significant Flame Radiation", Comb. Sci. Tech., 39, p. 195, 1984.

[24] Kulkarni, A. K., Fisher, S., "A Model for Upward Flame Spread on Vertical Wall", National Bureau of Standards, Center for Fire Research, Gaithersburg, 1988.

[25] Magnusson, S. E., Personal communication, Dept. of Fire Safety Eng. Lund University, Lund, 1989.

[26] McCaffrey, B. J., Quintiere, J. Q., Harkleroad, M.F., "Estimating Room Temperatures and the Likelyhood of Flashover Using Fire Test Data Correlations". Fire Technology, Vol 17, pp 98-119; 1981.

[27] Quintiere, J. G., "An Assessment of Correlations Between Laboratory and Full-Scale Experiments for the FAA Aircraft Fire Safety Program, Part 2: Rate of Energy Release in Fire", NBSIR 82-2536, National Bureau of Standards, Washington DC, 1982.

[28] Östman, B., "Ignitability as Proposed by the International Standards Organisation Compared with Some European Fire Tests for Building Panels", Fire and Materials, Vol. 5, no. 4, 1981.

[29] Mitler, H.E., "The Physical Bases for the Harvard Computer Fire Code", Division of Applied Sciences, Harvard University, Home Fire Project Technical Report No. 34, Oct. 1978.

Table 1

Material no.	Material name	$\dot{Q}''_{max}$ kW/m²	λ s^{-1}	kρc * 10^{-3} $(w/m^2 K)^2$	φ $(m/s)K^2$
1	Insulating fiberboard	139.8	0.0070	41	63
2	Medium density fiberboard	162.4	0.0027	80	15
3	Particle board	199.8	0.0049	110	14
4	Gypsum plasterboard	27.7	0.0150	100	-
5	PVC cover on gypsum pl. board	107.5	0.0293	75	-
6	Paper cover on gypsum pl. board	105.3	0.0208	100	1
7	Textile cover on gypsum pl. board	222.0	0.0278	80	-
8	Textile cover on mineral wool	246.2	0.0382	4.3	34
9	Melamine-faced particle board	40.9	-0.0032	105	-
10	Expanded polystyren	-	-	-	-
11	Rigid polyurethane foam	130.6	0.0217	4.0	-
12	Wood panel, spruce	149.7	0.0086	85	-
13	Paper cover on particle board	164.1	0.0035	110	19

Surface Spread of Flame Test
Flamespread correlations

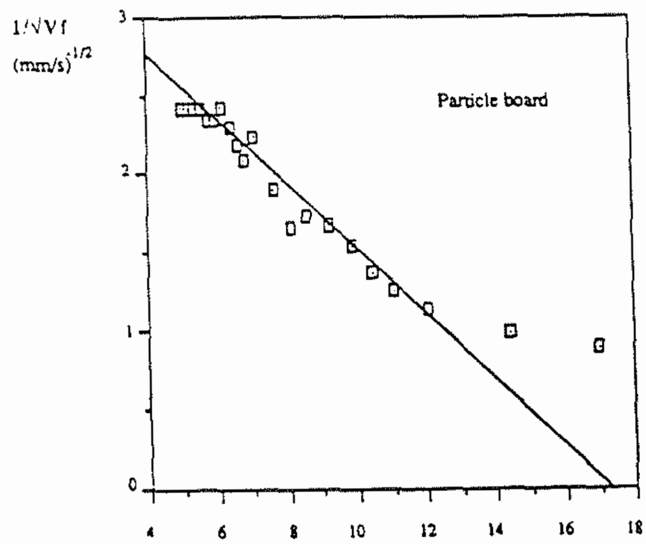

Fig. 1.

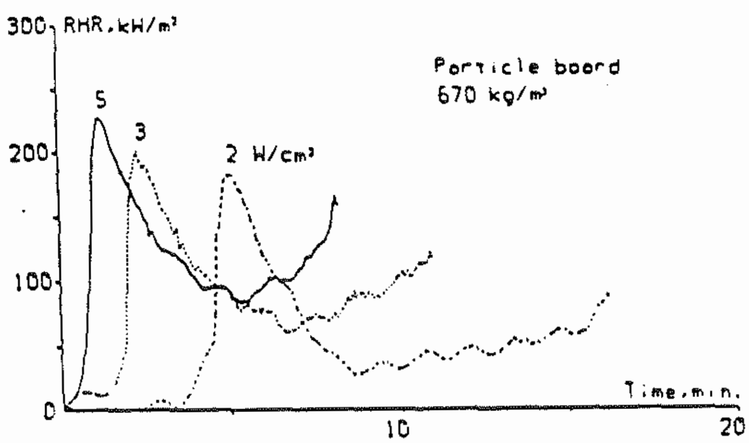

Fig. 2. Results from RHR bench-scale test

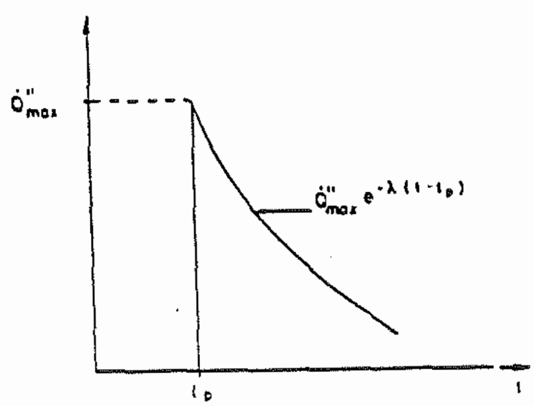

Fig. 3. Principle for analytical approximation of experimental RHR curves

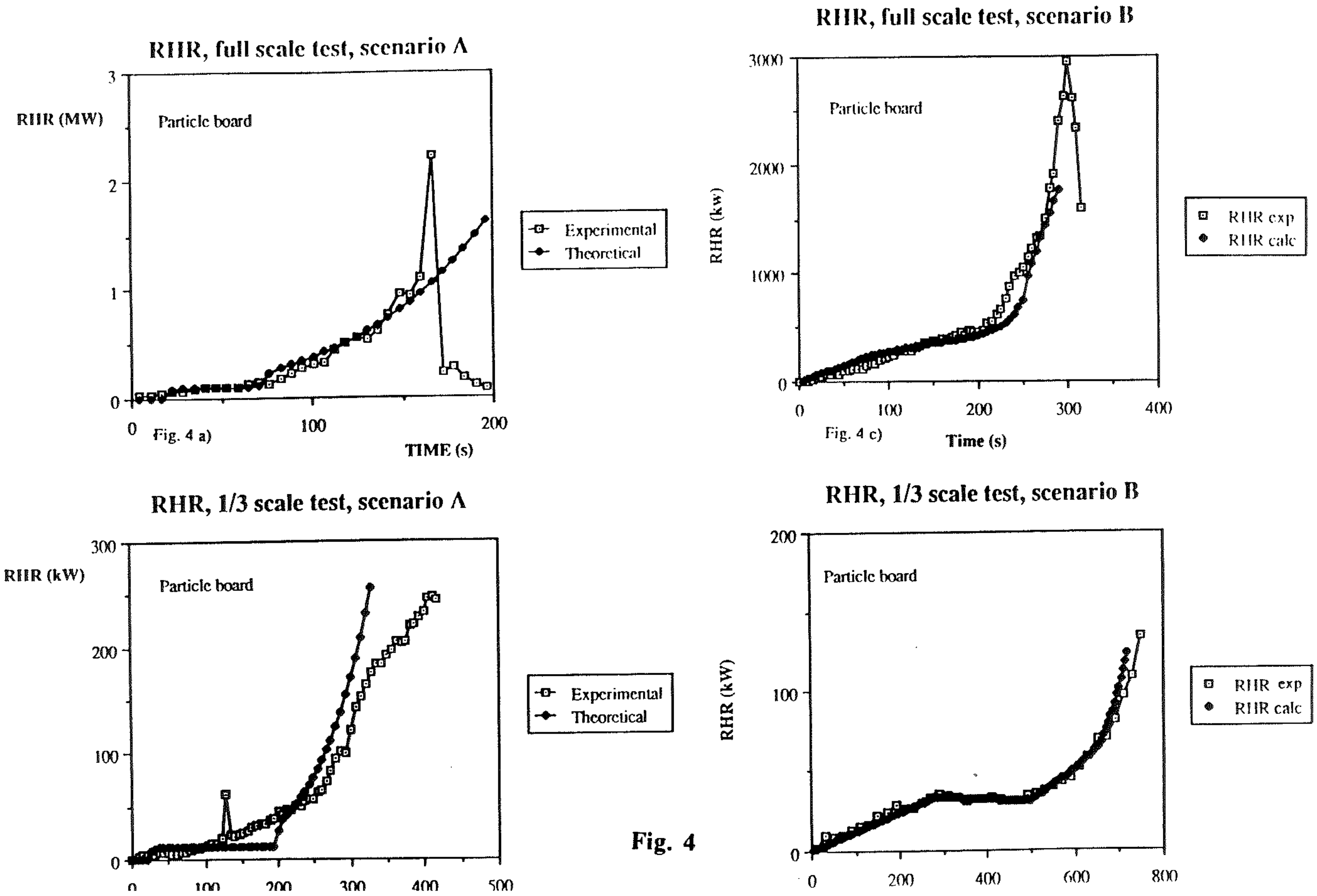

RHR, full scale test, scenario A
RHR (MW)
Particle board
Experimental
Theoretical
0
1
2
3
100
200
TIME (s)
Fig. 4 a)
RHR, full scale test, scenario B
RHR (kw)
Particle board
RHR exp
RHR calc
1000
2000
3000
300
400
Time (s)
Fig. 4 c)
RHR, 1/3 scale test, scenario A
RHR (kW)
Particle board
Experimental
Theoretical
500
RHR, 1/3 scale test, scenario B
RHR (kW)
Particle board
RHR exp
RHR calc
600
800

Fig. 4

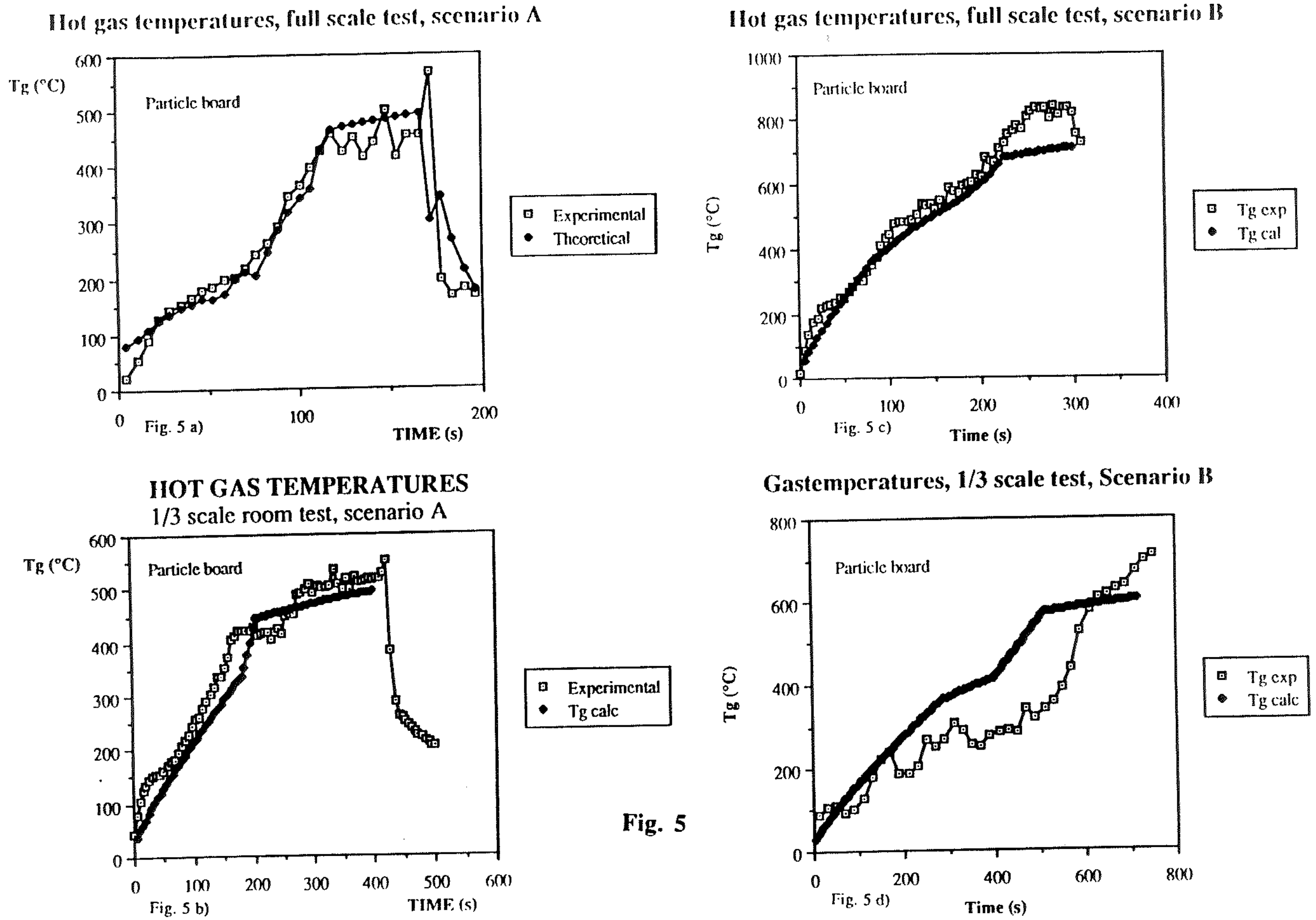
Hot gas temperatures, full scale test, scenario A
Tg (°C)
Particle board
Experimental
Theoretical
TIME (s)
Fig. 5 a)
Hot gas temperatures, full scale test, scenario B
Tg (°C)
Particle board
Tg exp
Tg cal
Time (s)
Fig. 5 c)
HOT GAS TEMPERATURES
1/3 scale room test, scenario A
Tg (°C)
Particle board
Experimental
Tg calc
TIME (s)
Fig. 5 b)
Gastemperatures, 1/3 scale test, Scenario B
Tg (°C)
Particle board
Tg exp
Tg calc
Time (s)
Fig. 5 d)

Fig. 5

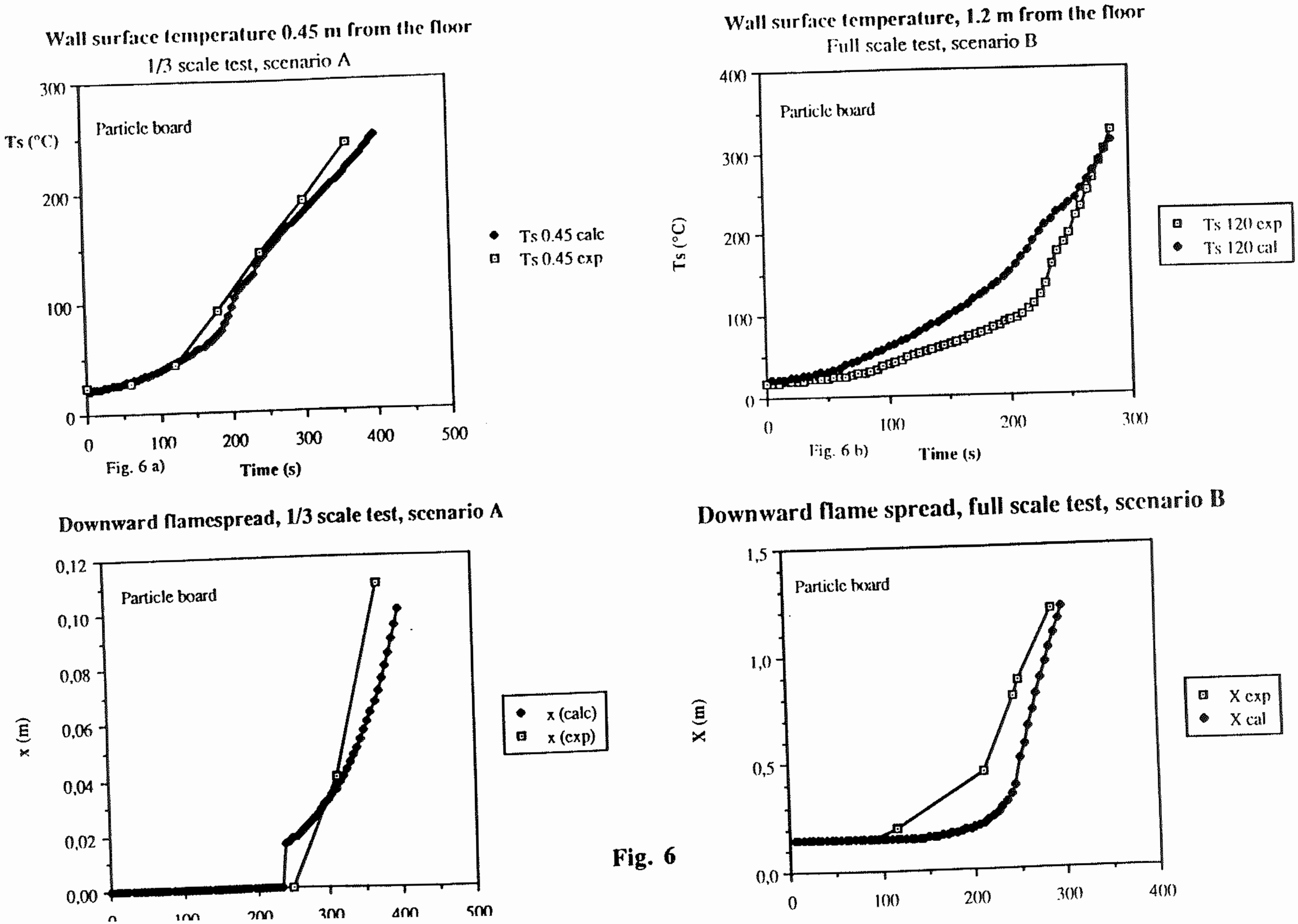
Wall surface temperature 0.45 m from the floor
1/3 scale test, scenario A
Ts (°C)
Particle board
Ts 0.45 calc
Ts 0.45 exp
Time (s)
Fig. 6 a)
Wall surface temperature, 1.2 m from the floor
Full scale test, scenario B
Ts (°C)
Particle board
Ts 120 exp
Ts 120 cal
Time (s)
Fig. 6 b)
Downward flamespread, 1/3 scale test, scenario A
x (m)
Particle board
x (calc)
x (exp)
Downward flame spread, full scale test, scenario B
X (m)
Particle board
X exp
X cal

Fig. 6

Appendix

Contents | Page

Appendix A

Bench - Scale Test Results

Contents | Page

Table A-1

Mat.no see Table 1	C (BA) [s cm / mm W]	C (JQ) [s cm / mm W]	$q''_{0,ig}$(BA) [kW/m]	$q''_{0,ig}$(JQ) [kW/m]	T_{ig} (BA) [°C]	T_{ig} (JQ) [°C]	Φ (BA) [K m/s]	Φ (JQ) [K m/s]
1	1,0	1,3	15,4	12,0	375	330	63,0	42,0
2	2,0	1,8	13,9	15,0	385	372	15,0	18,0
3	2,1	2,2	17,3	16,0	385	390	14,0	11,0
4	-	0,9	-	35,0	469	-	-	-
5	0,7	-	17,8	-	385	-	121,0	-
6	6,3	5,8	15,9	10,0	416	412	1,0	1,0
7	1,9	-	17,4	-	402	-	16,0	-
8	1,3	1,2	16,2	17,0	325	400	46,0	34,0
9	-	-	-	-	496	-	-	-
10	-	-		-	558	-	-	-
11	0.4 *	1,0	16,3	9,0	270	280	650 *	82,0
12	0.4 *	1,1	30,1	16,0	416	385	323 *	43,0
13	1,7	-	19,5	-	410	-	19,0	-

(BA) refers to results published in reference [4].
(JQ) refers to results published in reference [3].
* These values are erroneous

Surface Spread of Flame Test
Flamespread correlations

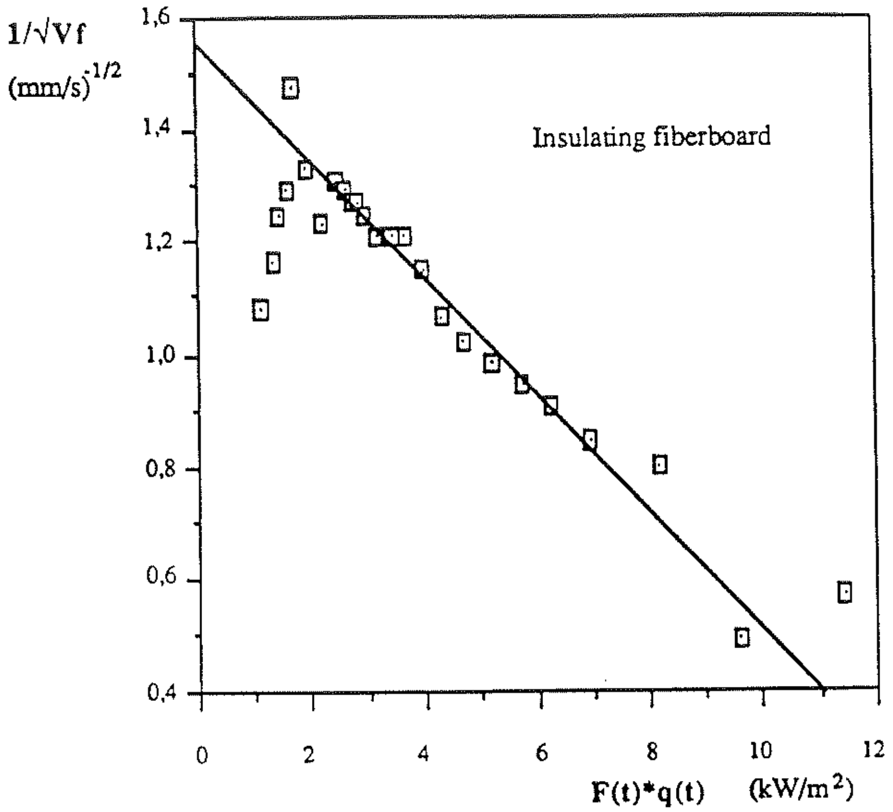

Surface Spread of Flame Test
Flamespread correlations

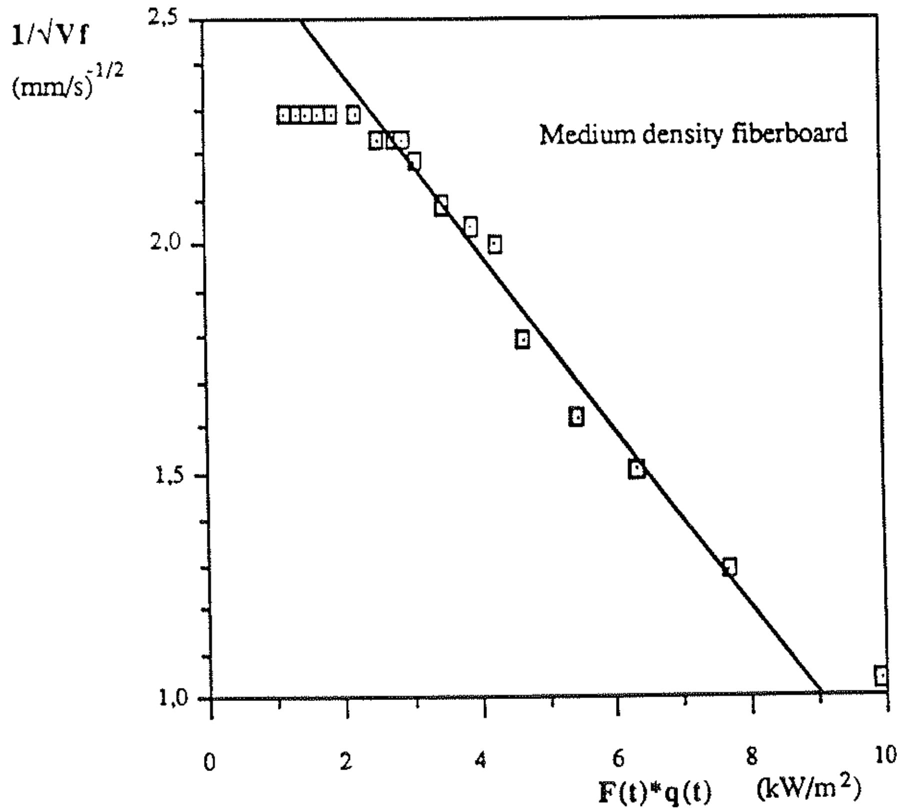

Surface Spread of Flame Test
Flamespread correlations

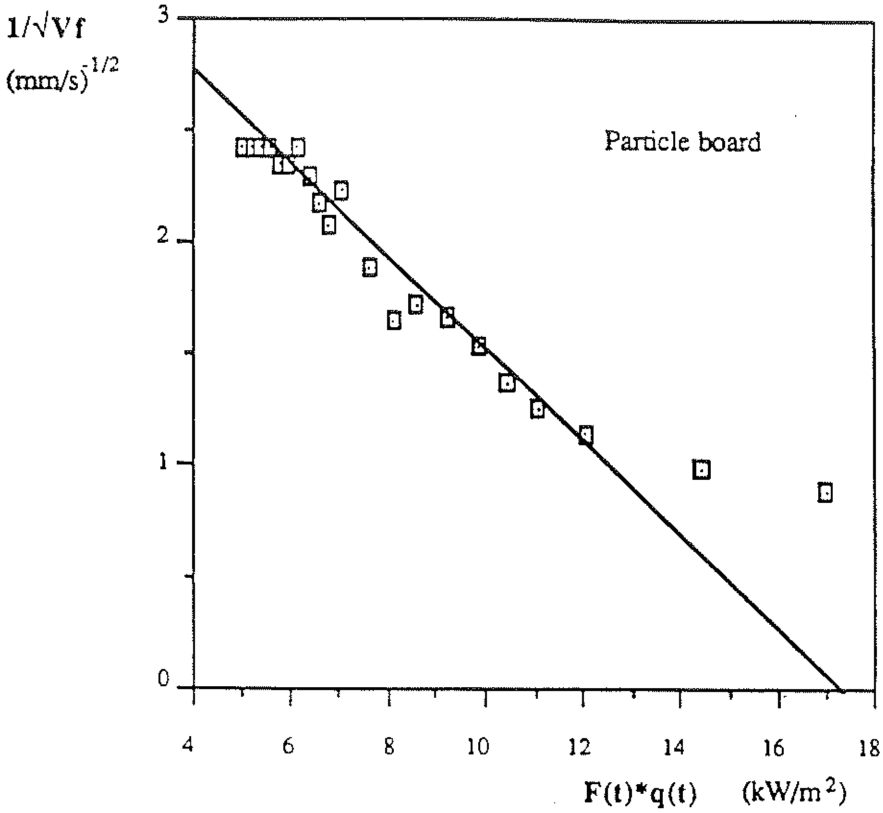

Surface Spread of Flame Test
Flamespread correlations

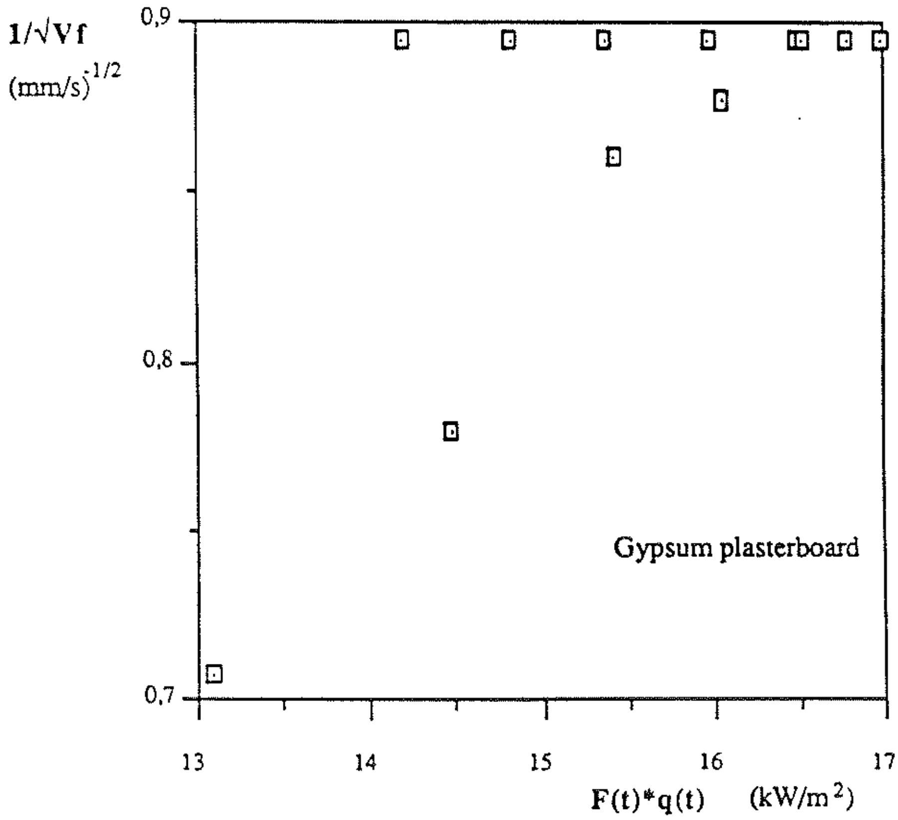

Surface Spread of Flame Test
Flamespread correlations

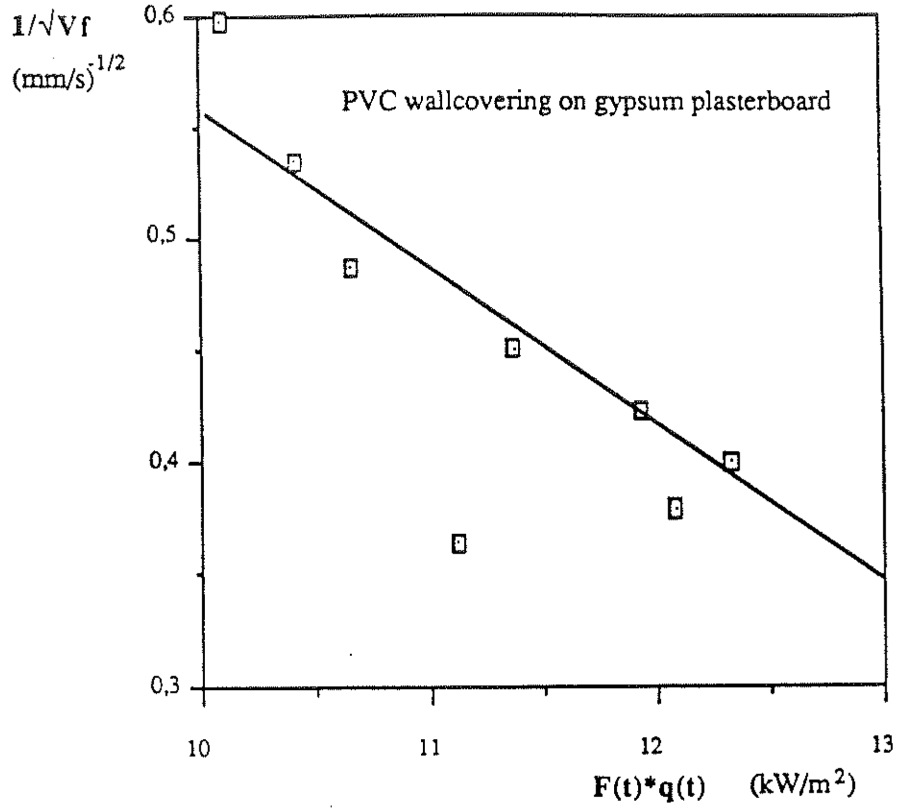

Surface Spread of Flame Test
Flamespread correlations

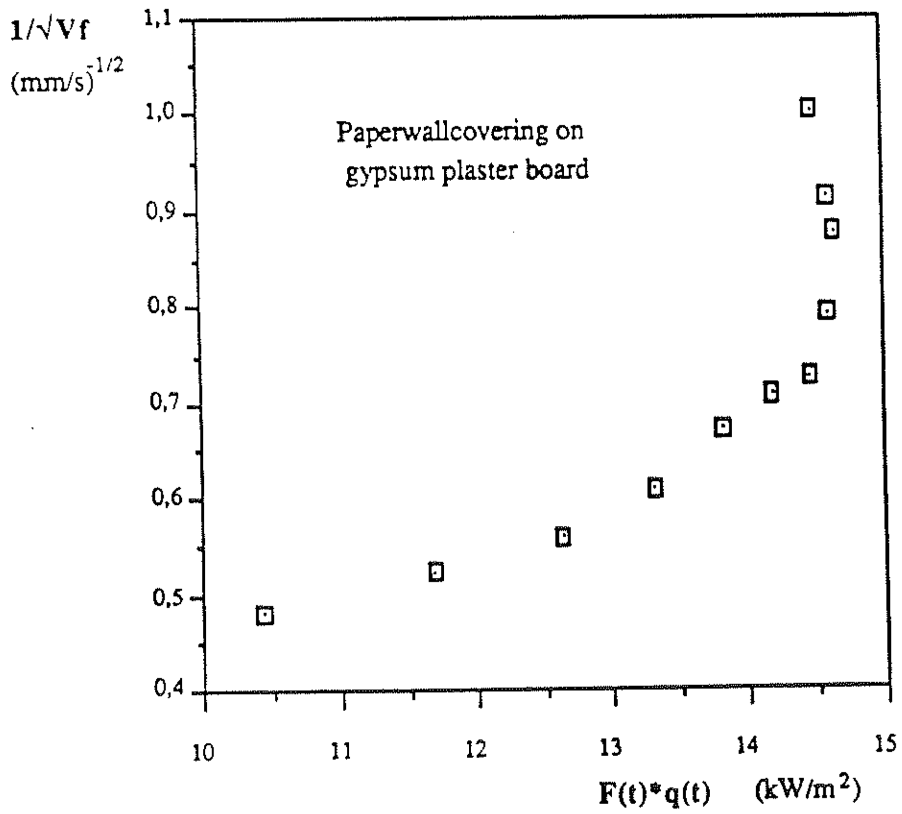

Surface Spread of Flame Test
Flamespread correlations

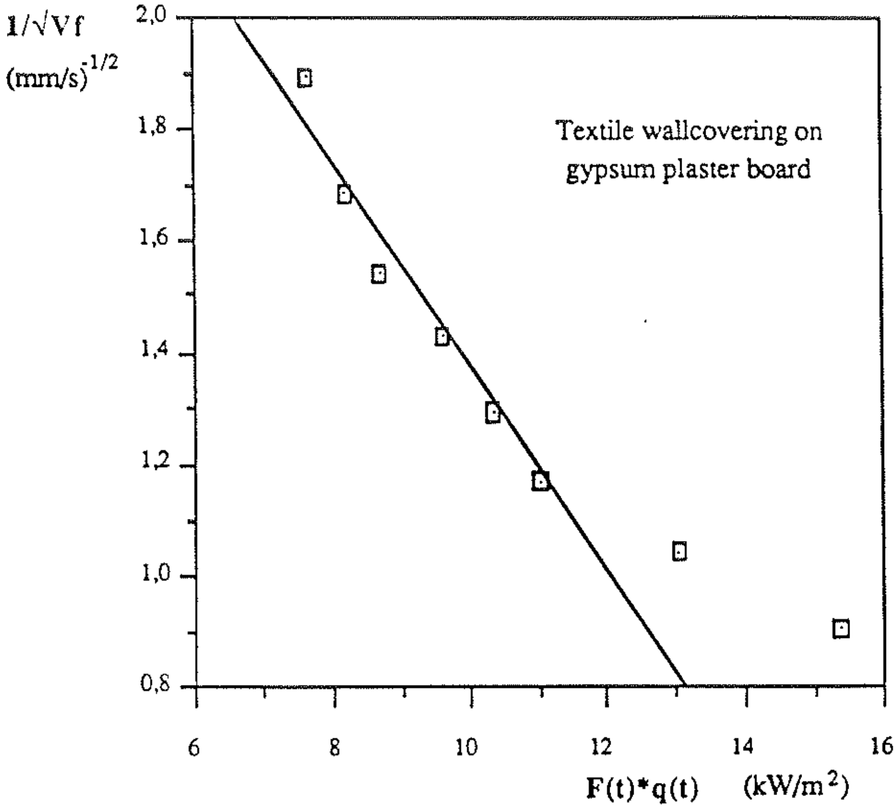

Surface Spread of Flame Test
Flamespread correlations

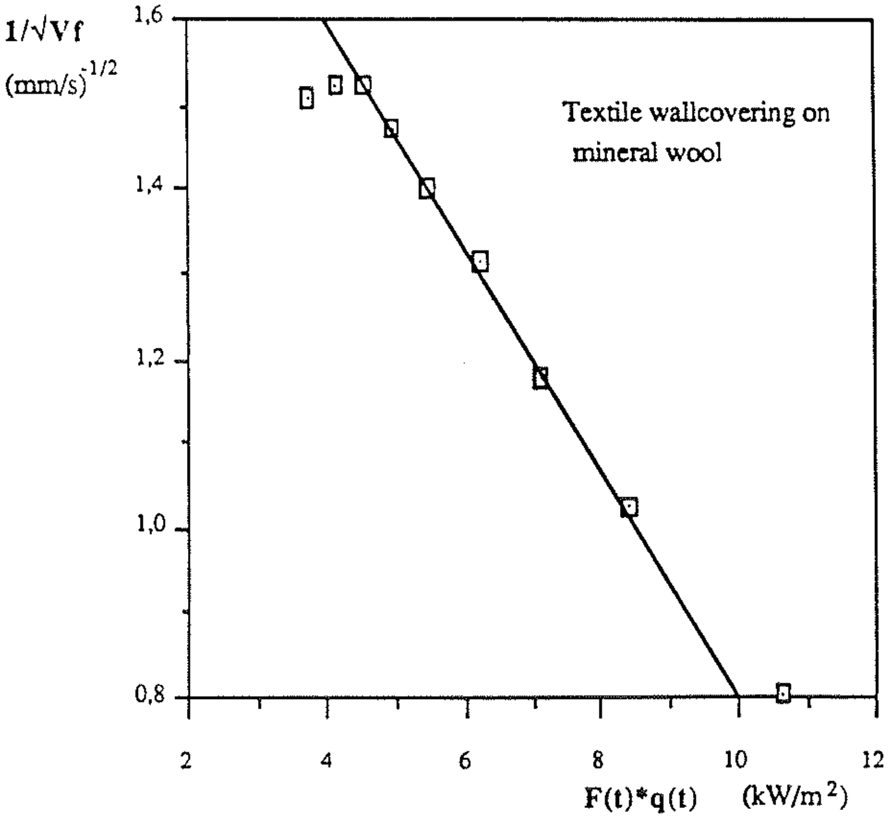

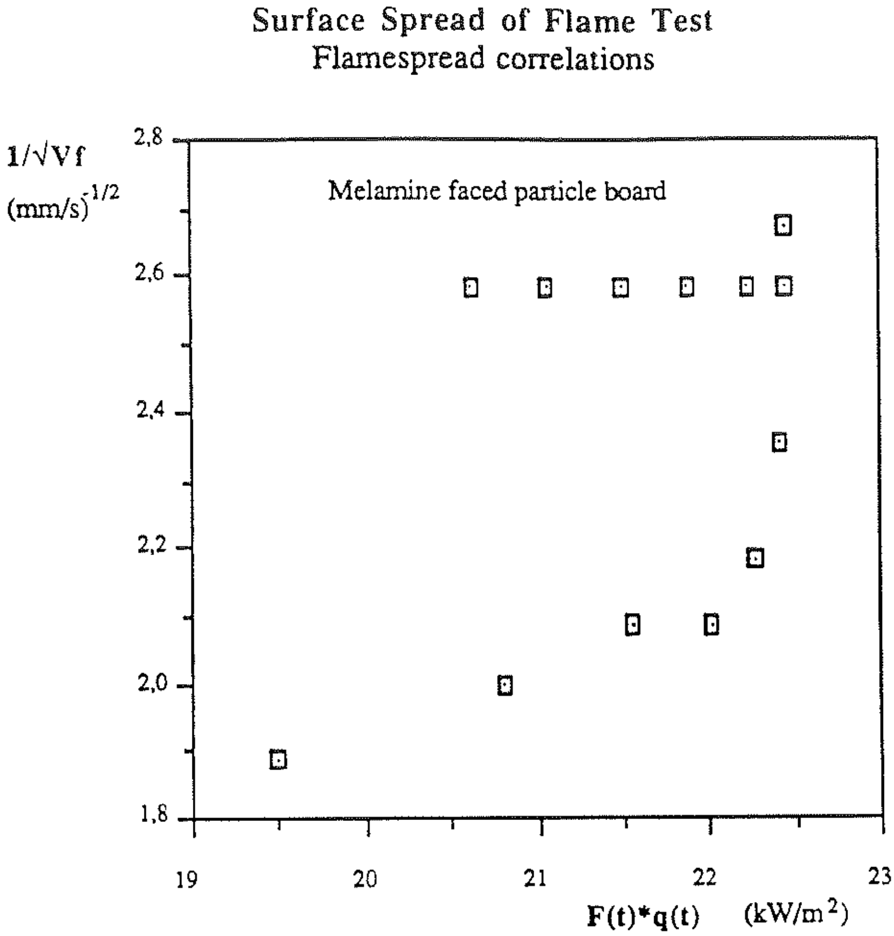
Surface Spread of Flame Test
Flamespread correlations
1/√Vf
(mm/s)^-1/2
Melamine faced particle board
2,8
2,6
2,4
2,2
2,0
1,8
19
20
21
22
23
F(t)*q(t) (kW/m2)

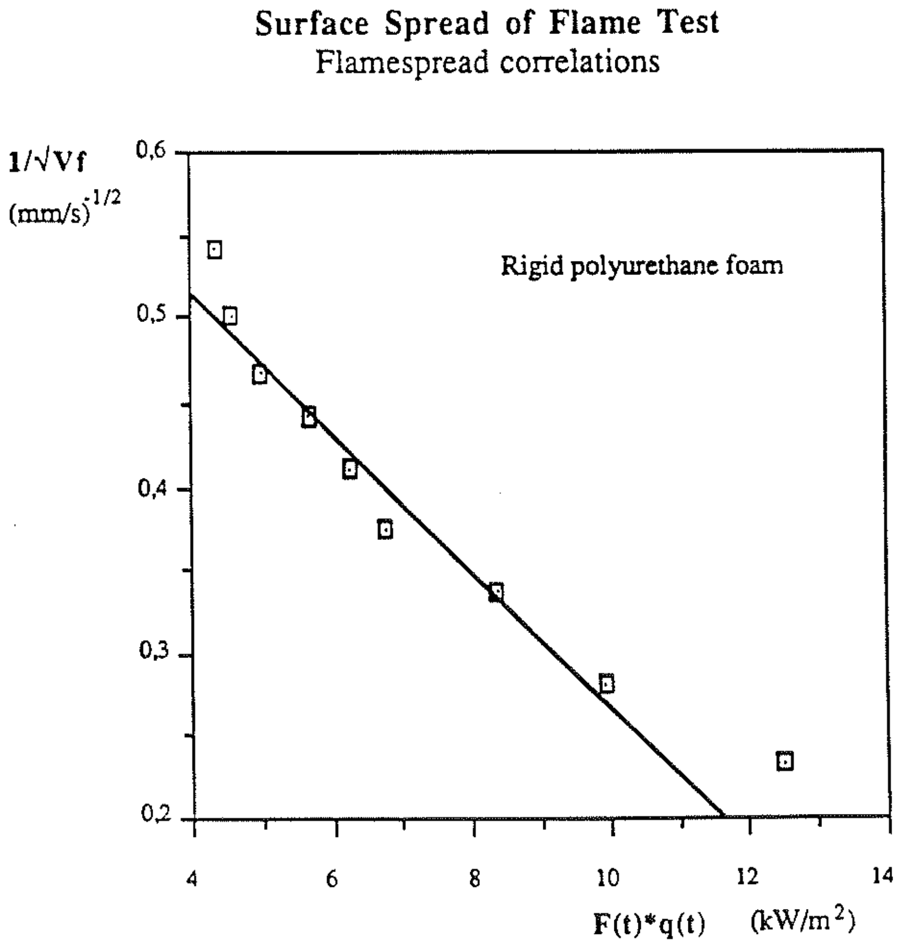
Surface Spread of Flame Test
Flamespread correlations
1/√Vf
(mm/s)^-1/2
Rigid polyurethane foam
0,6
0,5
0,4
0,3
0,2
4
6
8
10
12
14
F(t)*q(t) (kW/m2)

Surface Spread of Flame Test
Flamespread correlations

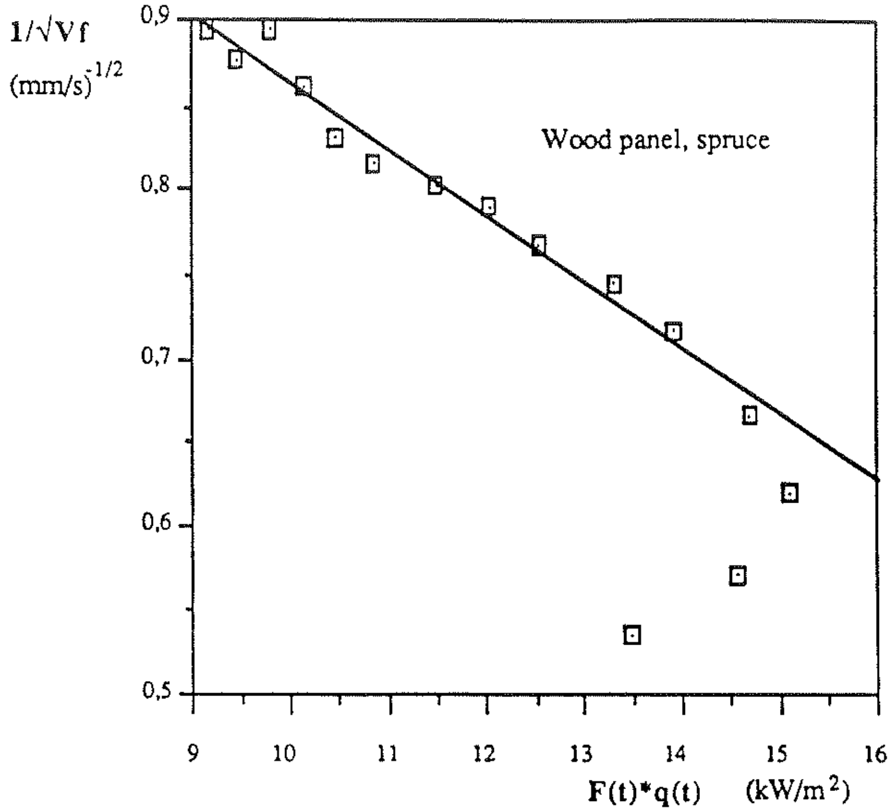

Surface Spread of Flame Test
Flamespread correlations

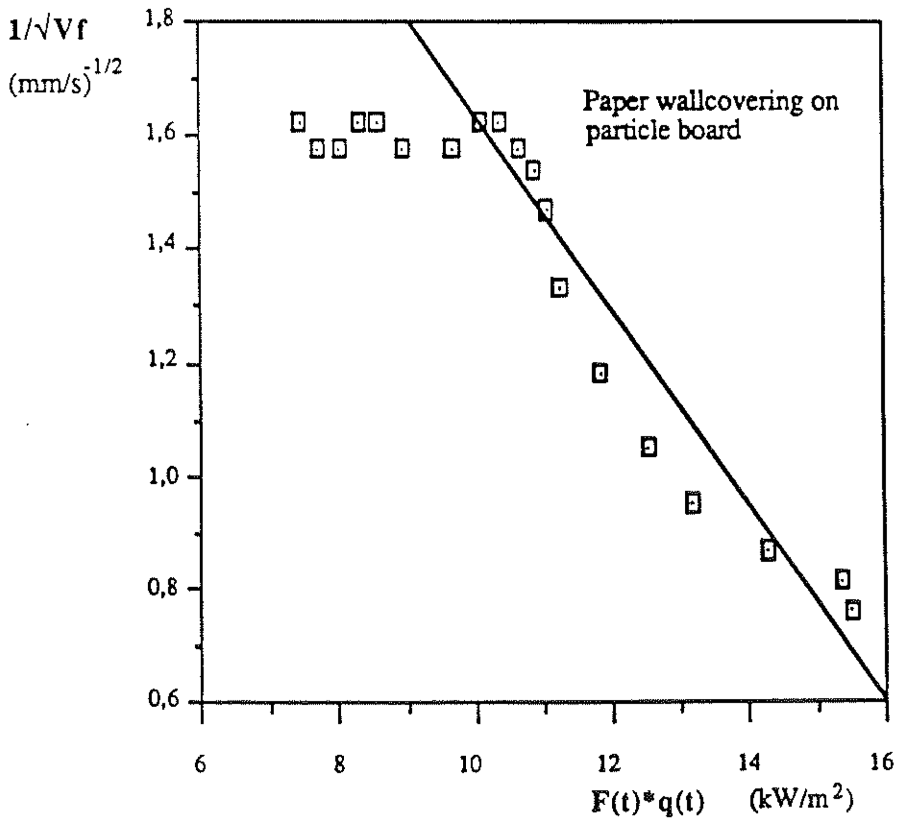

Appendix B

Comparison of experimental and calculated data from full scale test series, scenario A

<u>Contents</u> <u>Page</u>

Note: No experimental data of wall temperatures or downward flame spread exists for this series

RHR from full scale room test

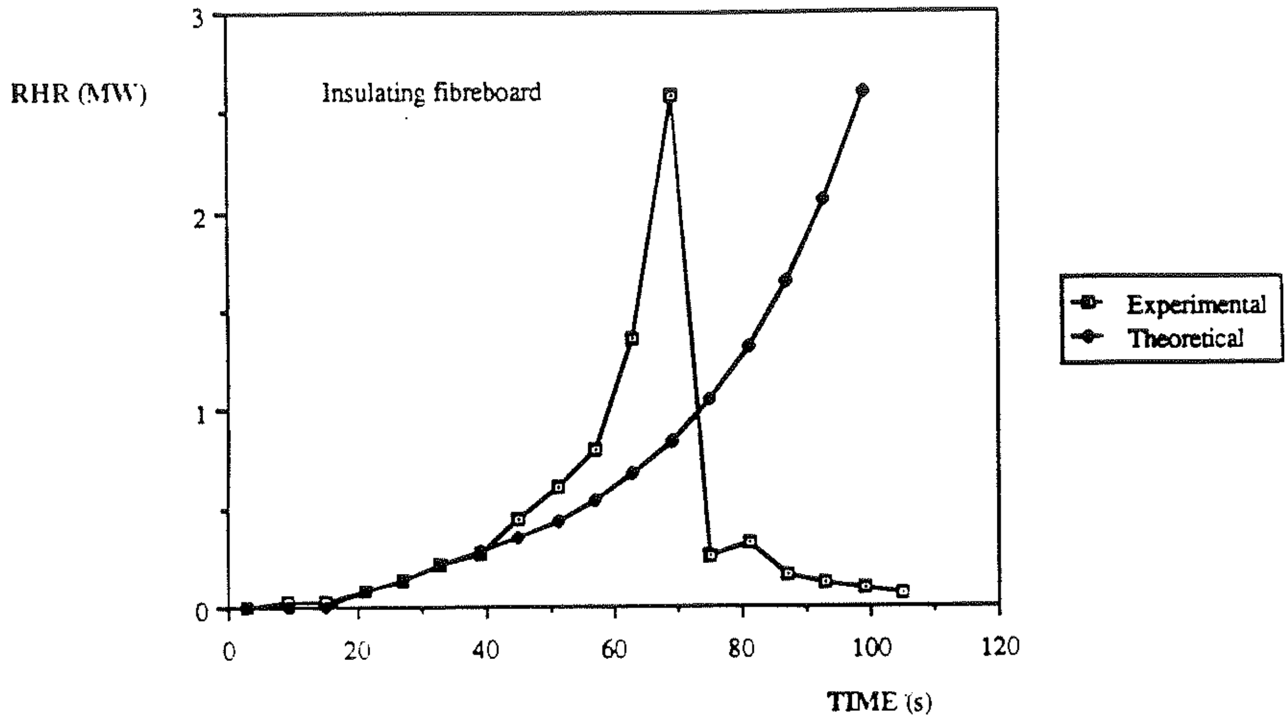

RHR from full scale room test

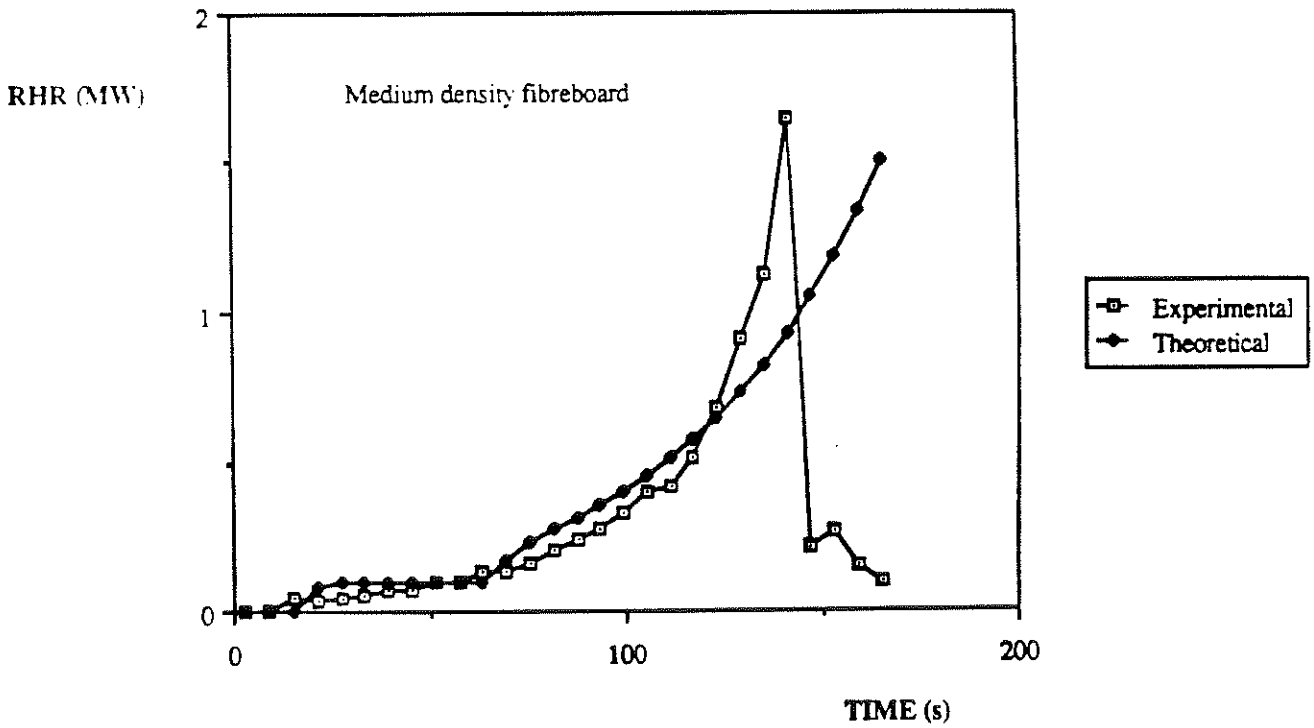

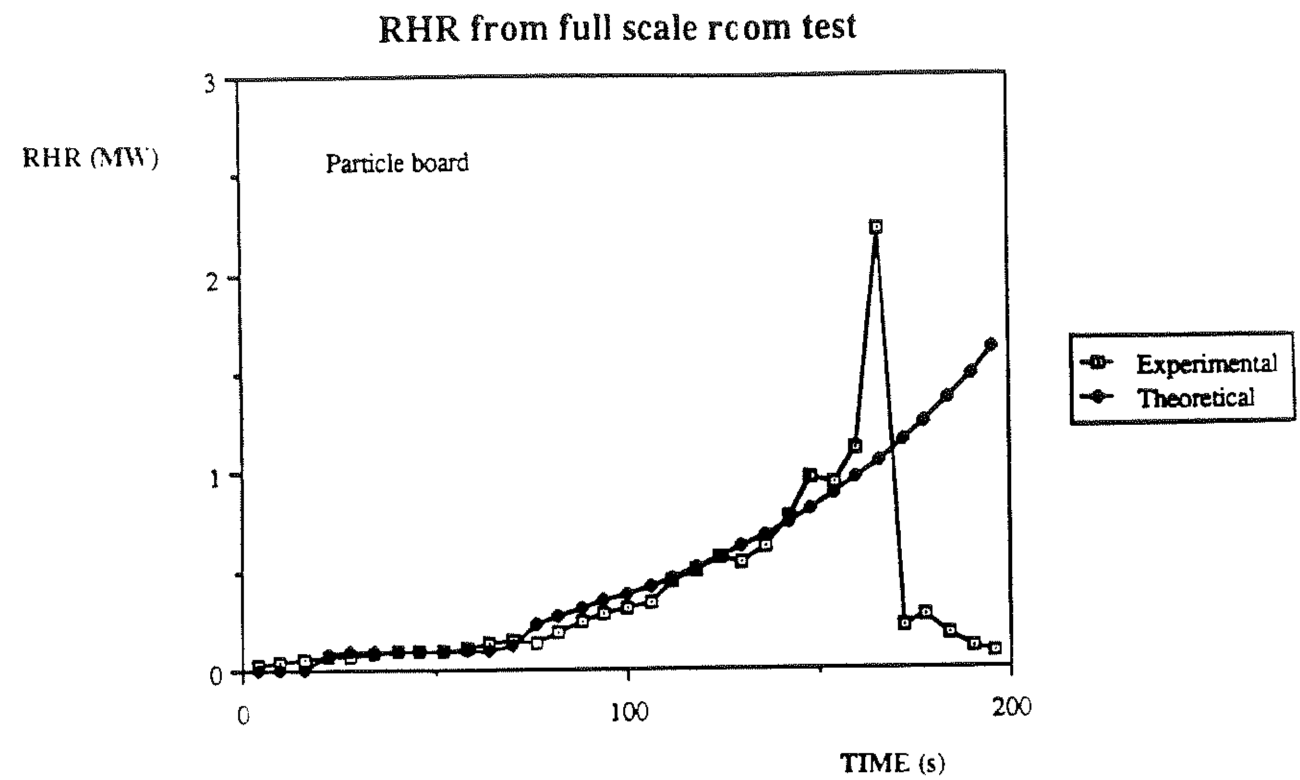
RHR from full scale rcom test
RHR (MW)
Particle board
Experimental
Theoretical
0
1
2
3
0
100
200
TIME (s)

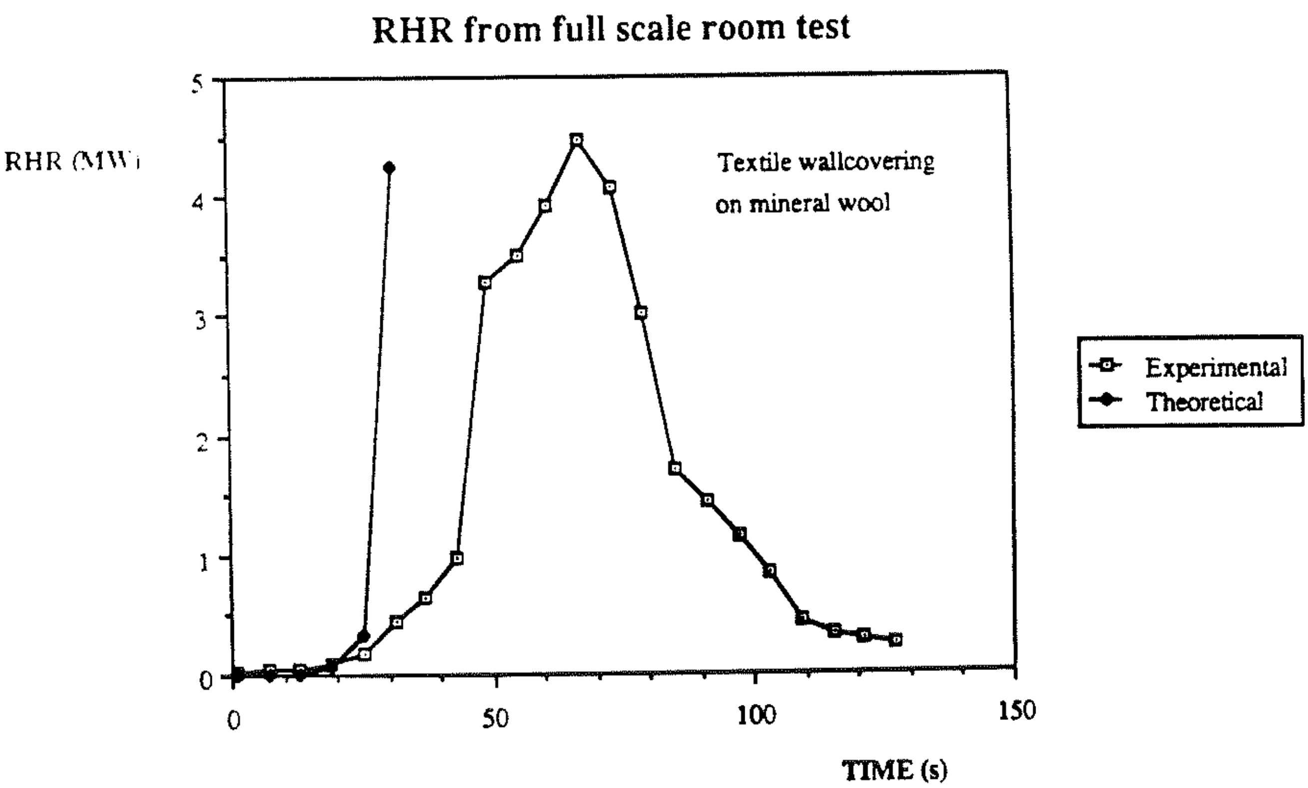
RHR from full scale room test
RHR (MW)
Textile wallcovering
on mineral wool
Experimental
Theoretical
0
1
2
3
4
5
0
50
100
150
TIME (s)

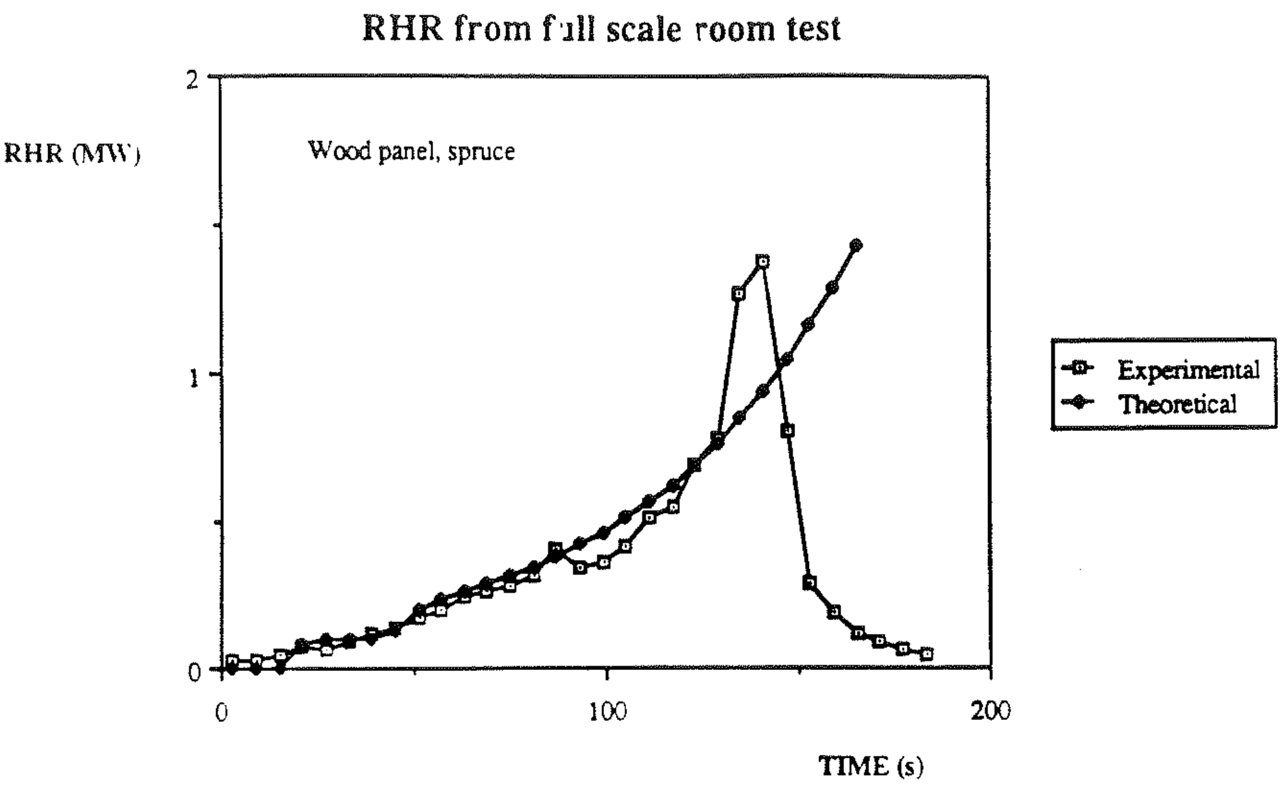
RHR from full scale room test
RHR (MW)
Wood panel, spruce
2
1
0
0
100
200
TIME (s)
Experimental
Theoretical

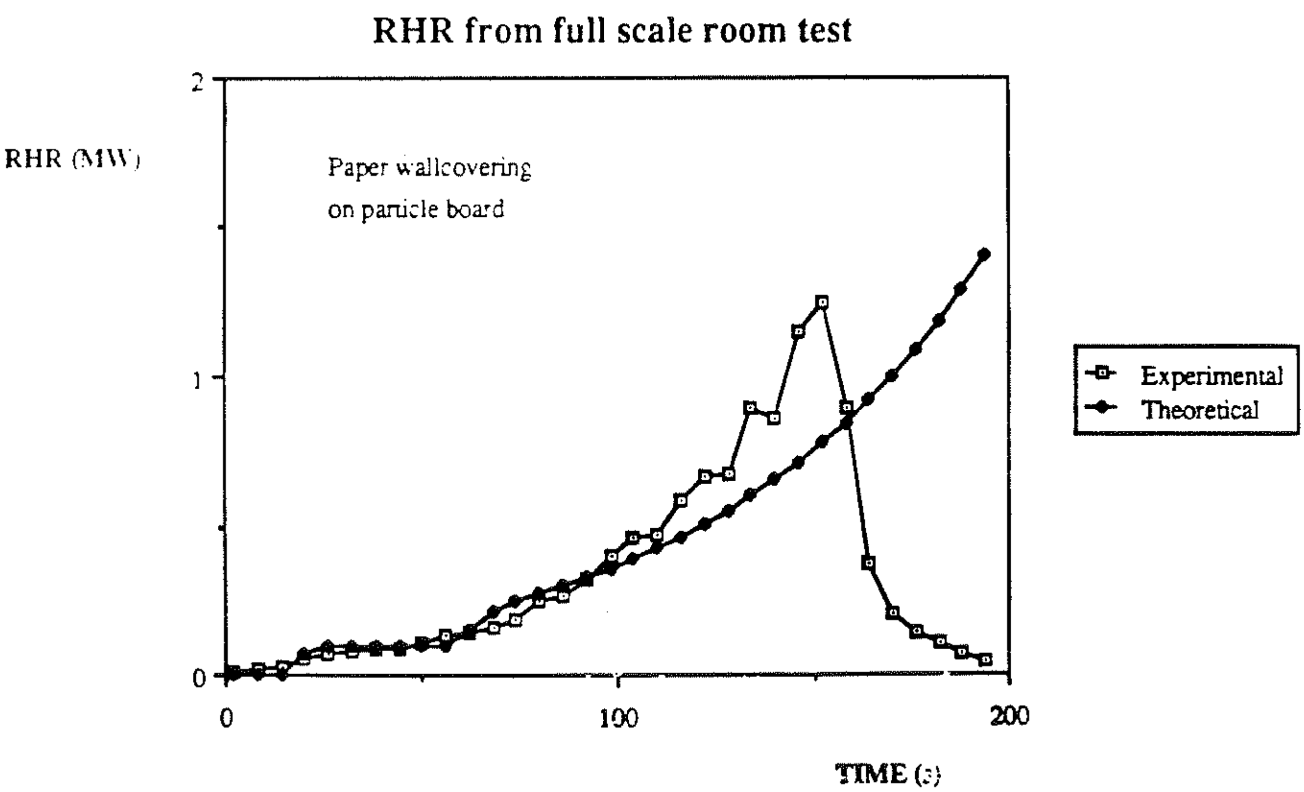
RHR from full scale room test
RHR (MW)
Paper wallcovering
on particle board
2
1
0
0
100
200
TIME (s)
Experimental
Theoretical

HOT GAS TEMPERATURES
Full scale room test

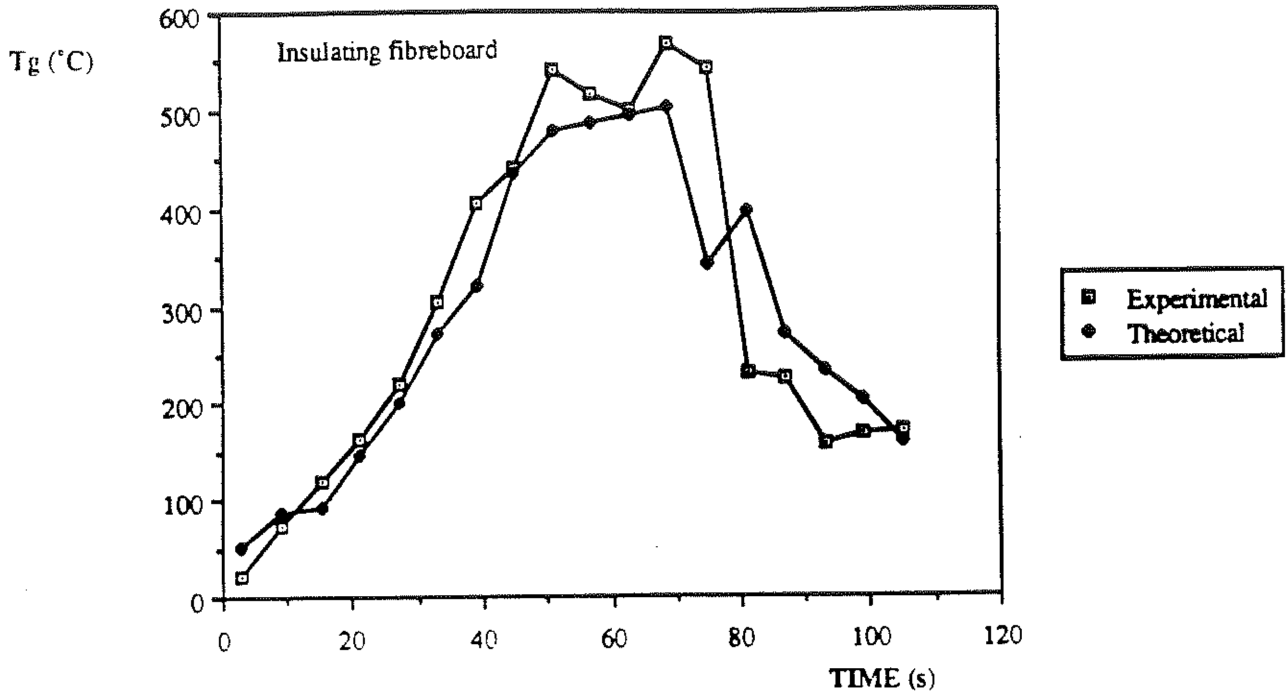

HOT GAS TEMPERATURES
Full scale room test

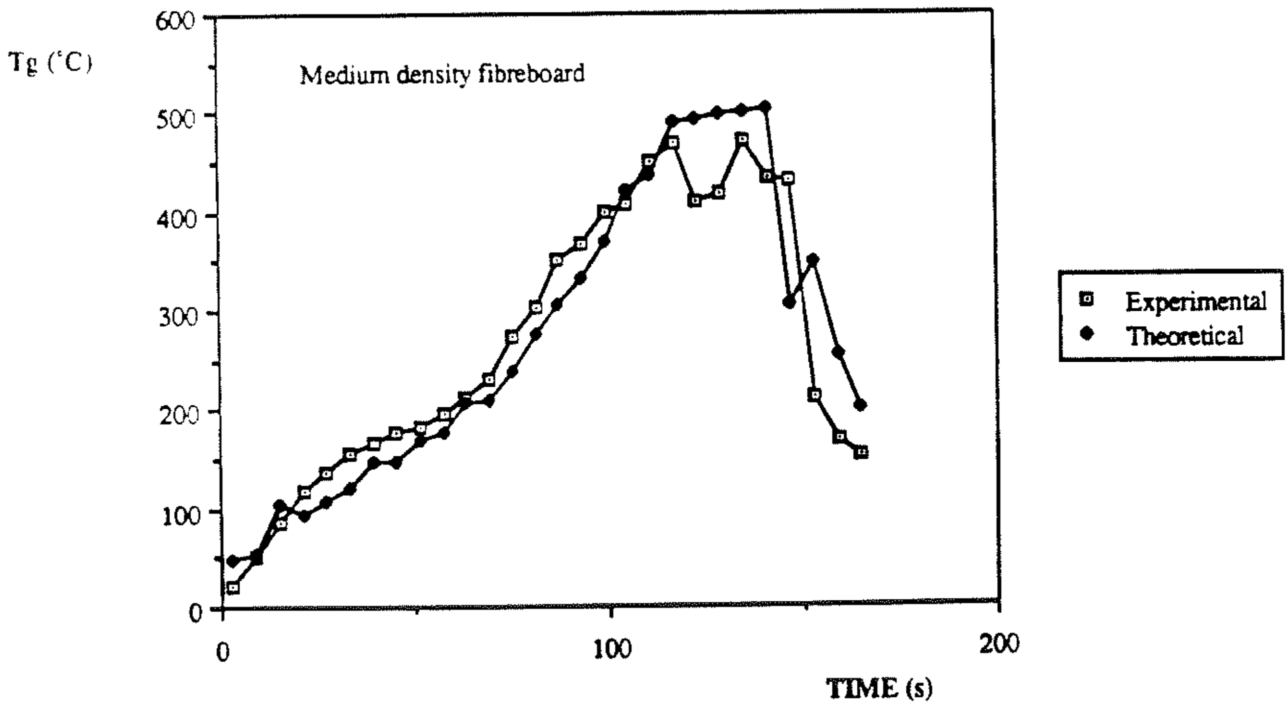

HOT GAS TEMPERATURES
Full scale room test

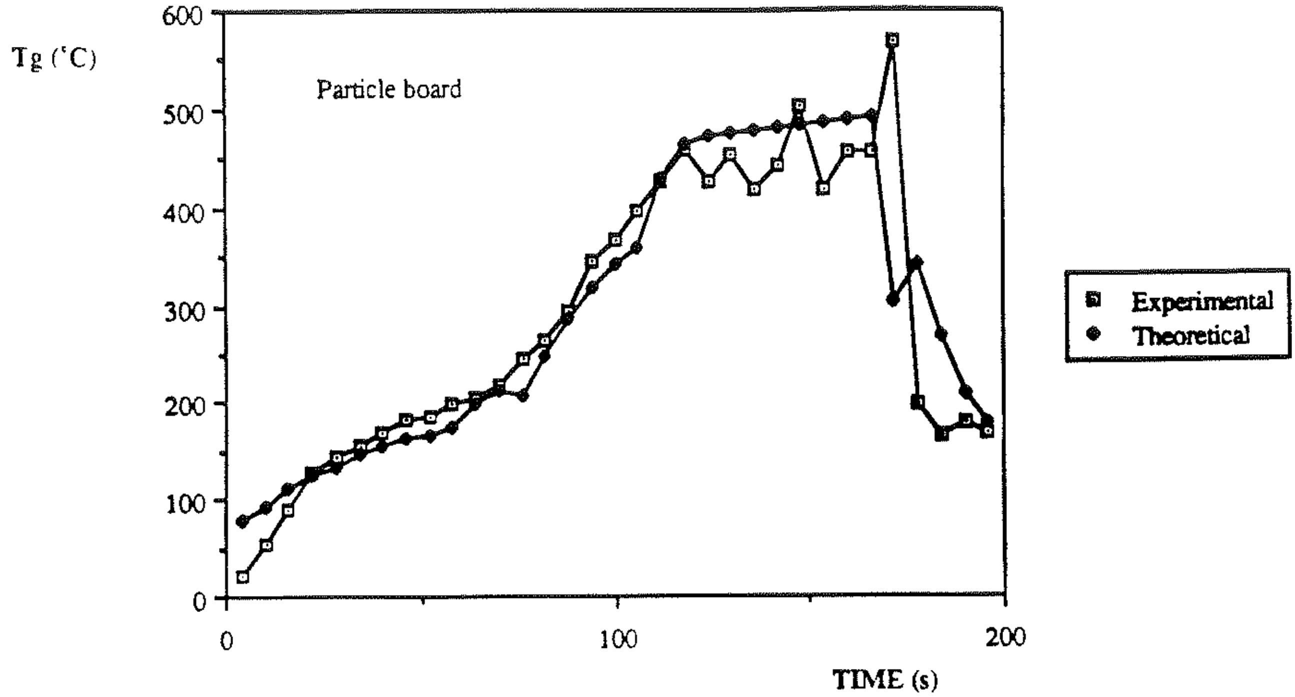

HOT GAS TEMPERATURES
Full scale room test

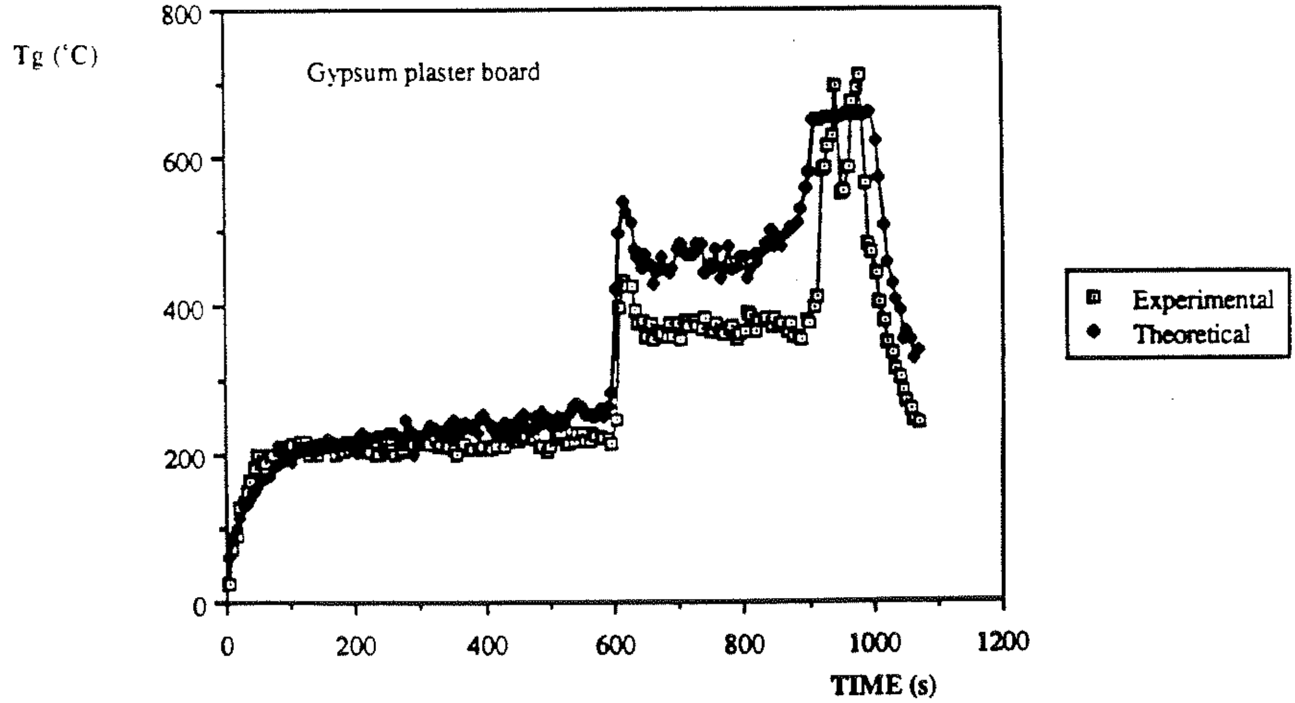

HOT GAS TEMPERATURES
Full scale room test

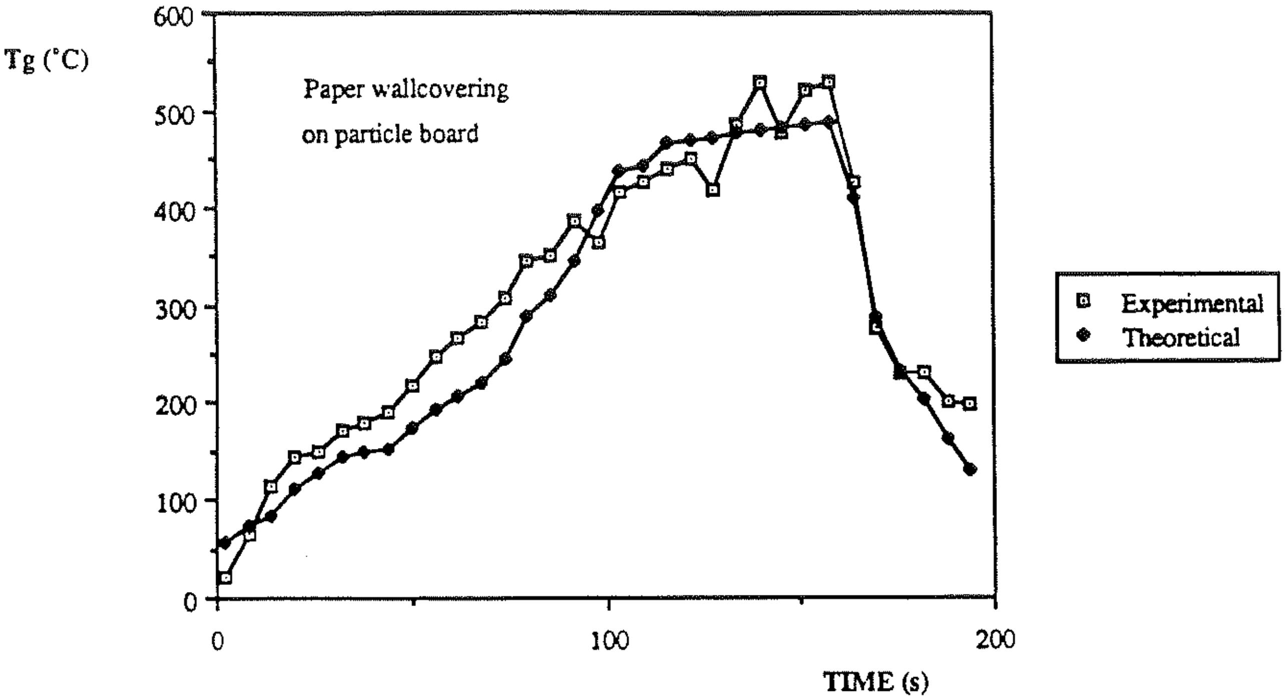

HOT GAS TEMPERATURES
Full scale room test

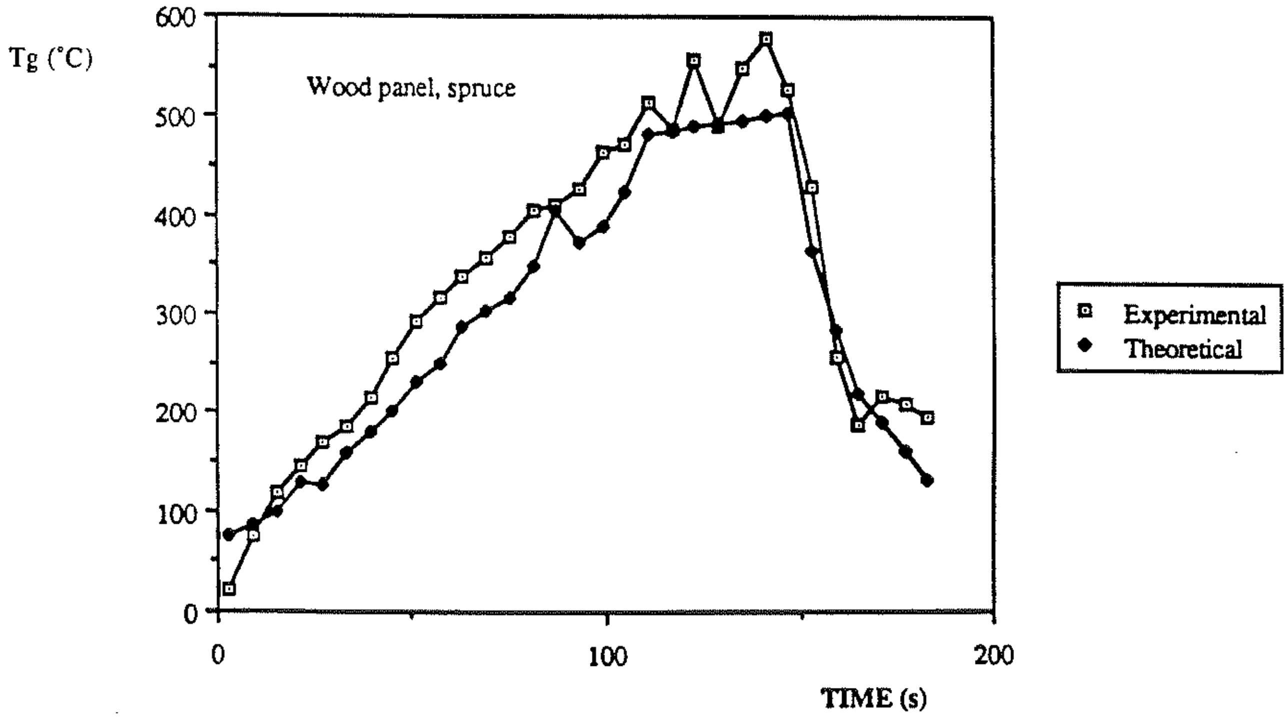

Heat flux to floor, full scale room test

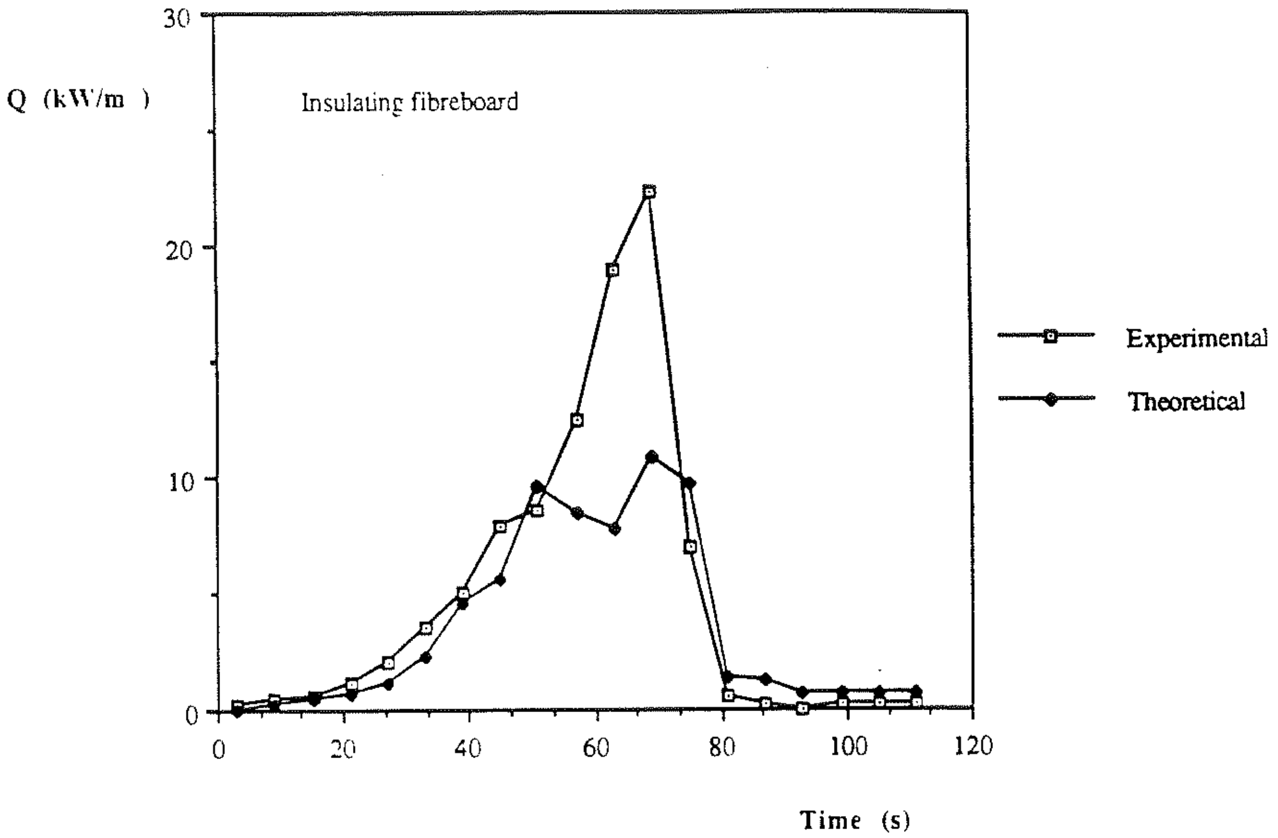

Heat flux to floor, full scale room test

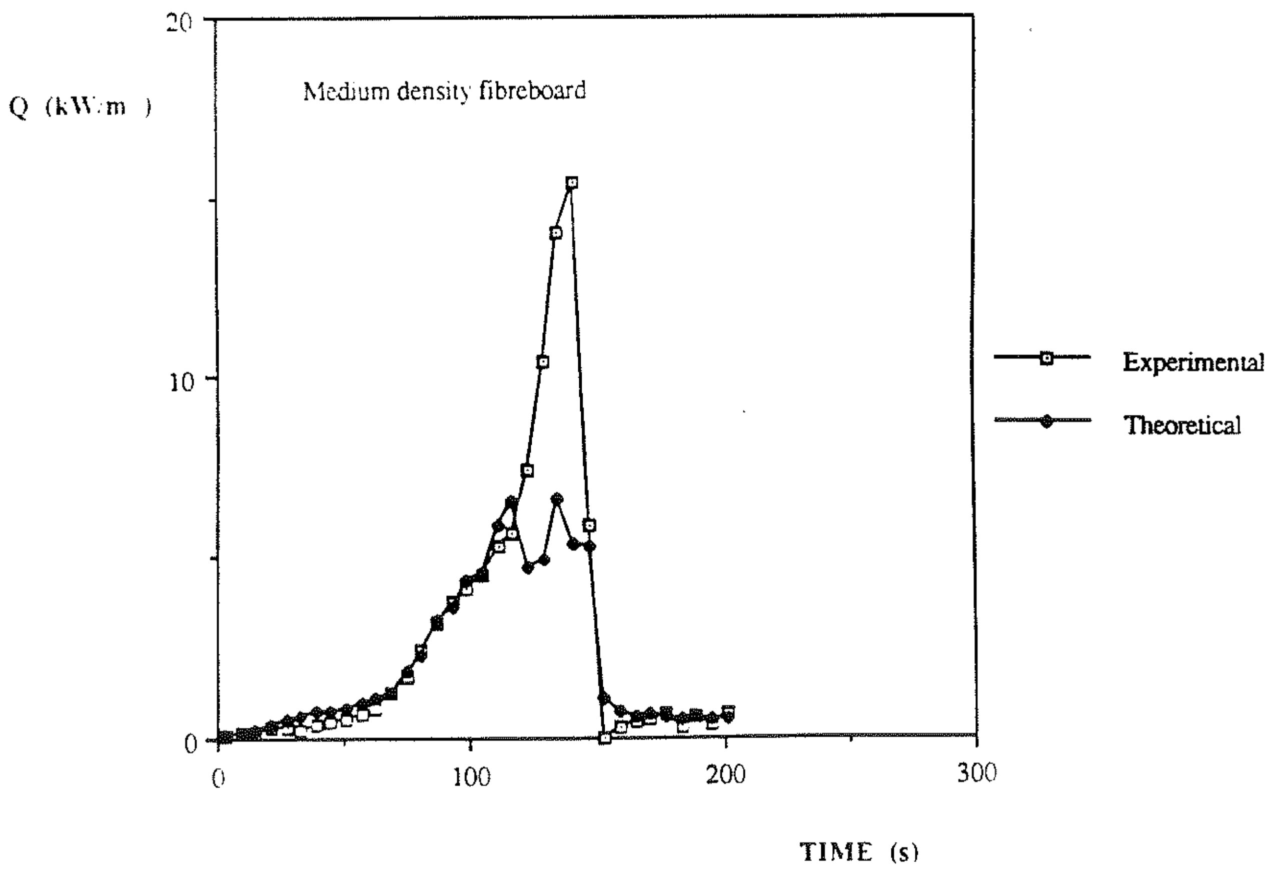

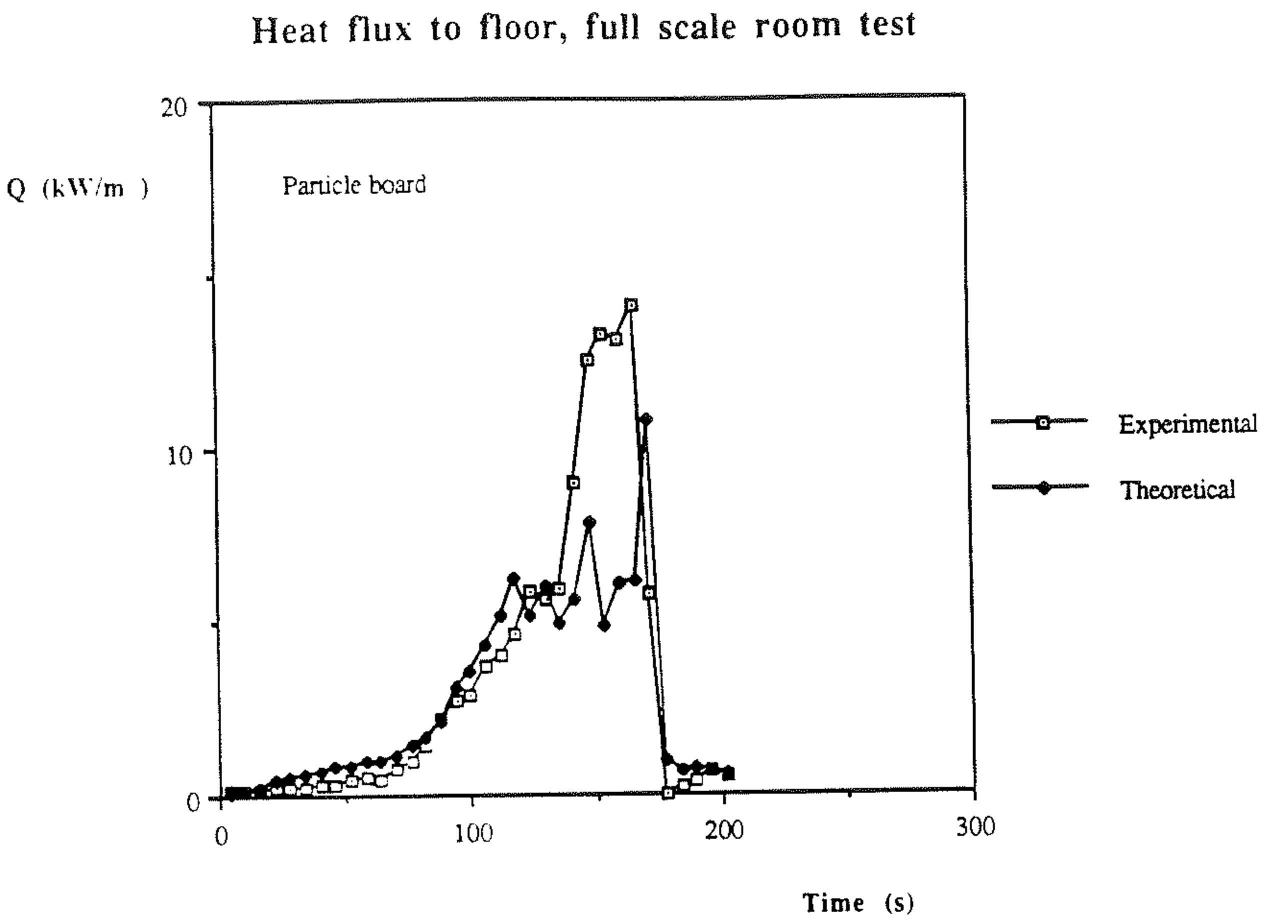
Heat flux to floor, full scale room test
Q (kW/m)
Particle board
Experimental
Theoretical
0
10
20
0
100
200
300
Time (s)

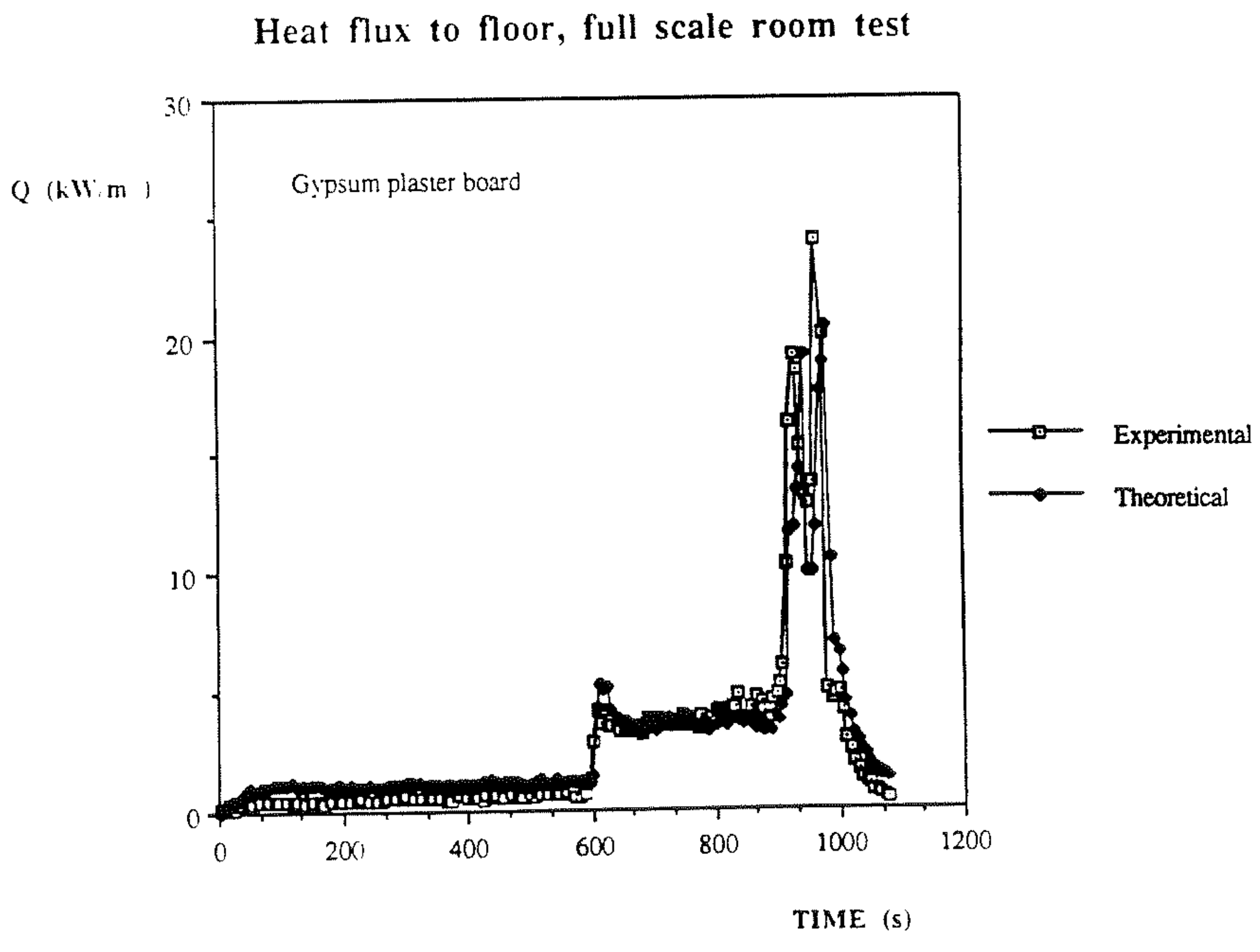
Heat flux to floor, full scale room test
Q (kW/m)
Gypsum plaster board
Experimental
Theoretical
0
10
20
30
0
200
400
600
800
1000
1200
TIME (s)

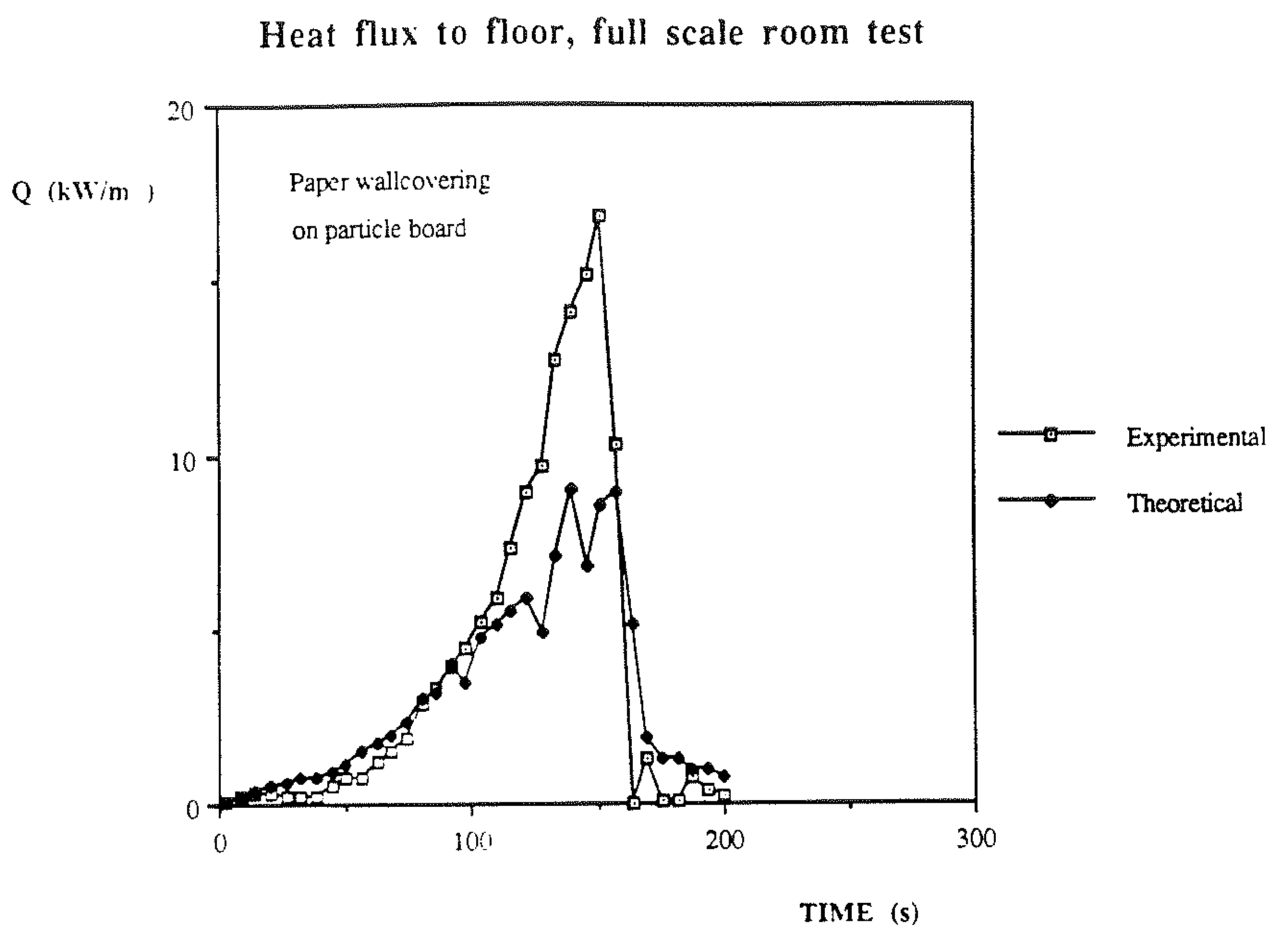
Heat flux to floor, full scale room test
Q (kW/m)
Paper wallcovering
on particle board
Experimental
Theoretical
TIME (s)
0
10
20
0
100
200
300

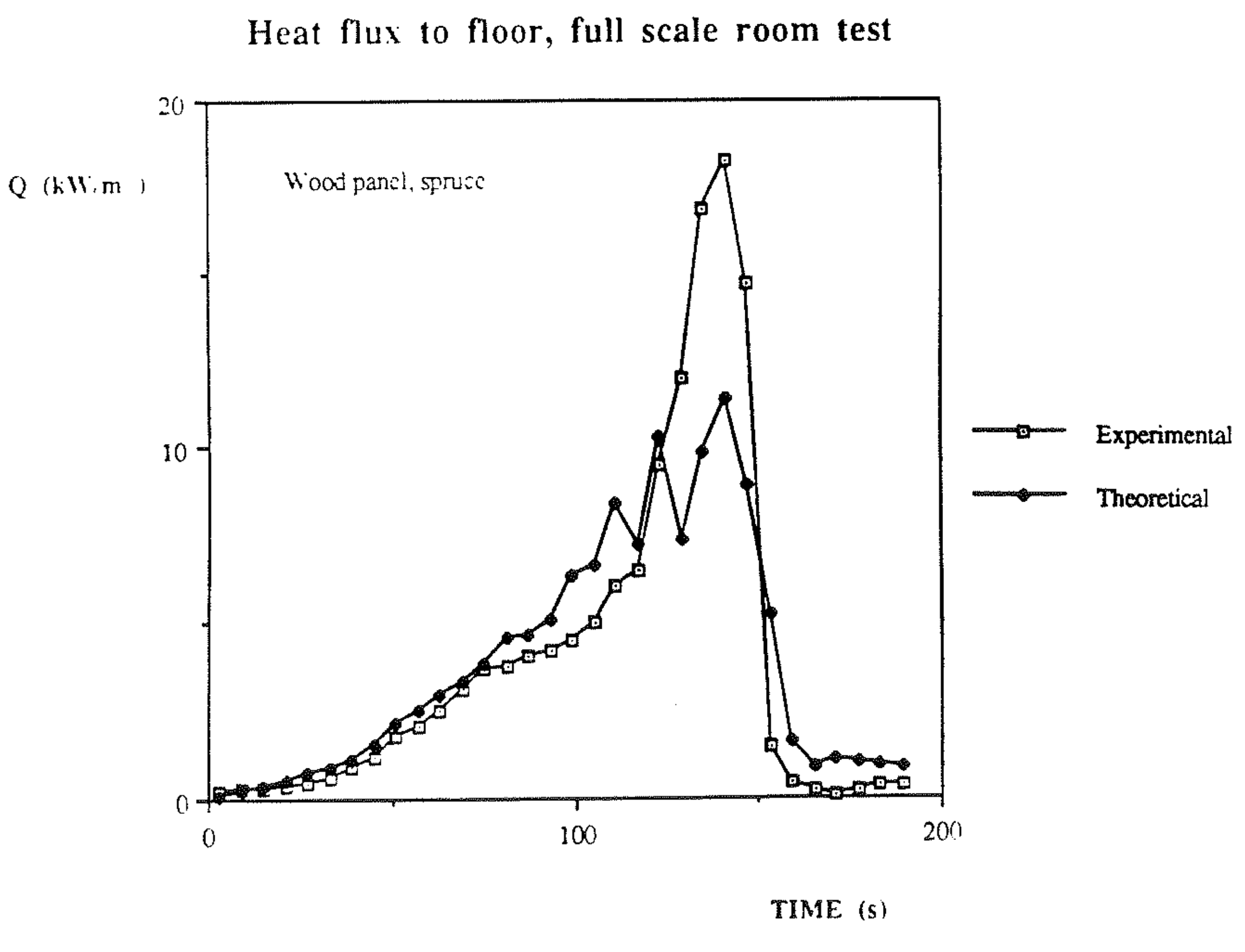
Heat flux to floor, full scale room test
Q (kW/m)
Wood panel, spruce
Experimental
Theoretical
TIME (s)
0
10
20
0
100
200

Appendix C

Comparison of experimental and calculated data from 1/3 scale test series, scenario A

Contents	Page

RHR from 1/3 scale room test

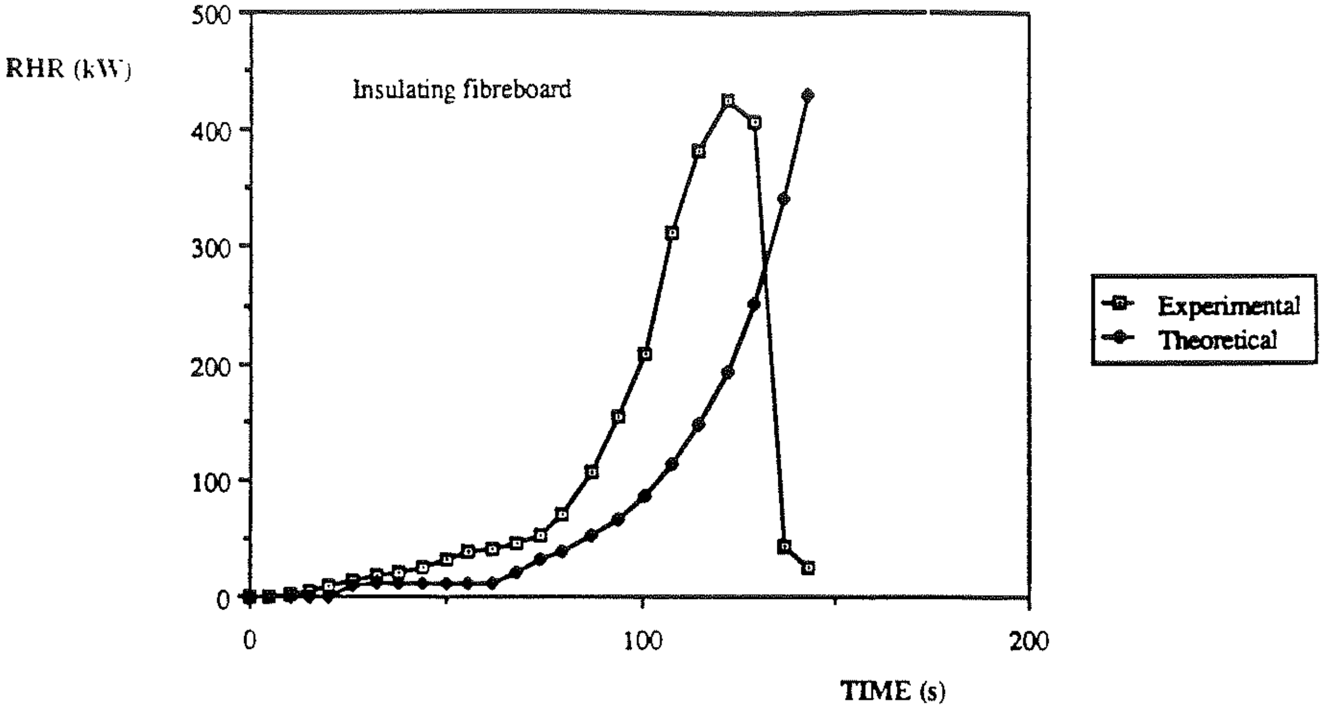

RHR from 1/3 scale room test

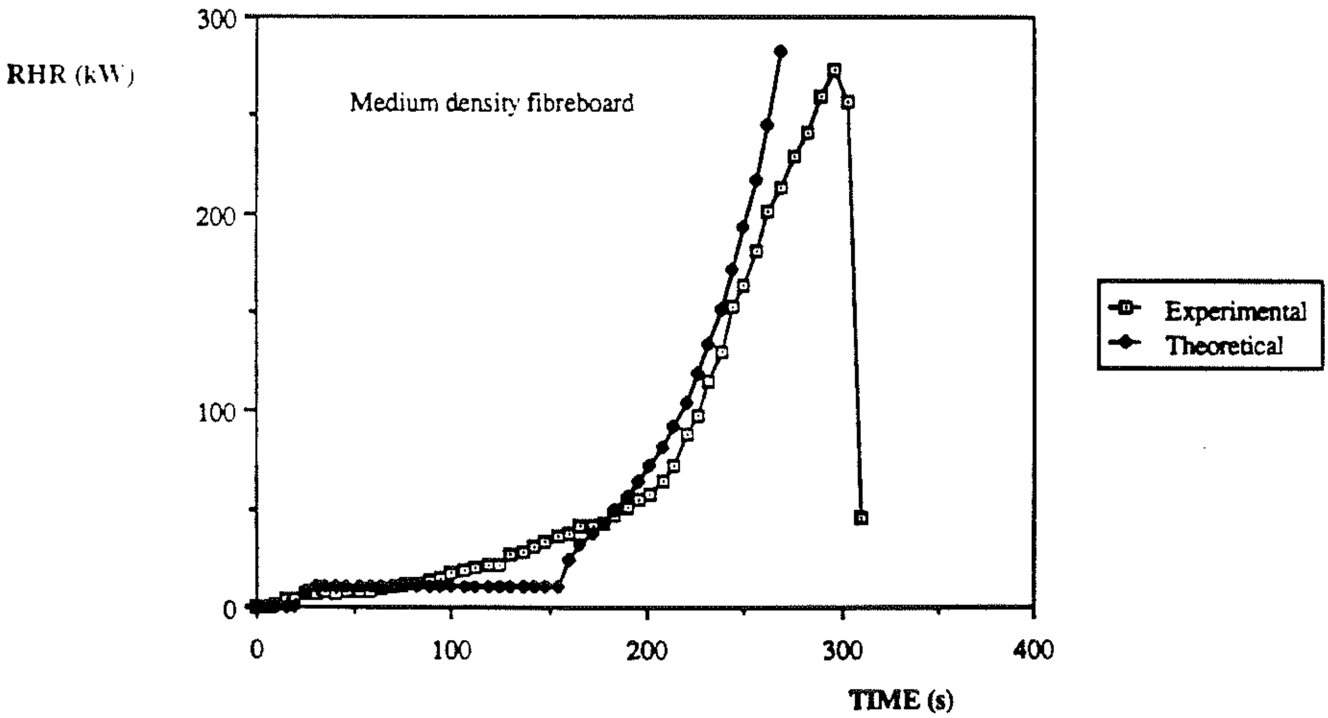

RHR from 1/3 scale room test

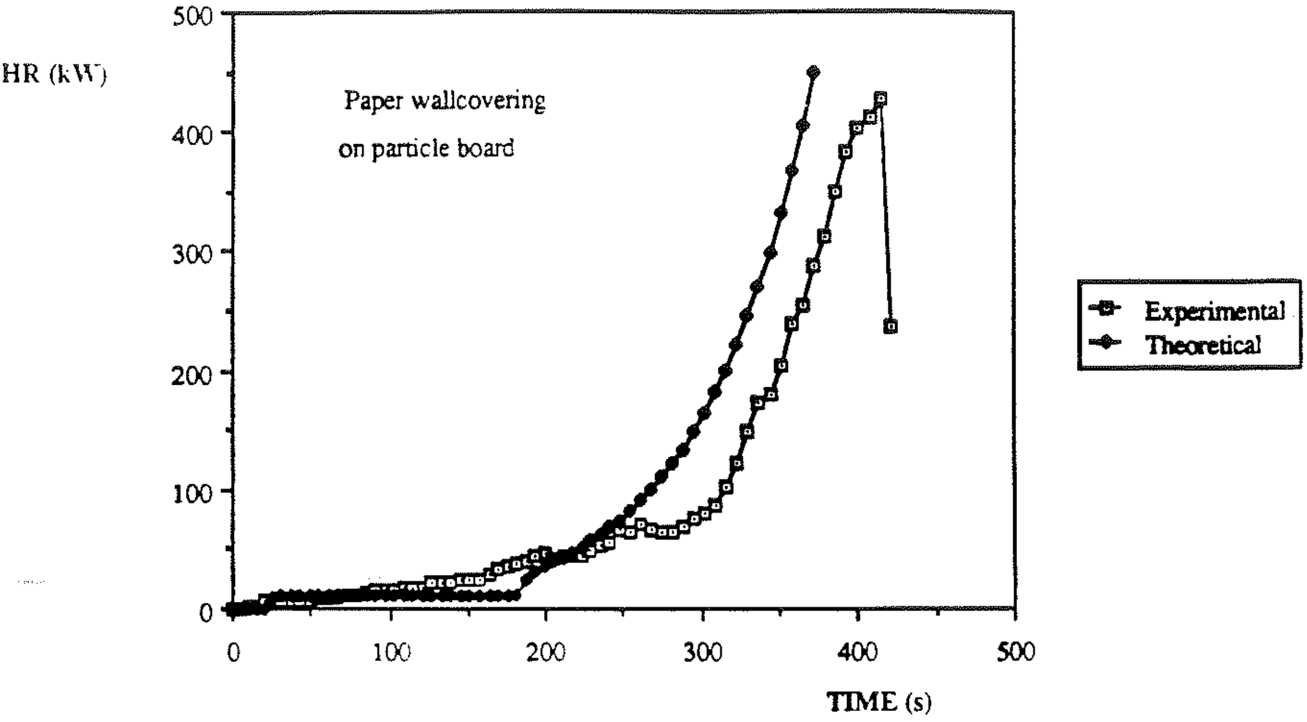

RHR, 1/3 scale test, scenario A

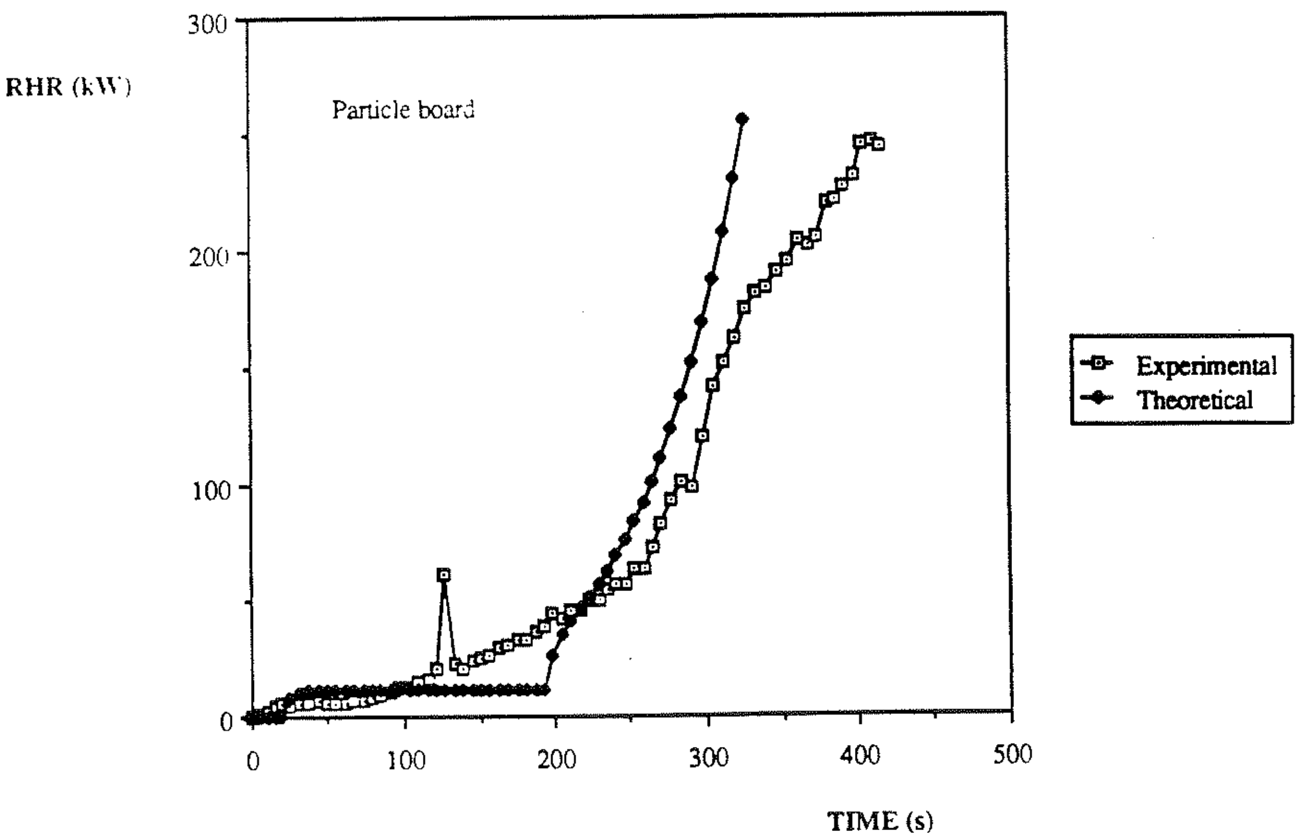

RHR from 1/3 scale room test

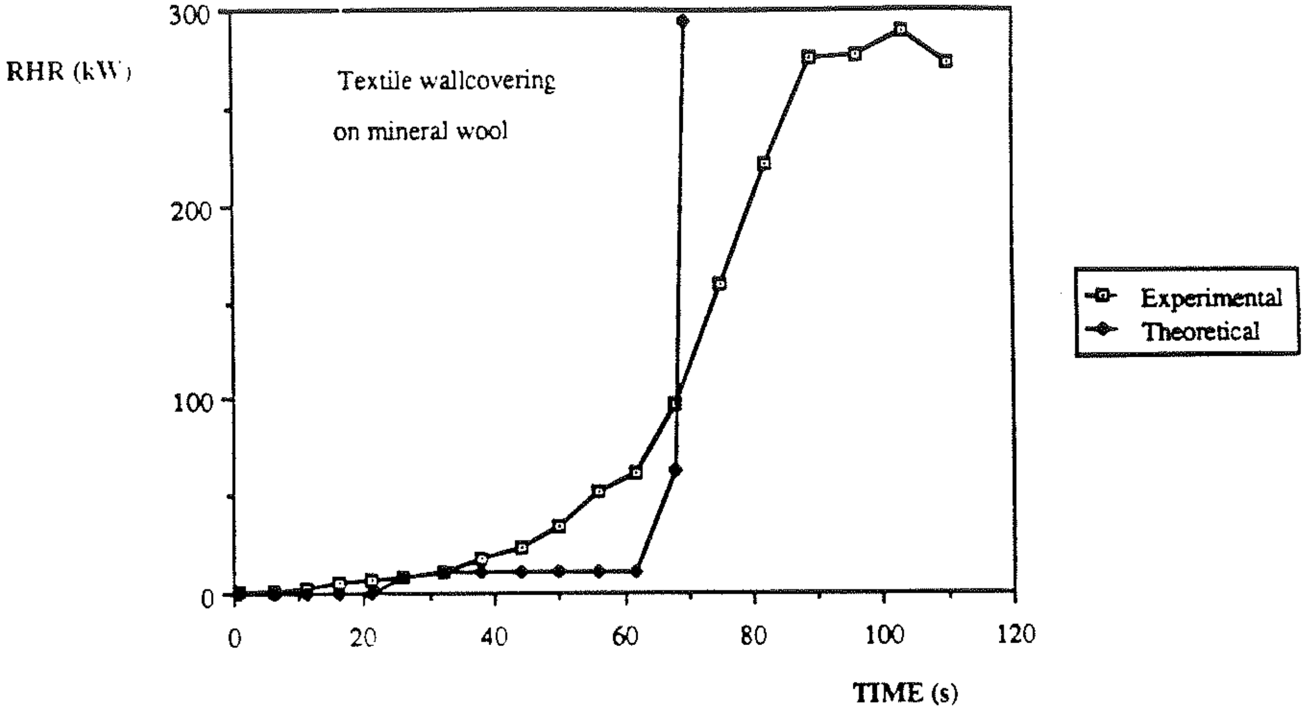

RHR from 1/3 scale room test

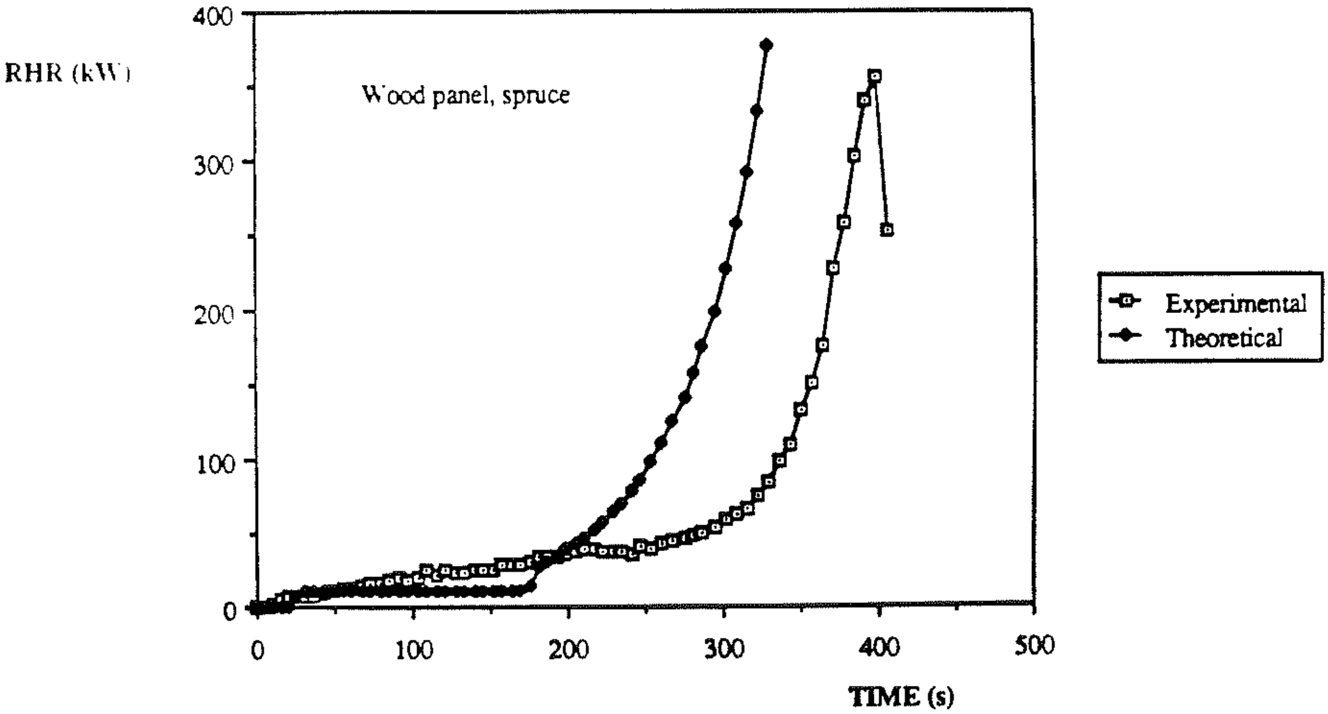

HOT GAS TEMPERATURES

1/3 scale room test

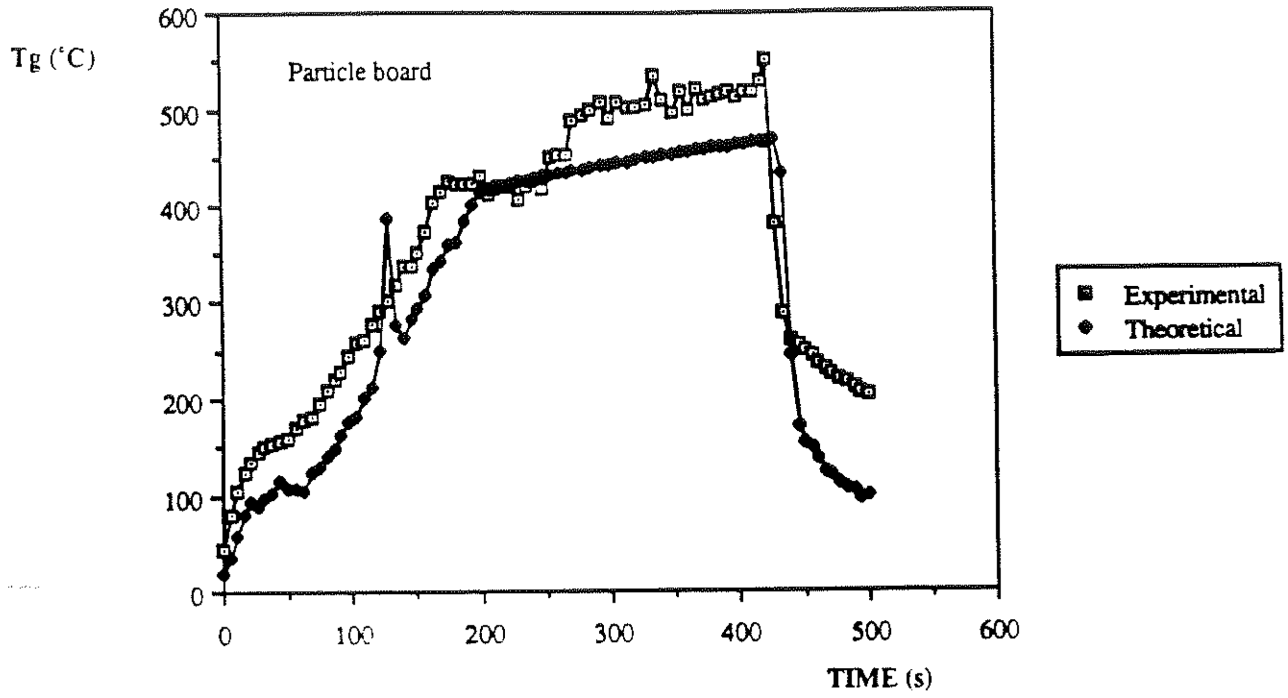

HOT GAS TEMPERATURES

1/3 scale room test

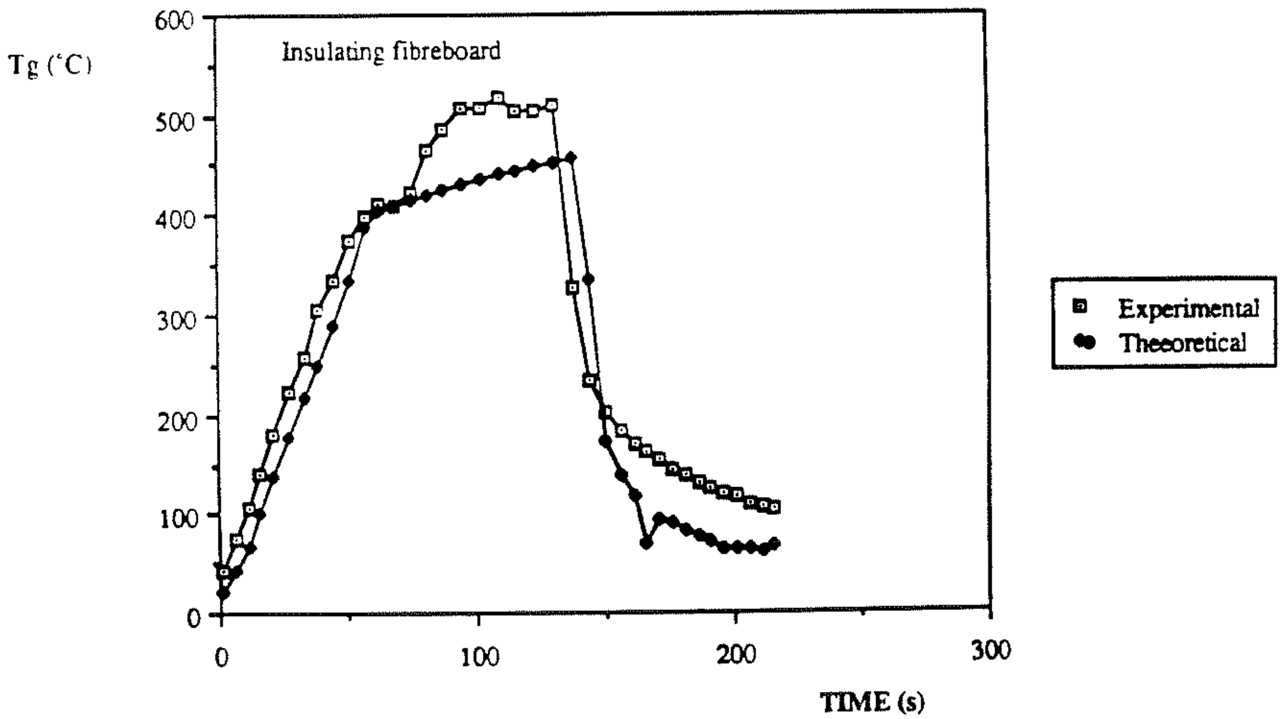

HOT GAS TEMPERATURES
1/3 scale room test

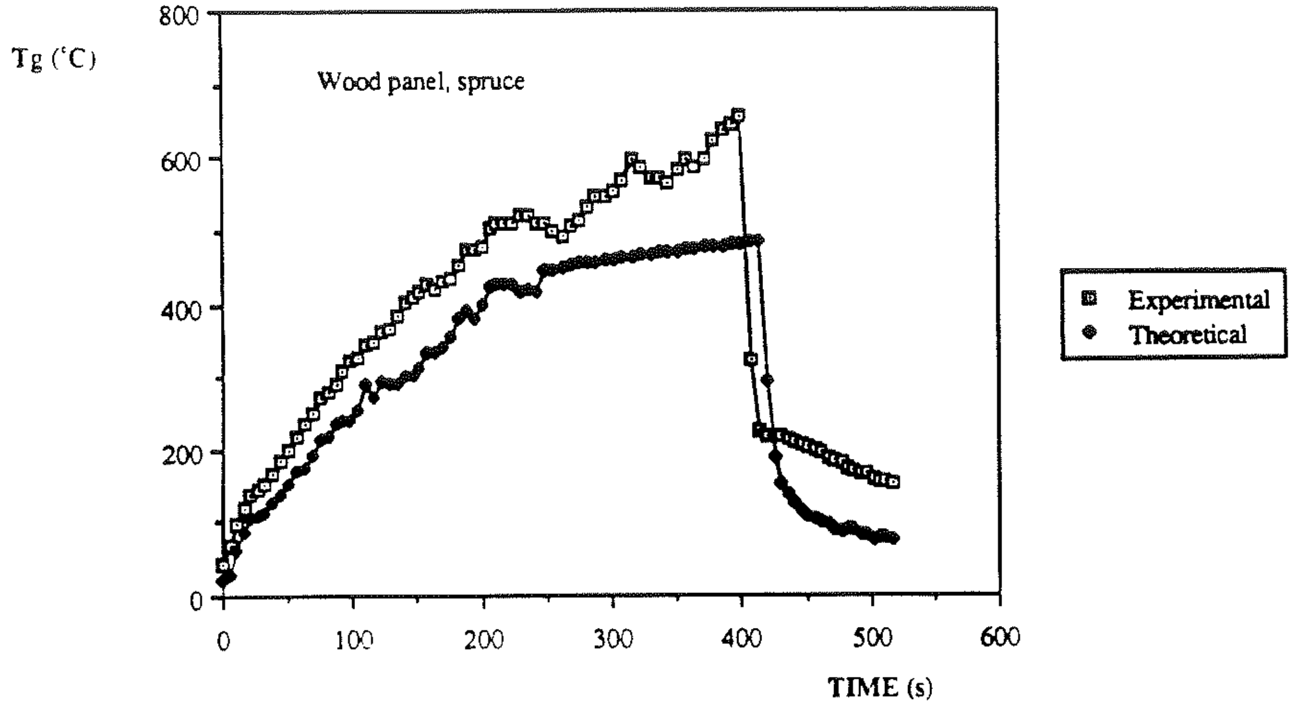

HOT GAS TEMPERATURES
1/3 scale room test

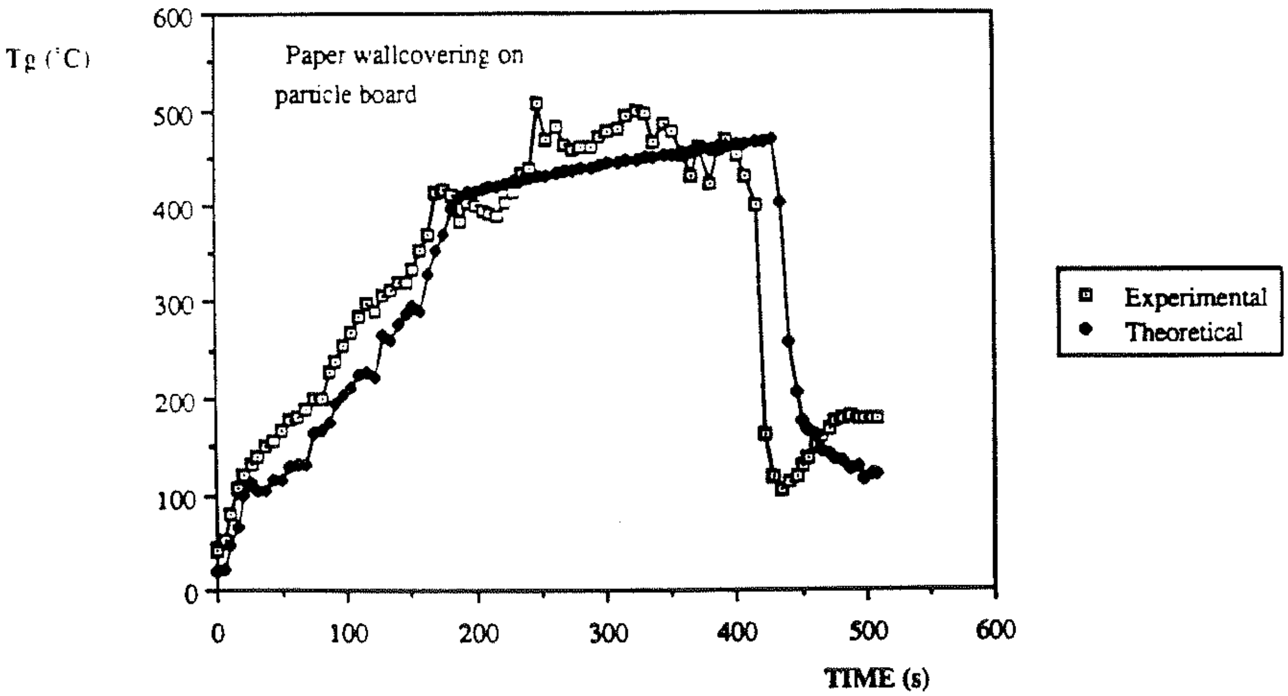

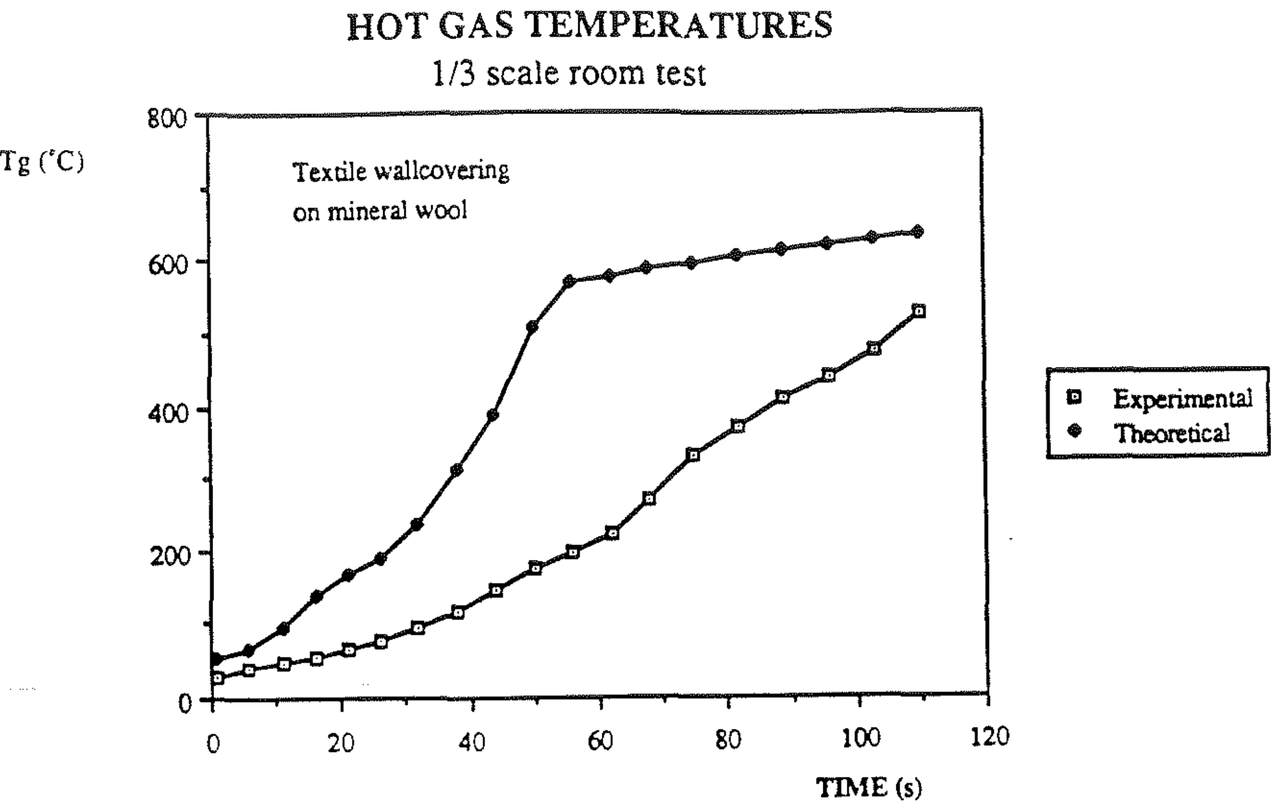

Note: No temperature data is availible for material no. 2, medium density fibreboard, due to thermocouple faliure during the test.

Wall surface temperatures, 1/3 scale test, scenario A

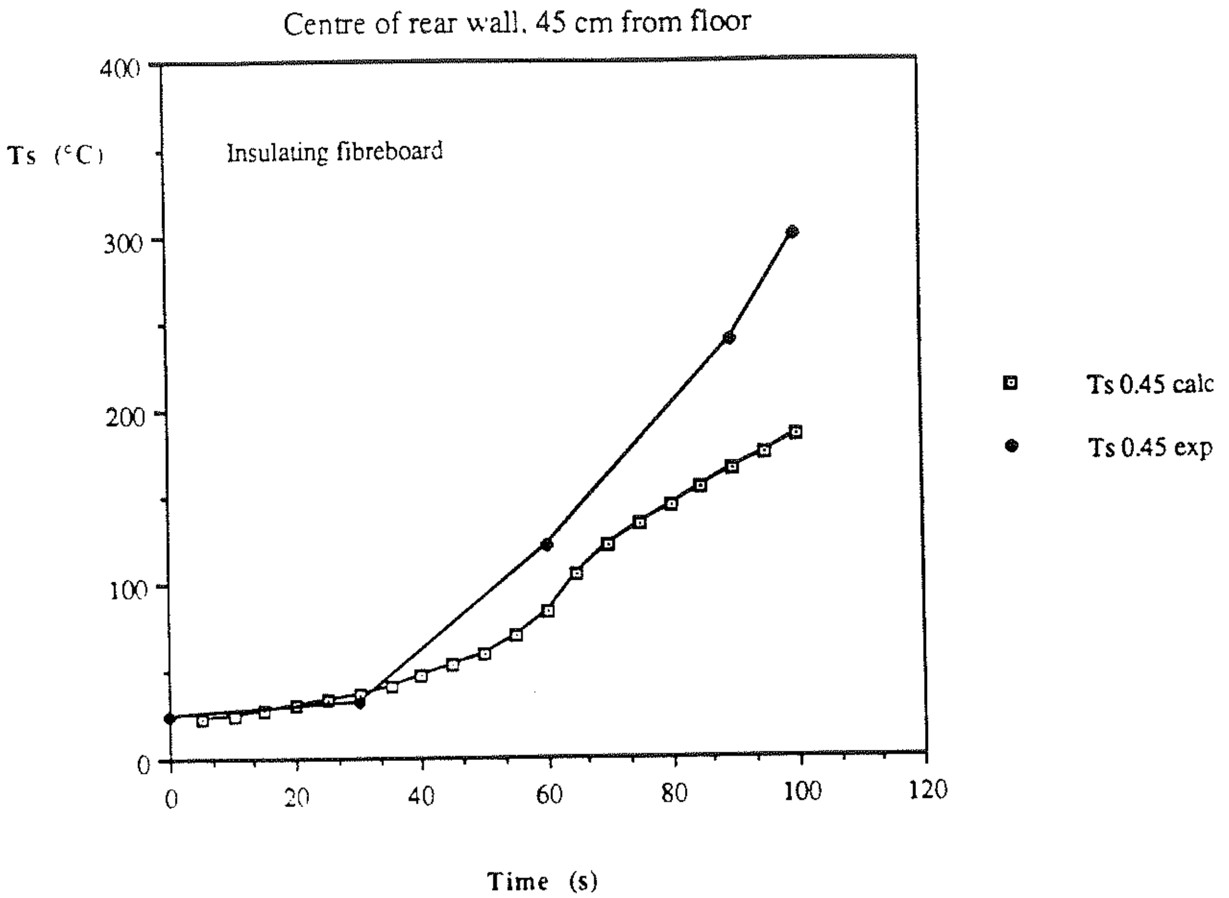

Wall surface temperatures, 1/3 scale test, scenario A

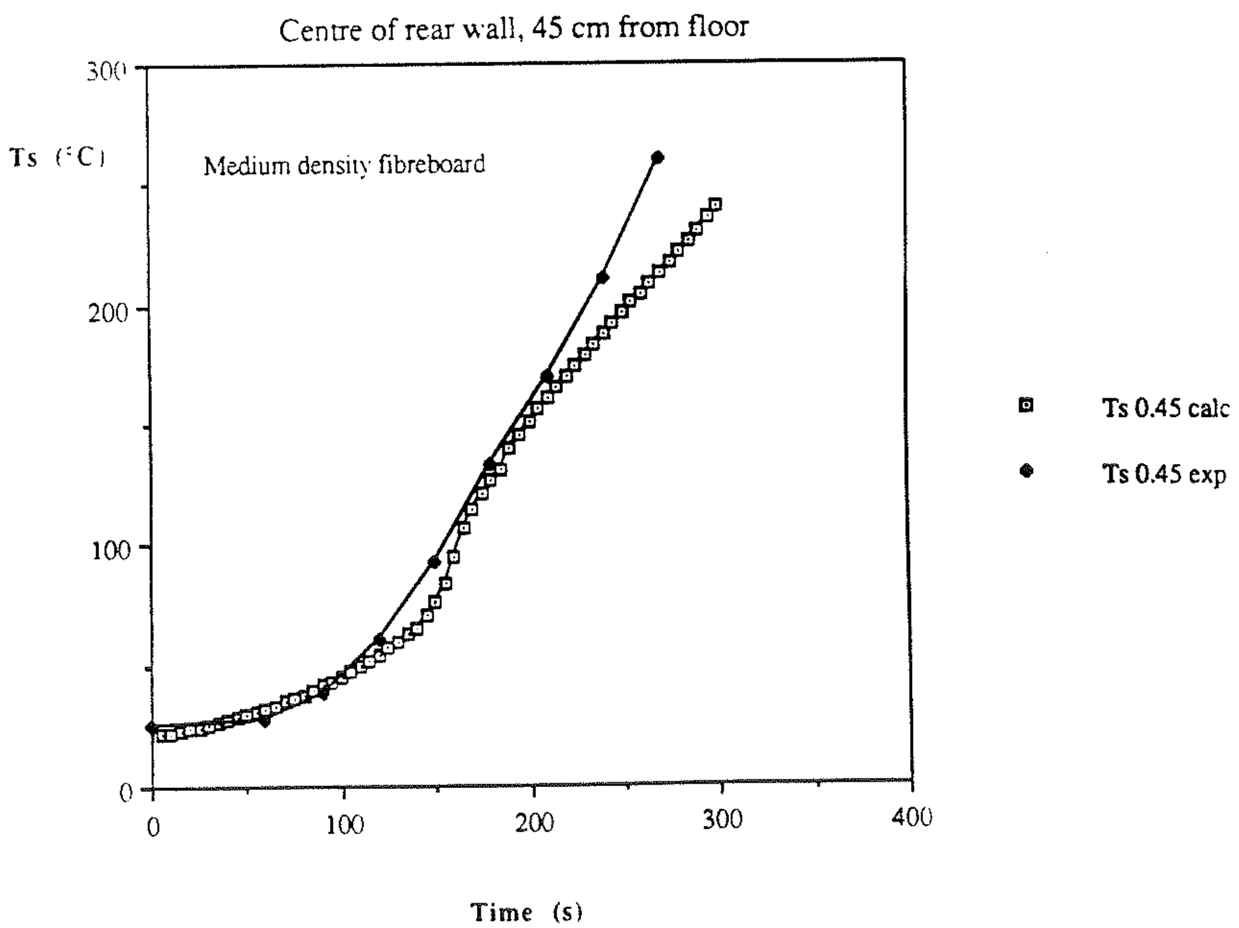

Wall surface temperature, 1/3 scale test, scenario A

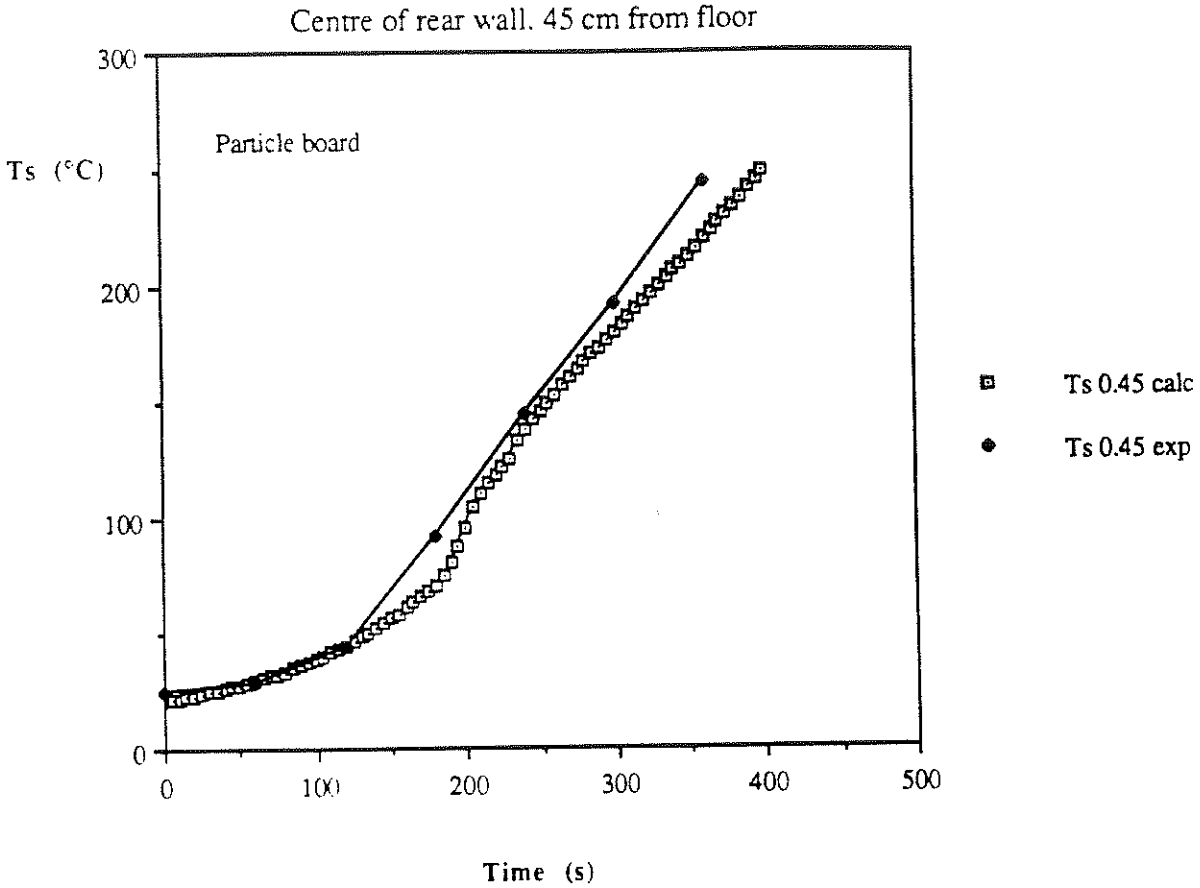

Wall surface temperatures, 1/3 scale test, scenario A

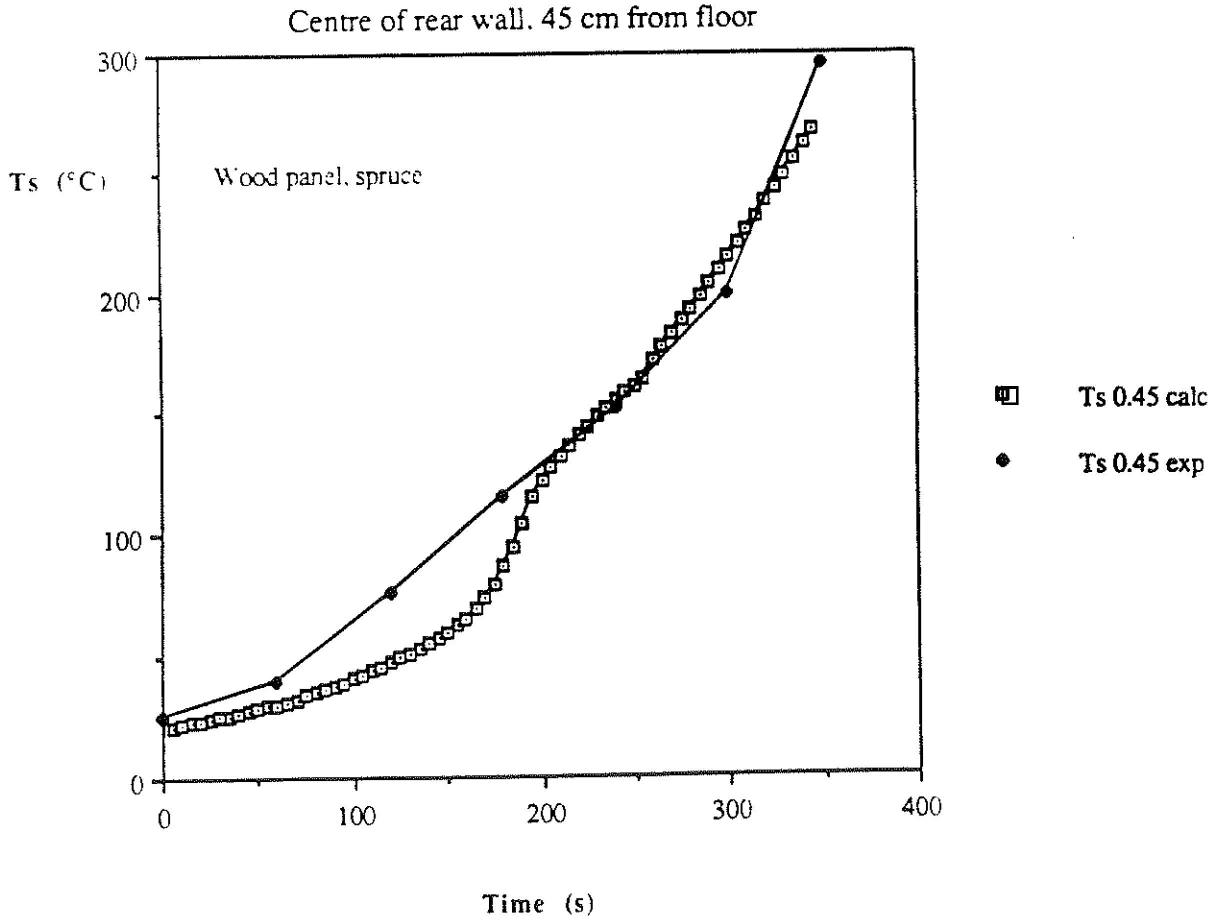

Wall surface temperatures, 1/3 scale test, scenario A

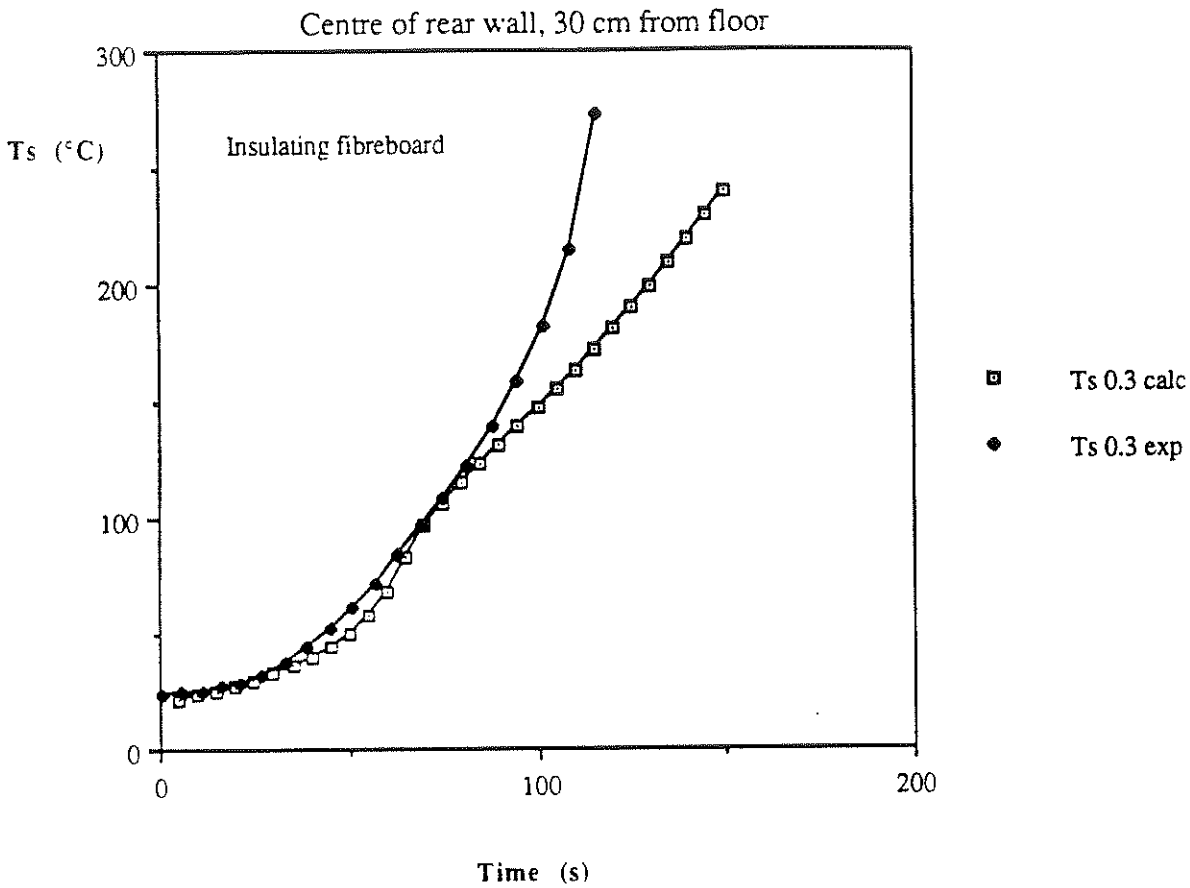

Wall surface temperature, 1/3 scale test, scenario A

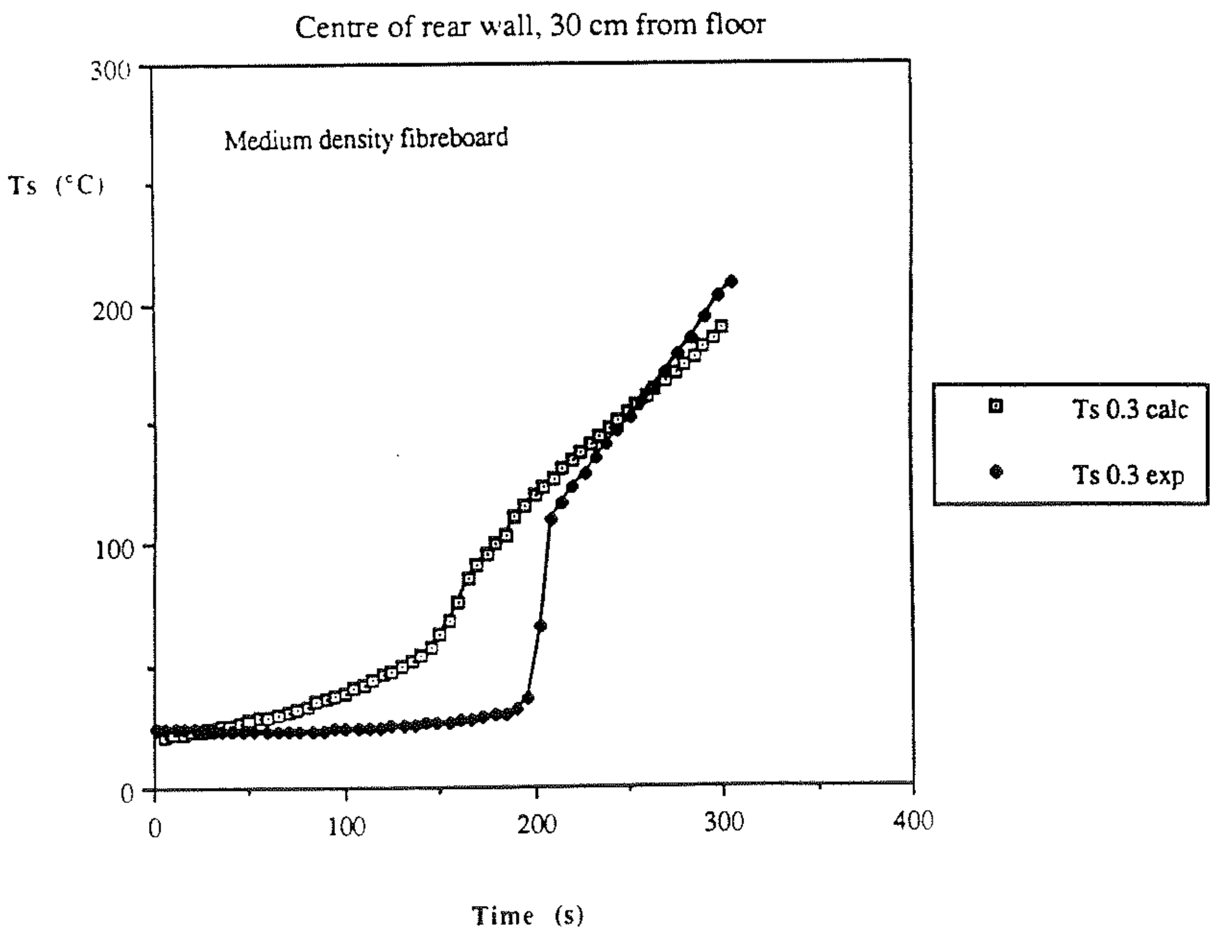

Wall surface temperatures, 1/3 scale test, scenario A

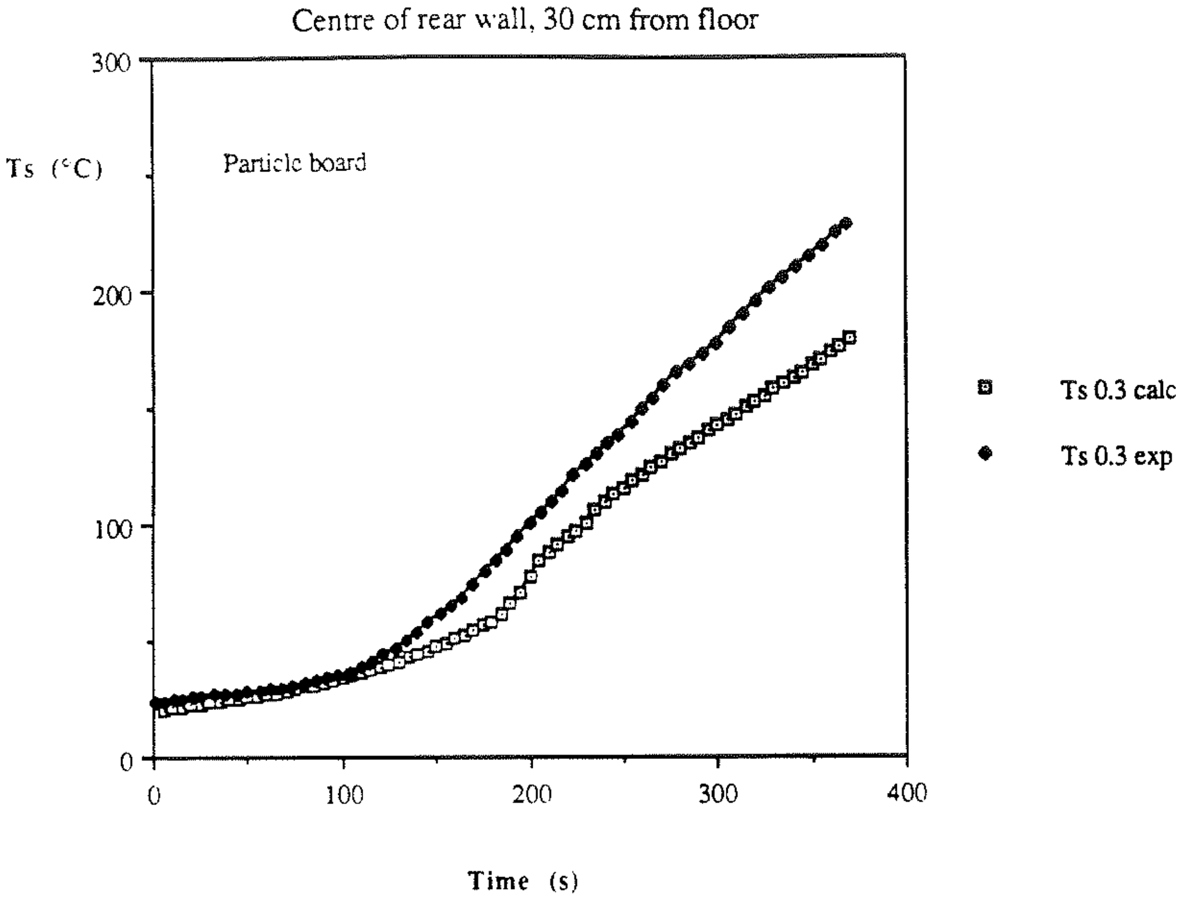

Wall surface temperatures, 1/3 scale test, scenario A

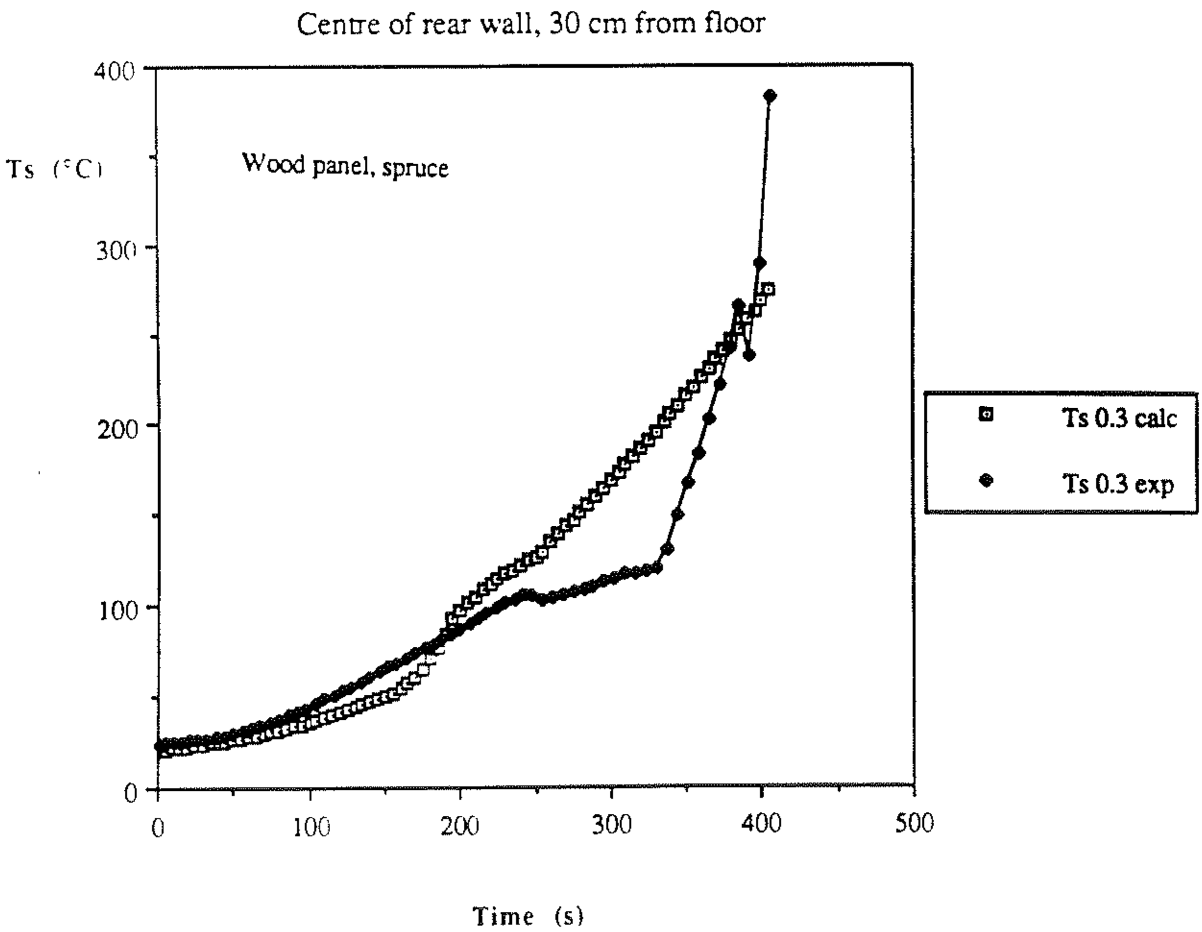

Downward flame spread, 1/3 scale test, scenario A

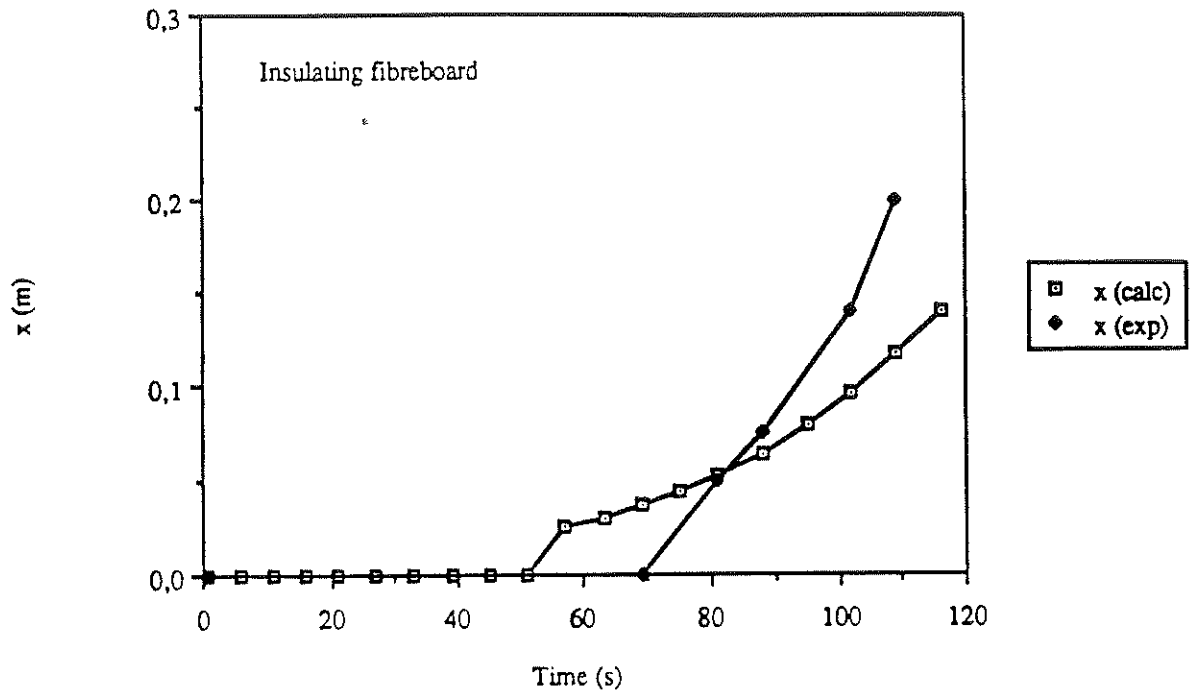

Downward flame spread, 1/3 scale test, scenario A

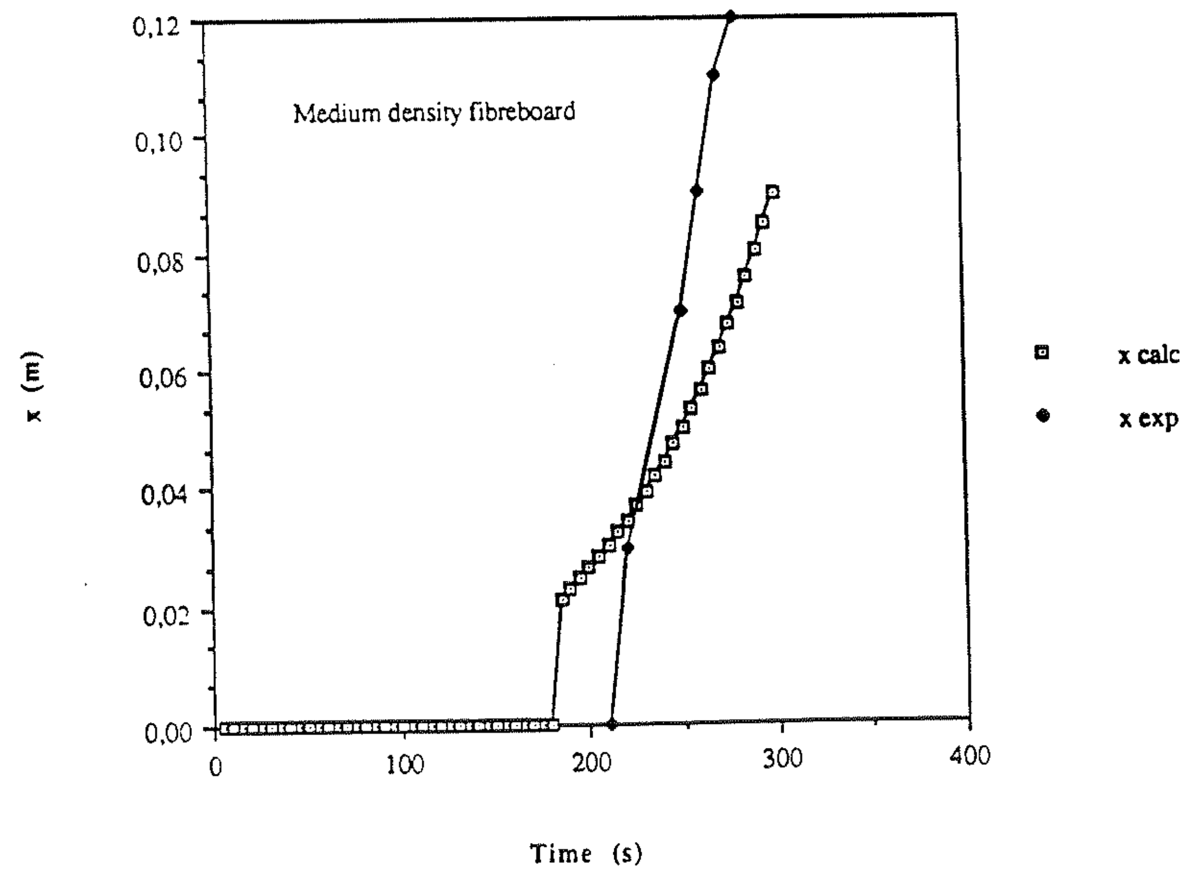

Downward flame spread, 1/3 scale test, scenario A

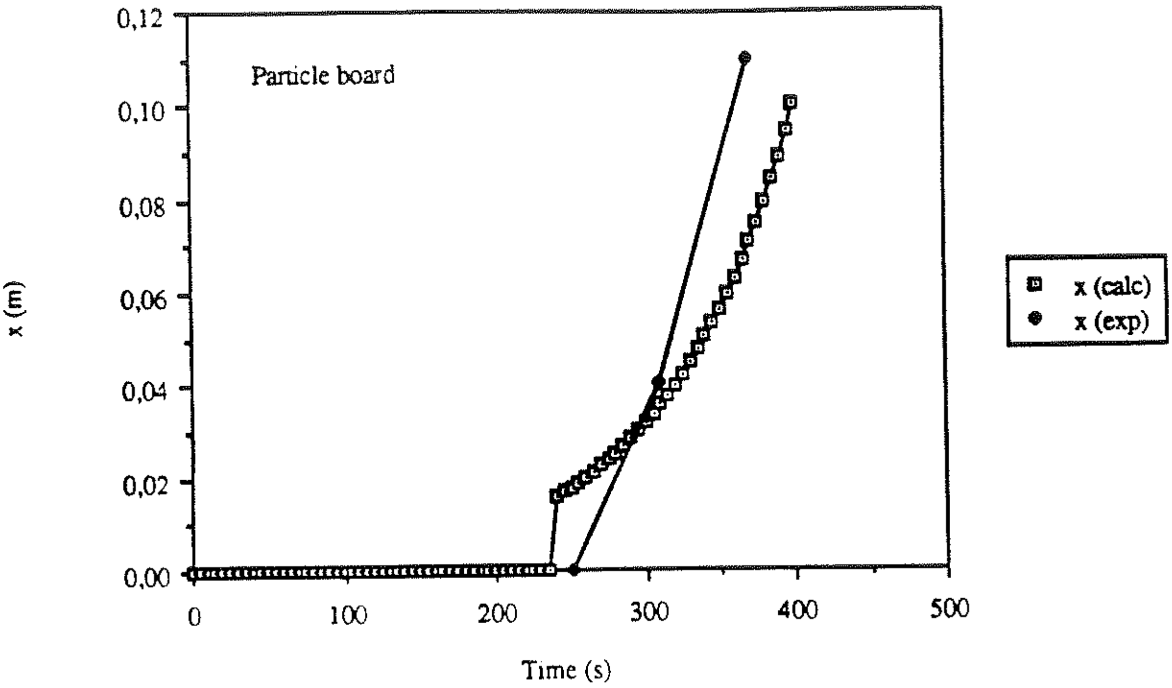

Downward flame spread, 1/3 scale test, scenario A

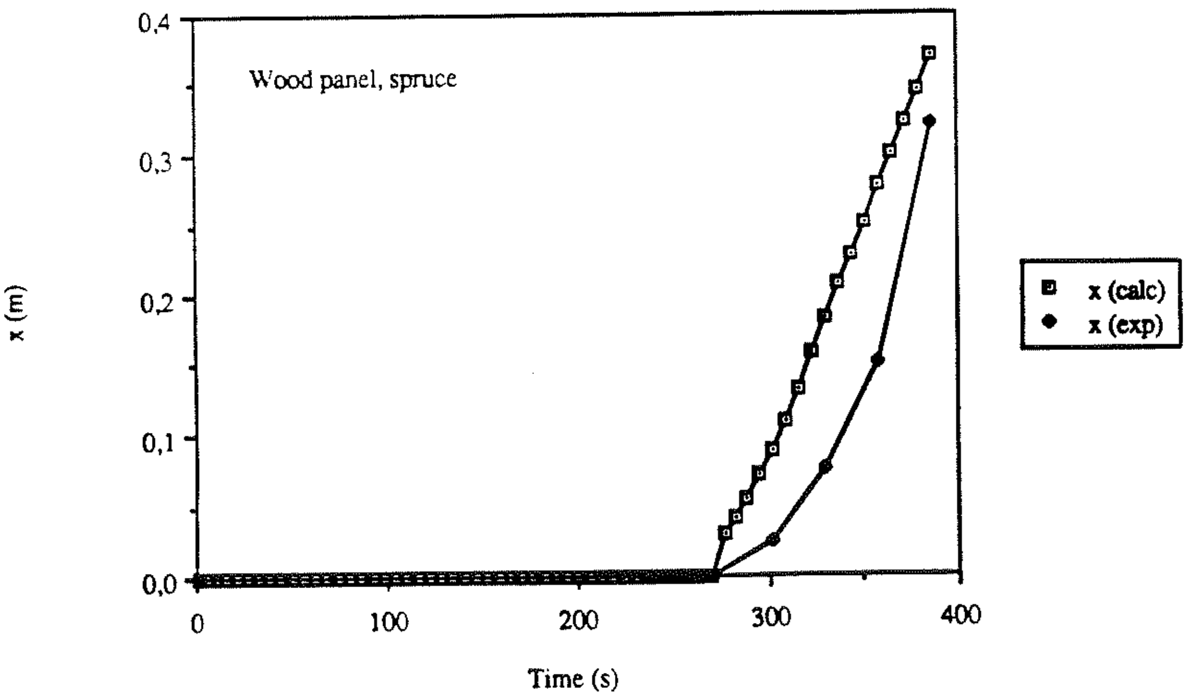

Downward flame spread, 1/3 scale test, scenario A

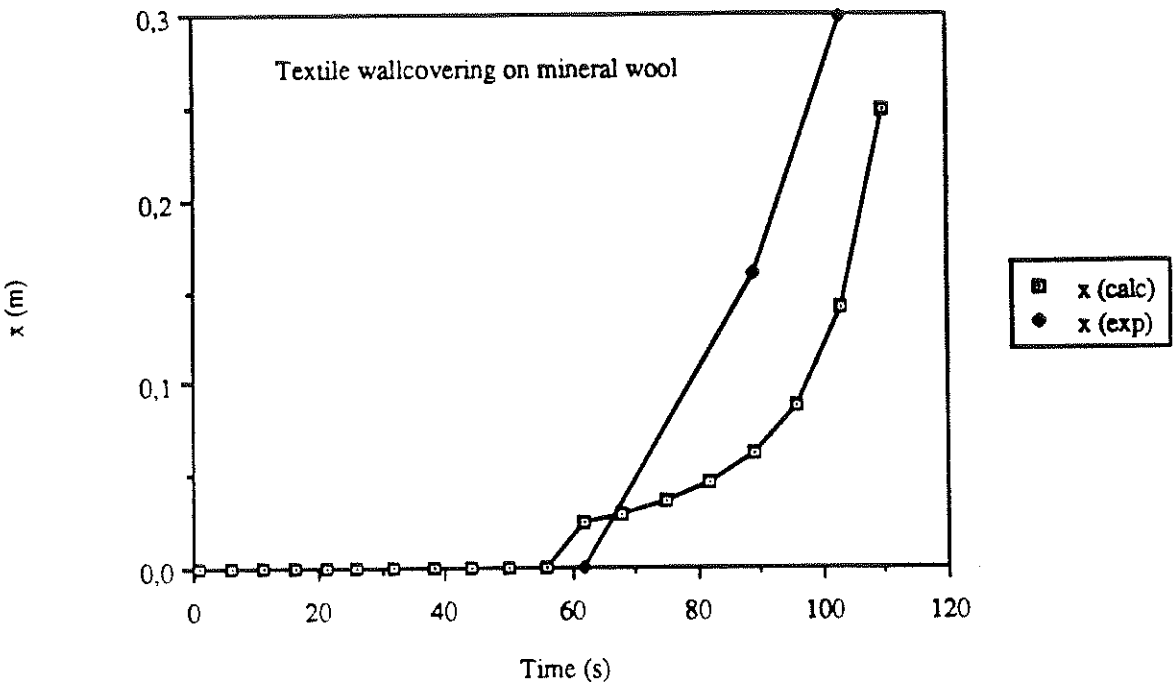

Appendix D

Comparison of experimental and calculated data from full scale test series, scenario B

Contents	Page

Note: Only results from Particle board

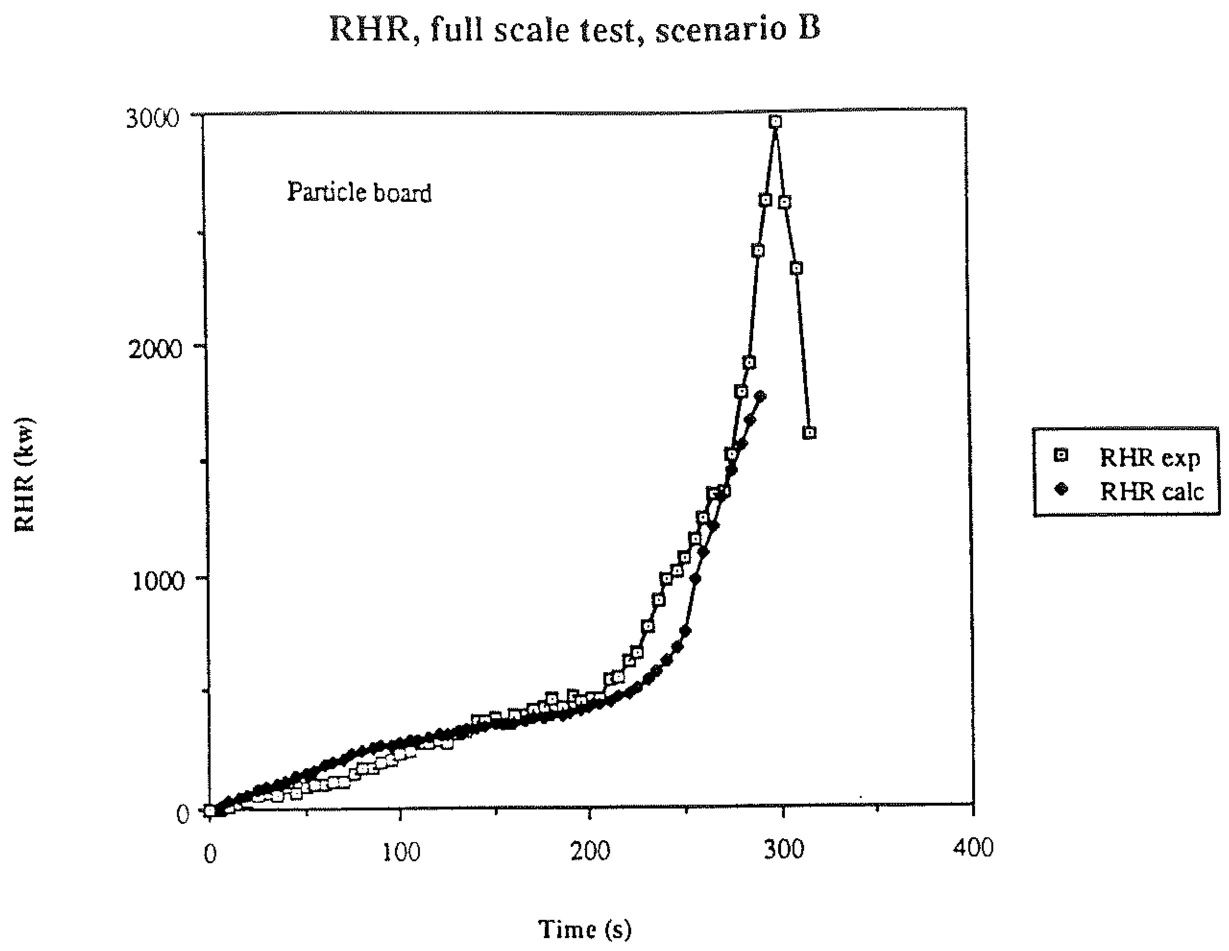
RHR, full scale test, scenario B
Particle board
RHR (kw)
3000
2000
1000
0
0
100
200
300
400
Time (s)
RHR exp
RHR calc

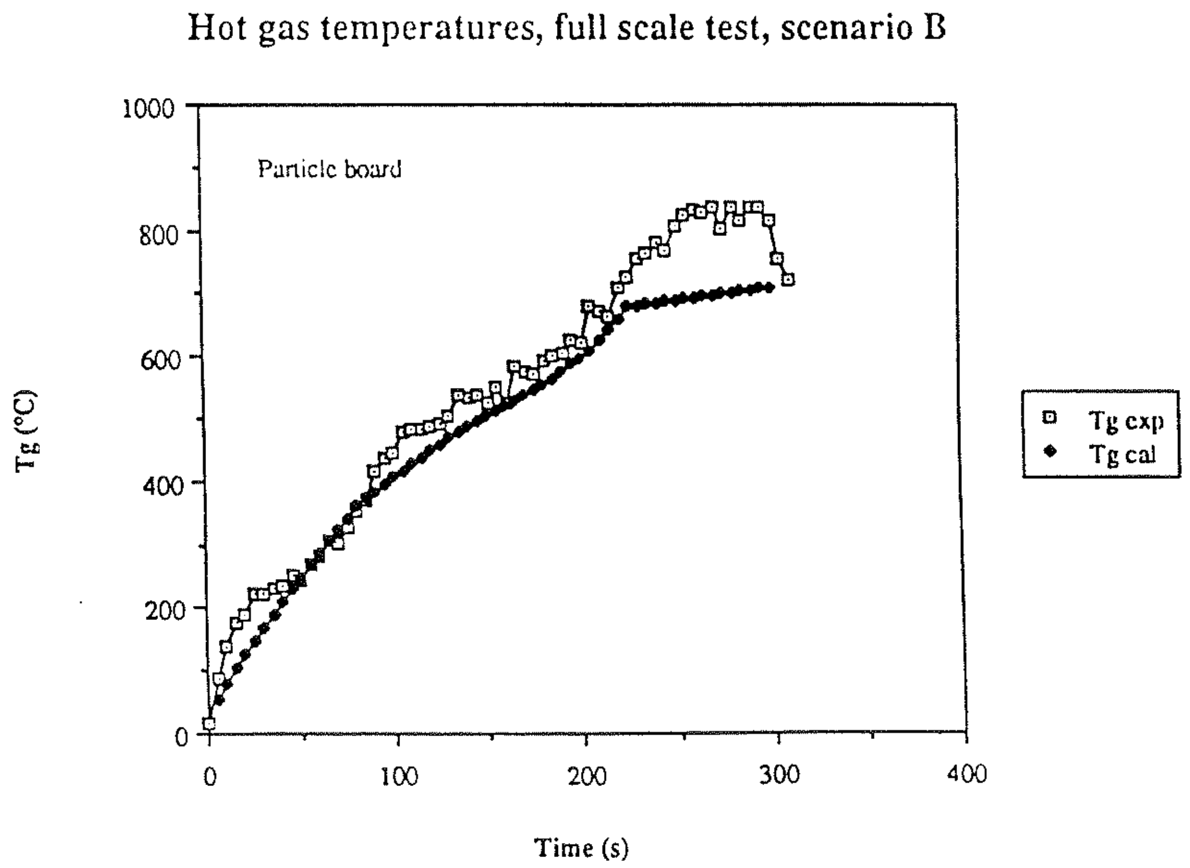
Hot gas temperatures, full scale test, scenario B
Particle board
Tg (°C)
1000
800
600
400
200
0
0
100
200
300
400
Time (s)
Tg exp
Tg cal

Heat flux to wall, full scale test, scenario B

Centre of long wall, 180 cm from floor

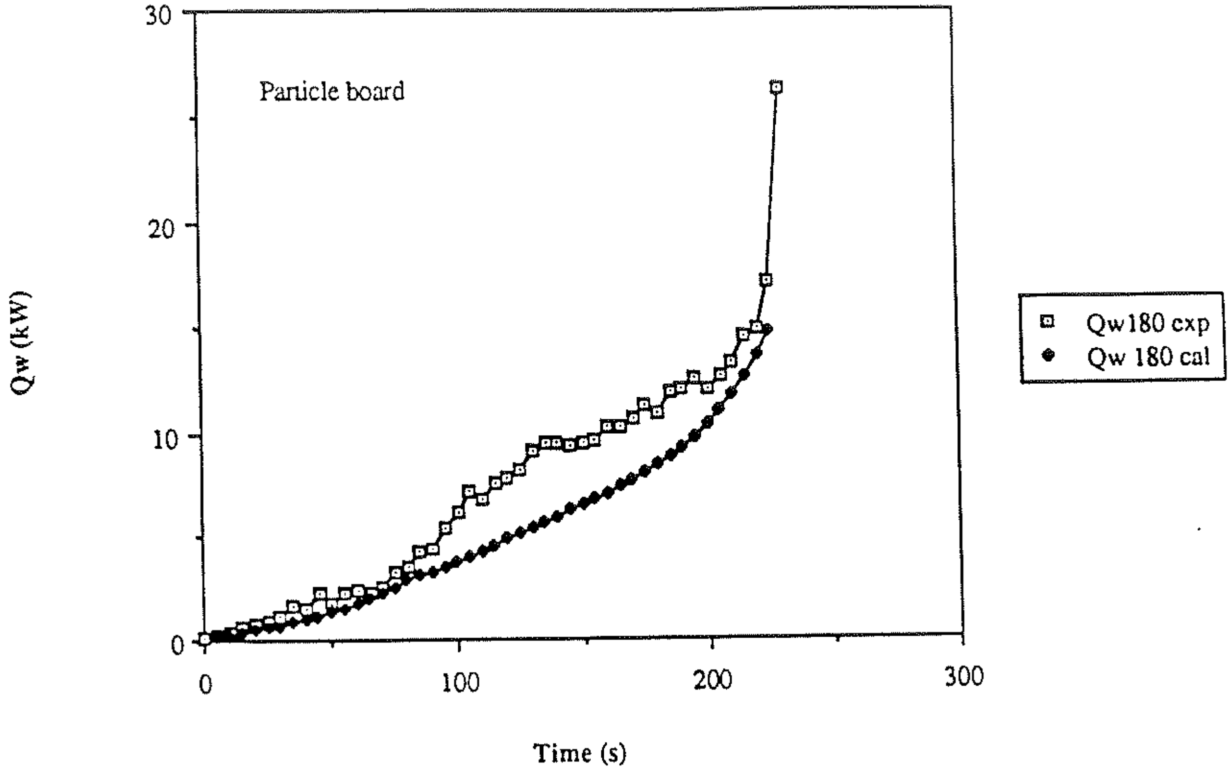

Heat flux to wall, full scale test, scenario B

Centre of long wall, 120 cm from floor

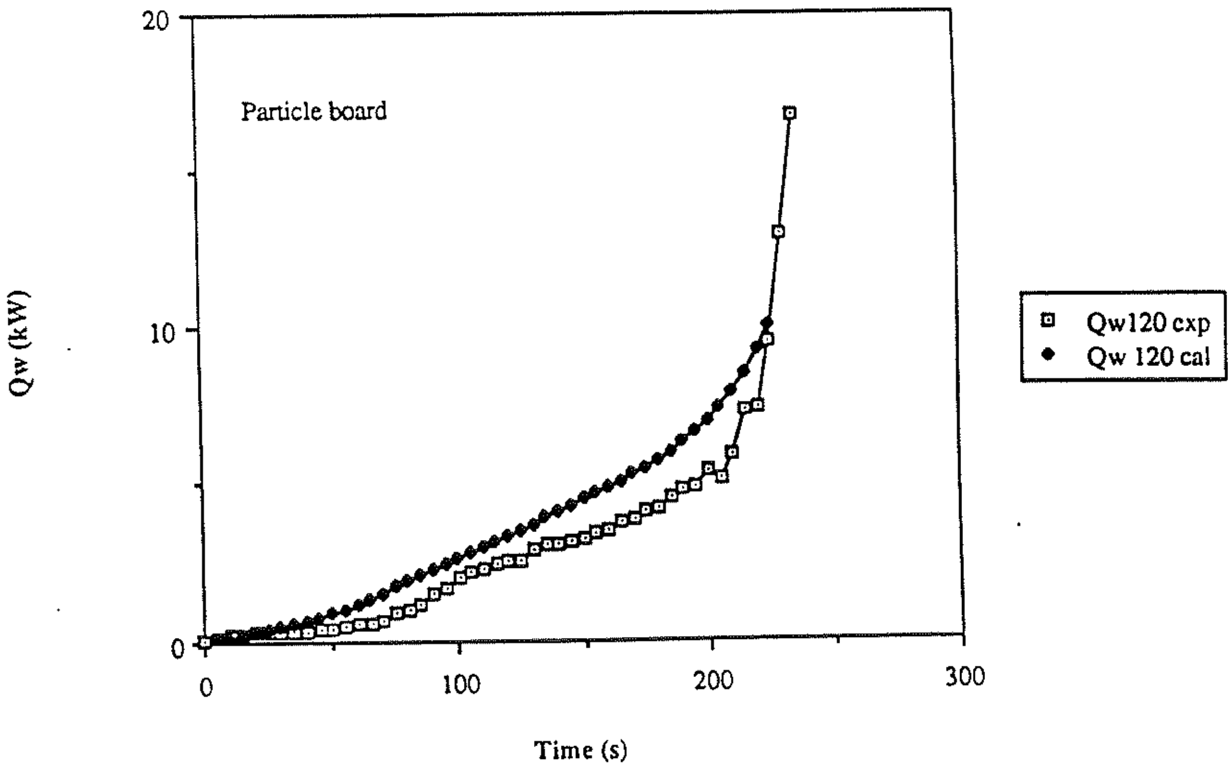

Heat flux to wall, full scale test, scenario B

Centre of long wall, 60 cm from floor

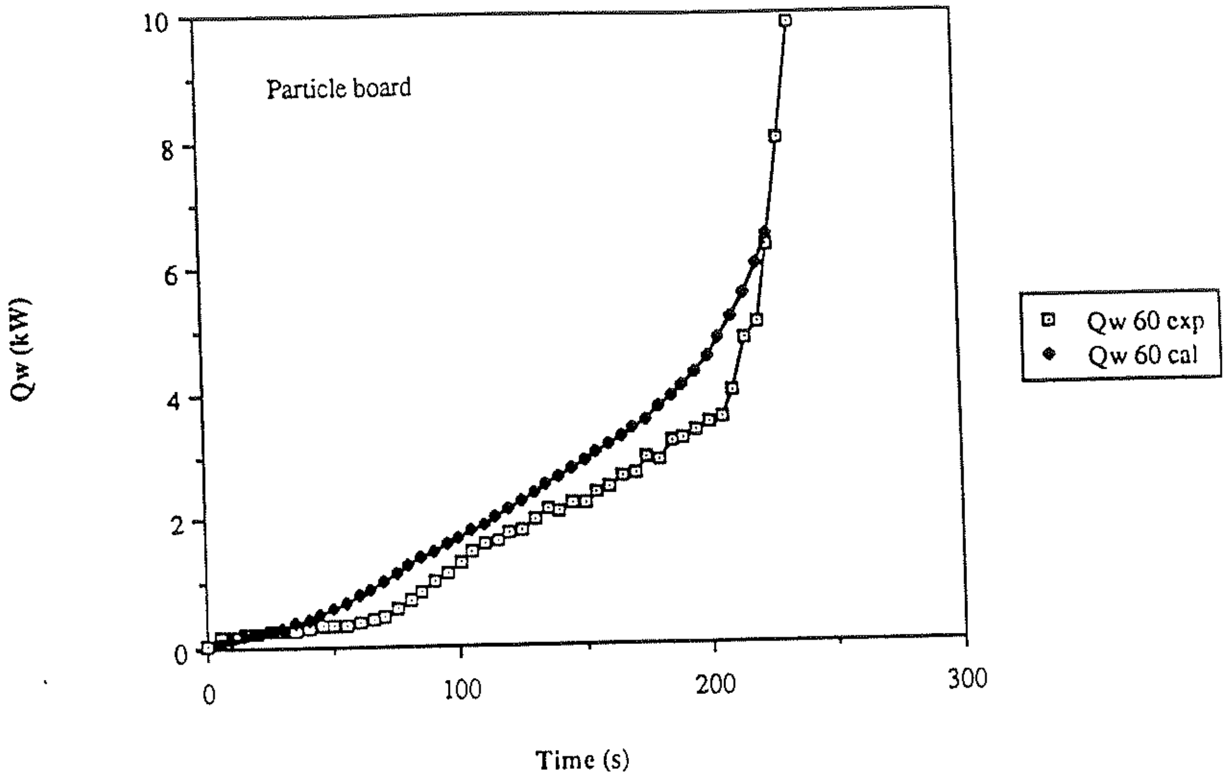

Heat flux to floor, full scale test, Scenario B

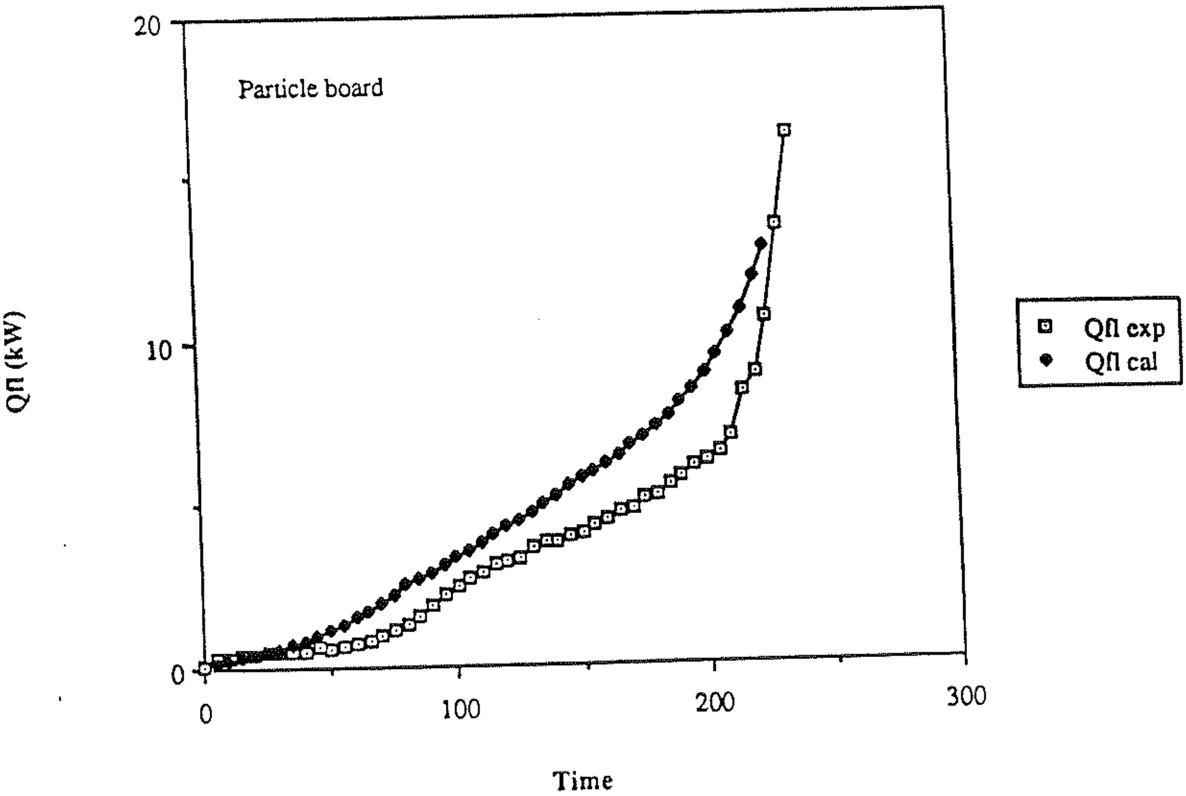

Surface Temperatures, full scale test, scenario B

Centre of long wall, 180 cm from floor

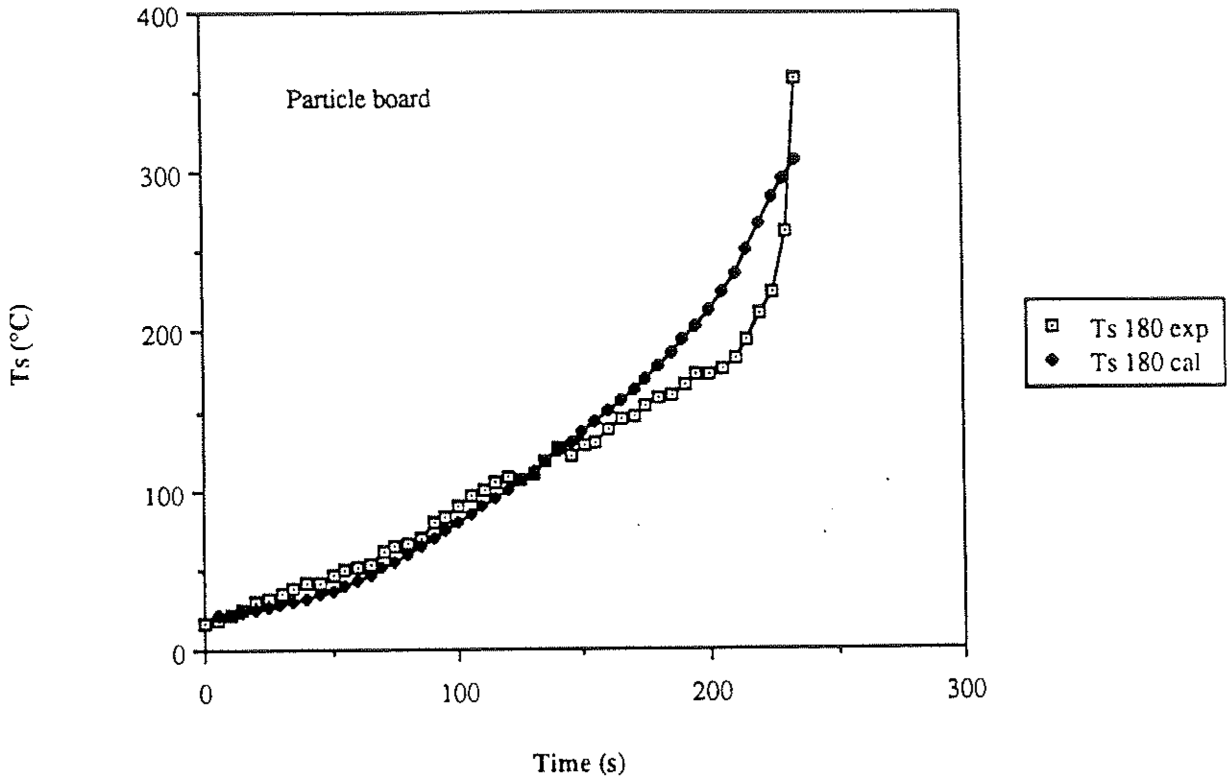

Surface temperatures, full scale test, Scenario B

Centre of long wall, 60 cm from floor

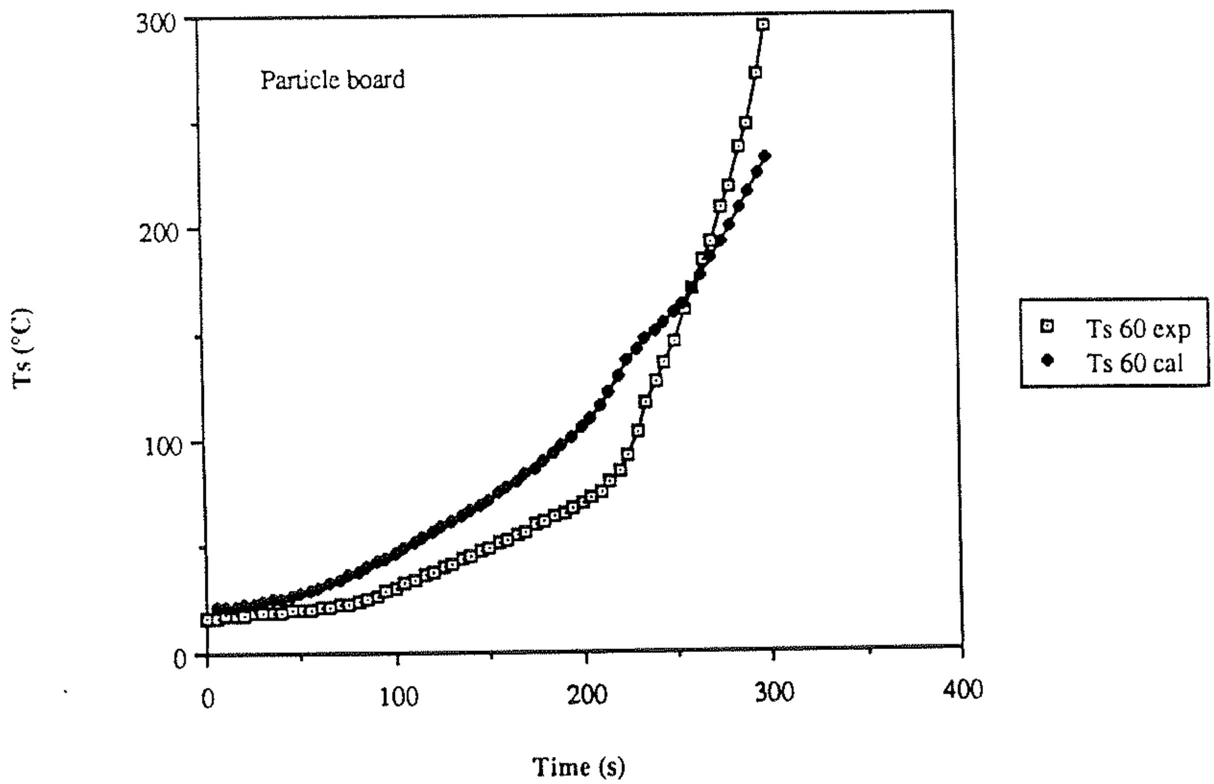

Surface temperatures, full scale test, scenario B

Centre of long wall, 120 cm from floor

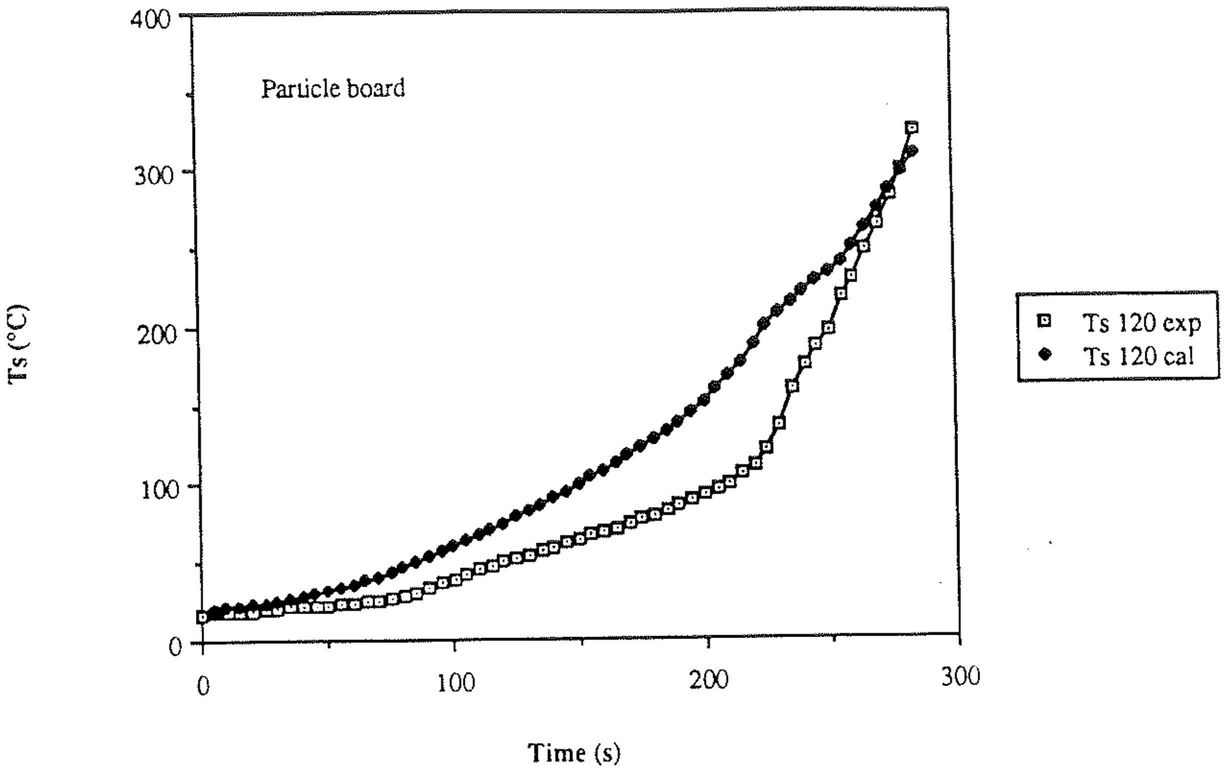

Downward flame spread, full scale test, scenario B

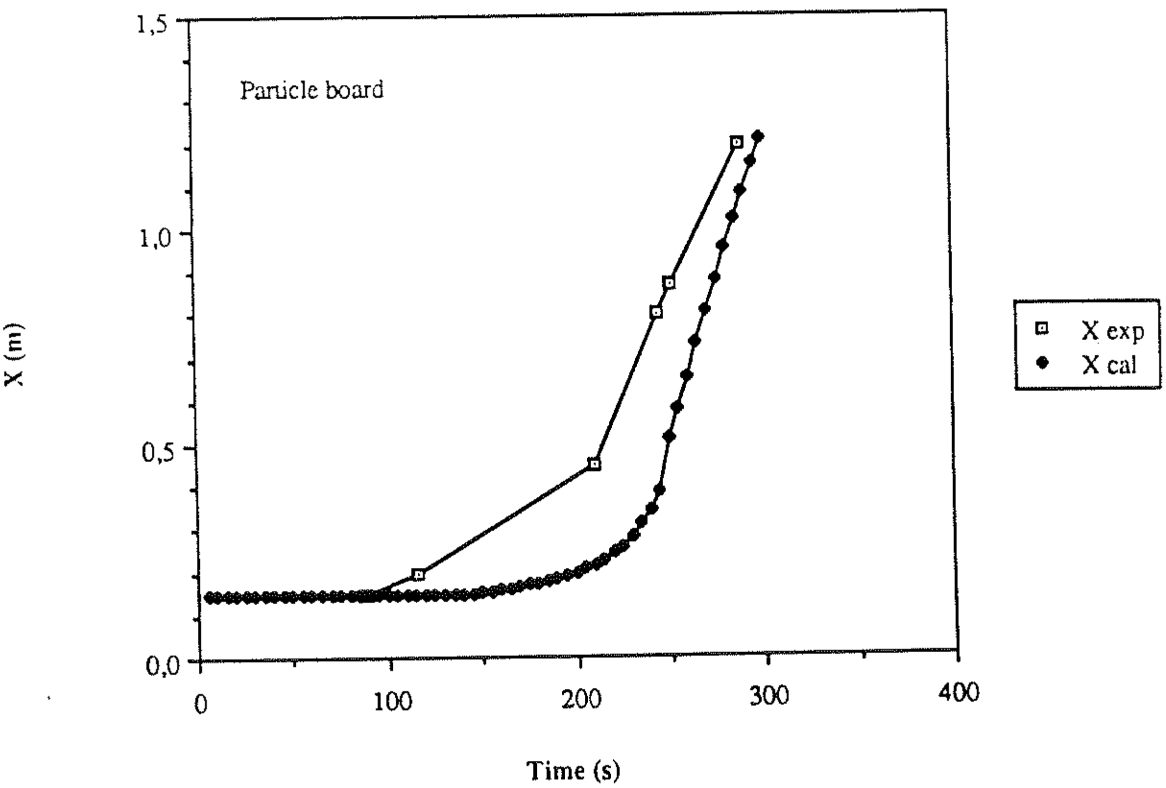

Appendix E

Comparison of experimental and calculated data from 1/3 scale test series, scenario B

Note: No experimental data of wall temperatures or downward flame spread exists for this series

RHR, 1/3 scale test, scenario B

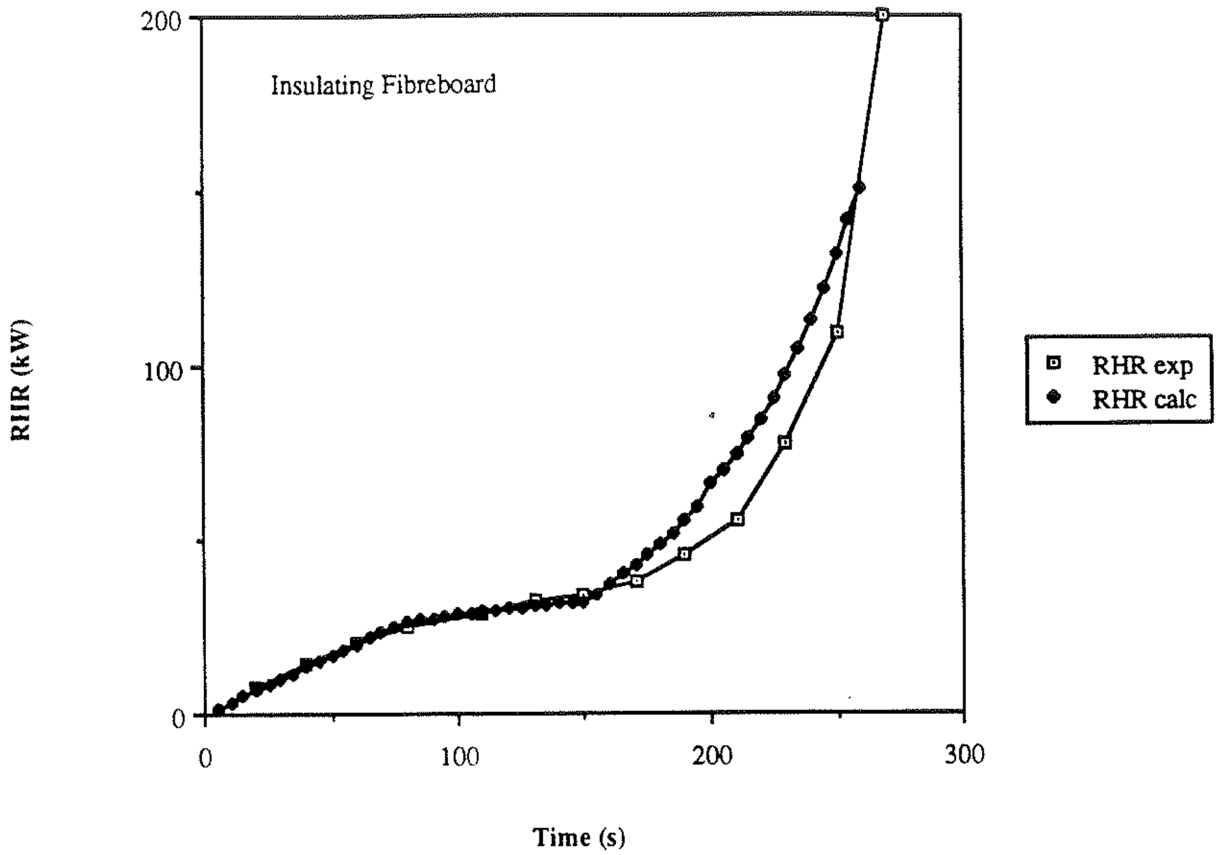

RHR, 1/3 scale, scenario B

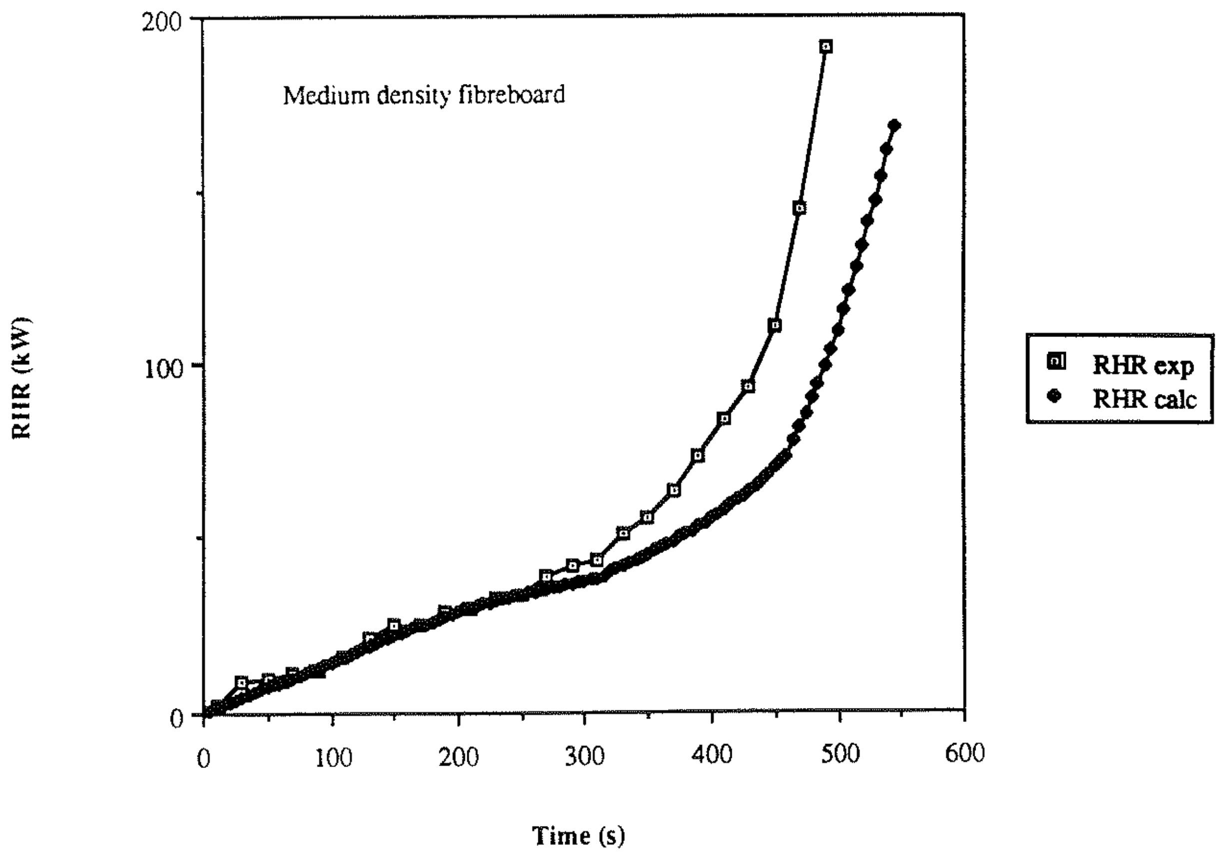

RHR, 1/3 scale test, Scenario B

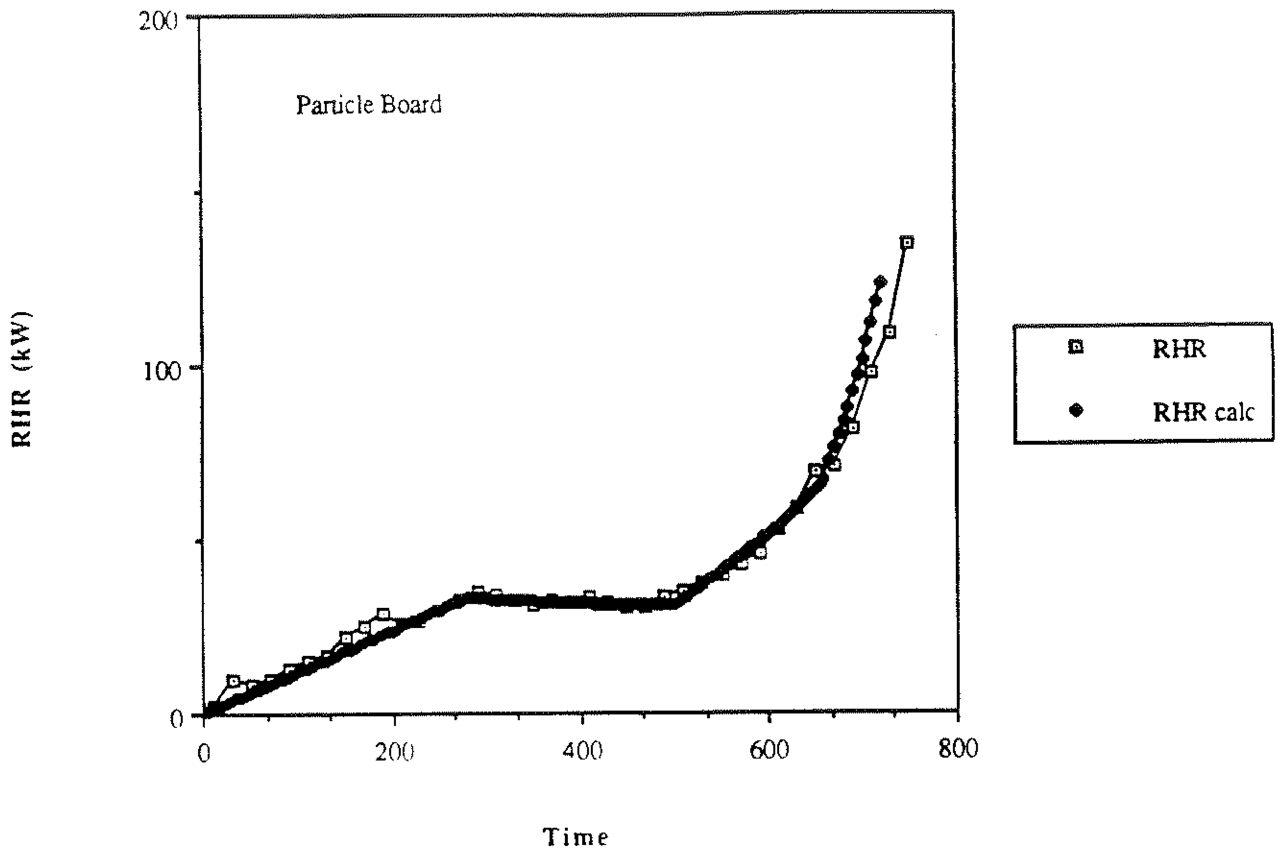

RHR, 1/3 scale test, scenario B

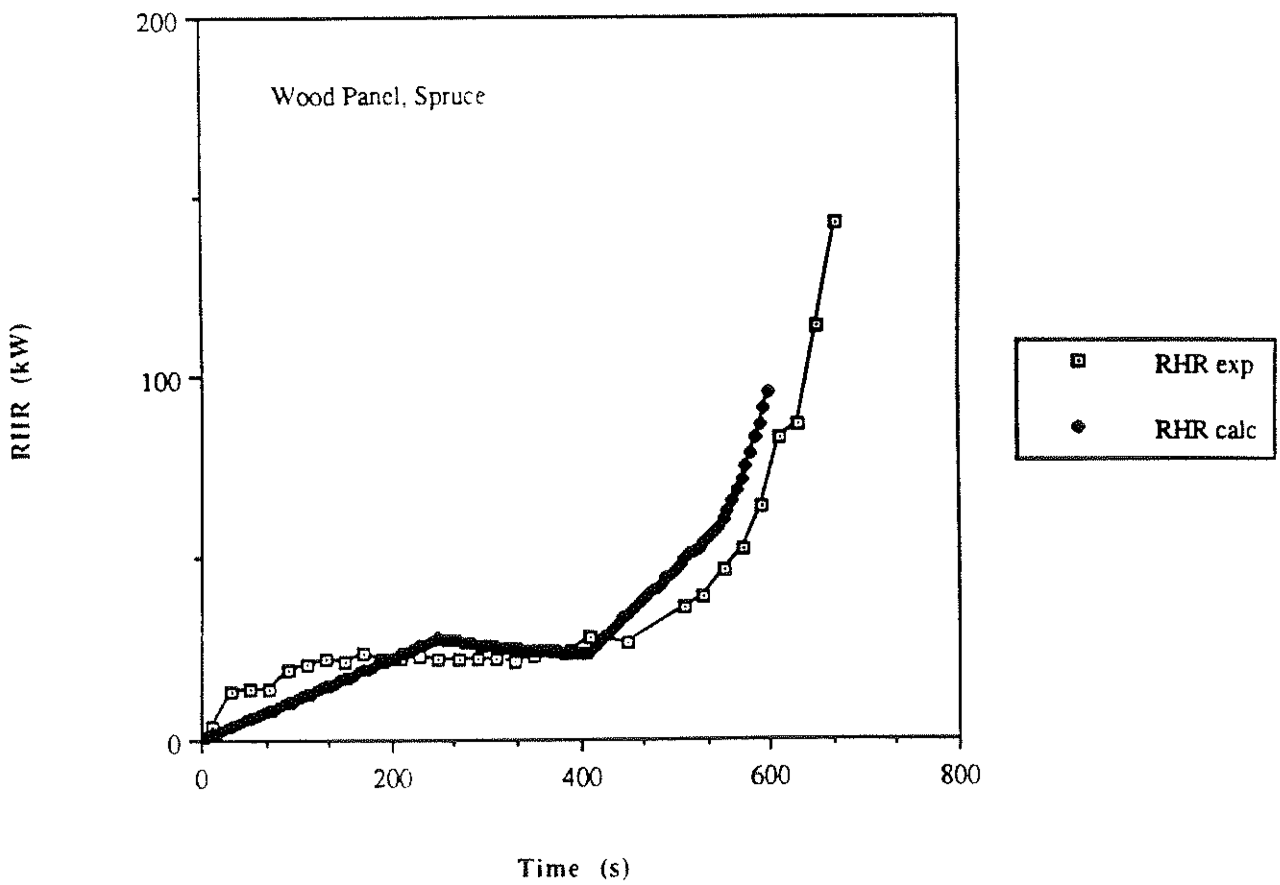

Gastemperatures, 1/3 scale, Scenario B

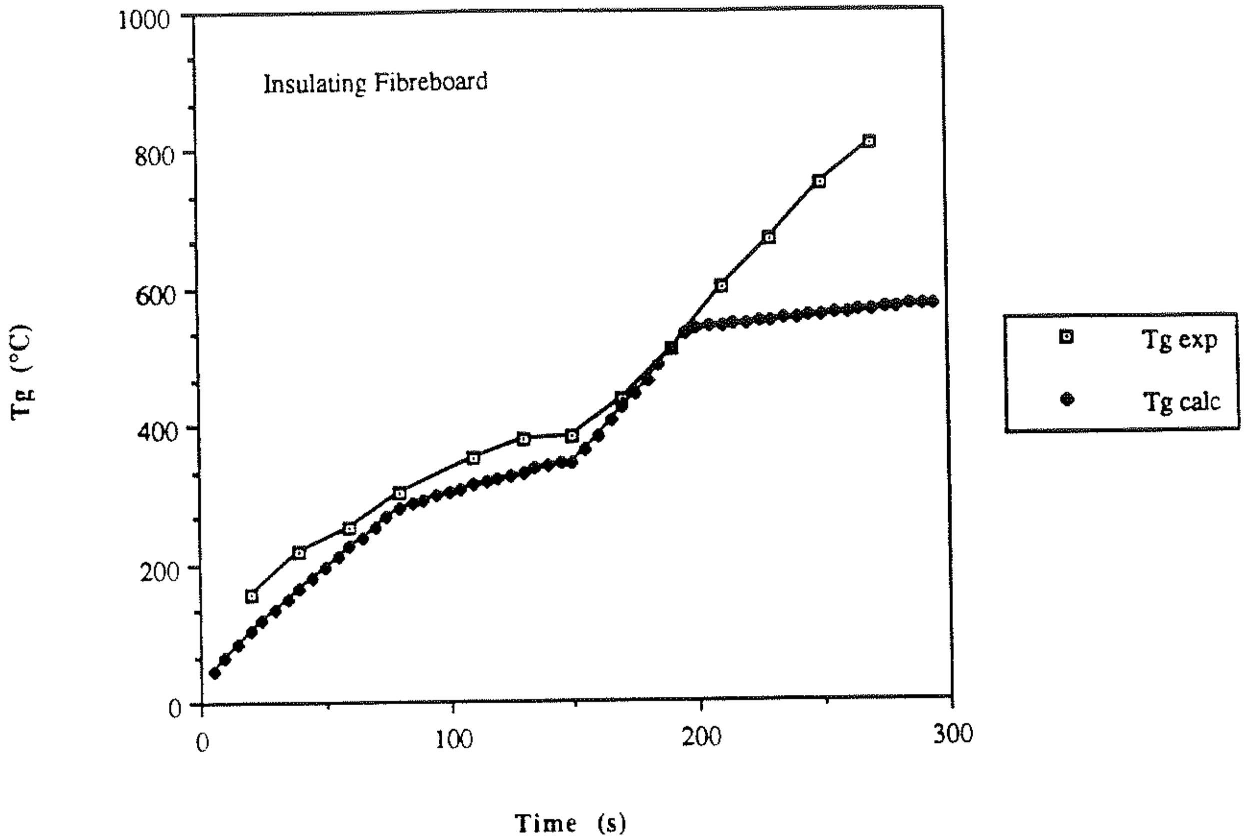

Gastemperatures, 1/3 scale, Scenario B

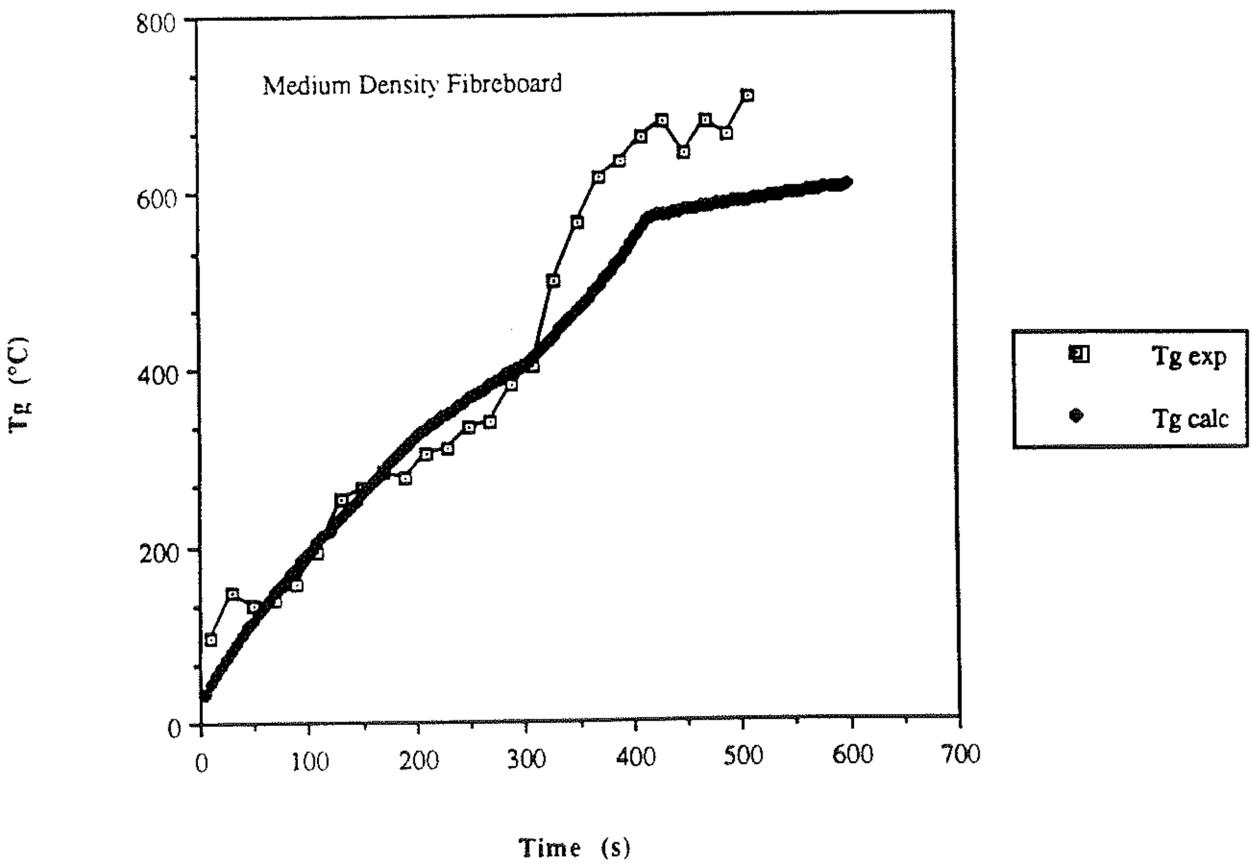

Gastemperatures, 1/3 scale test, Scenario B

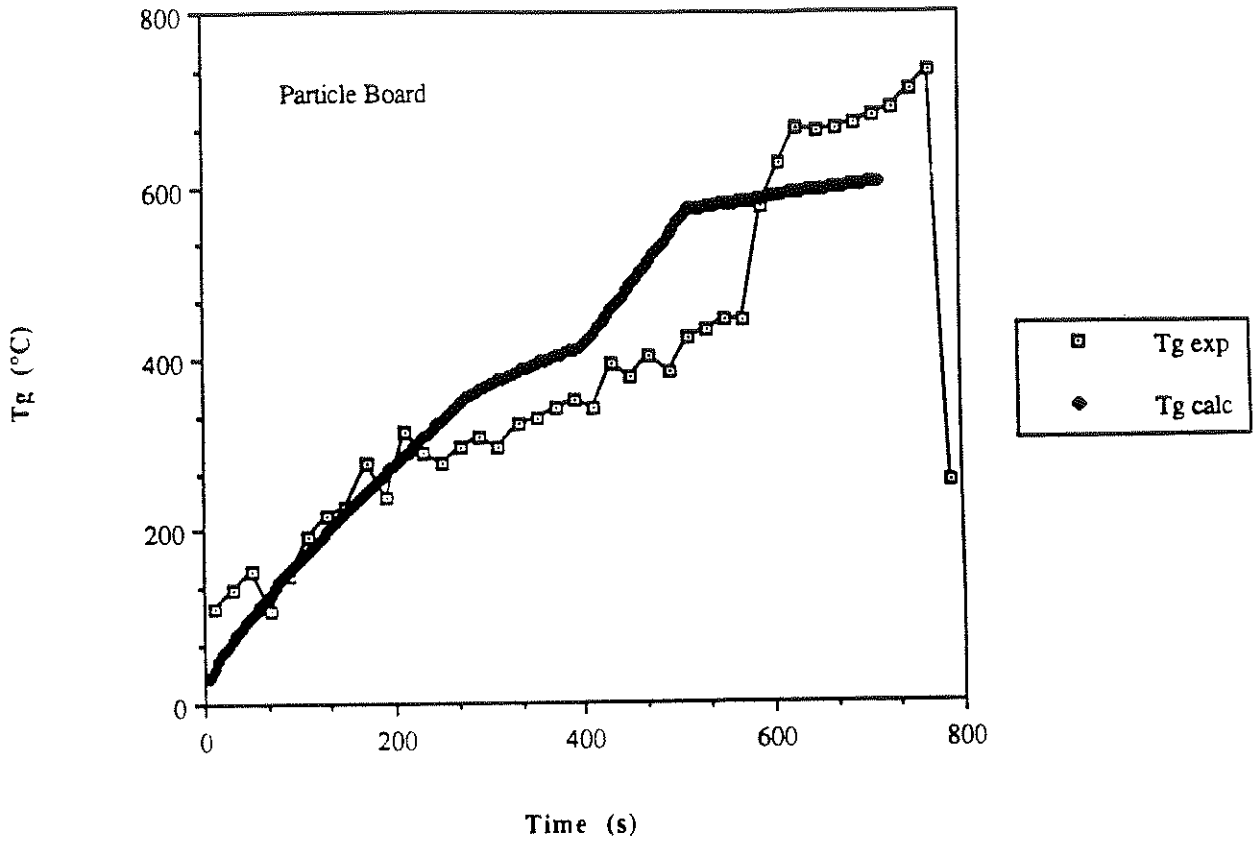

Gastemperatures, 1/3 scale, Scenario B